Supplementary Information (SI) for Chemical Science.
This journal is © The Royal Society of Chemistry 2026

Supporting Information

Synthesis, Characterization, and Imidogen Photochemistry of a Hydrazoic Acid Adduct of Rh_2

Arpan Paikar, Phong Thai, Matthew T. Figgins, Bodhisattwa Mandal, Matthew J. Lekas, Joseph H. Reibenspies, Gerard P. Van Trieste, and David. C. Powers*

Department of Chemistry, Texas A&M University, College Station, Texas 77843, United States

Email: powers@chem.tamu.edu

Table of Contents

A. General Considerations

Materials and Methods. Unless otherwise noted, all the chemicals and solvents (ACS reagent grade) were used as received. Sodium azide and stearic acid were purchased from Beantown Chemicals. Nitromethane was purchased from Sigma Aldrich. Dirhodium tetraacetate was obtained from Ark Pharm. *Cis*-4-octene, 1-octene, and cyclohexene were purchased from Ambeed. Norbornene was obtained from Bean Town Chemical. N_2 was purchased from Airgas. 2,2-Dimethylbutane (DMB) and *tert*-butylbenzene (TBB) were obtained from Tokyo Chemical Industry. ^{15}N-NaN_3, d_8-toluene, and CD_2Cl_2 were purchased from Cambridge Isotope Laboratories. CD_2Cl_2, d_8-toluene, and *cis*-4-octene were degassed by standard freeze-pump-thaw procedures (3 cycles) and stored over activated 4 Å molecular sieves in an N_2-filled glovebox. 1-Octene and cyclohexene were distilled over CaH_2 and stored over activated 4 Å molecular sieves. Anhydrous CH_2Cl_2 was obtained from a drying column and stored over activated 4 Å molecular sieves.[1] Sodium azide and stearic acid were dried under active vacuum at 50 °C for 12 h before every reaction. $Rh_2(esp)_2$ (**1**), aryl azides (**3a**, Ar = C_6H_5; **3b**, 4-CH_3-C_6H_4; **3c**,4-CF_3-C_6H_4) and [D_1]-stearic acid were prepared according to literature methods.[2]

Characterization Details. NMR spectra were recorded on either VNMRS 500 or Bruker Avance NEO 500 NMR operating at 500 MHz for ^1H, ^{13}C, and acquisitions and were referenced against solvent signals: CD_2Cl_2 (5.32 ppm, 1H; 53.84 ppm, ^{13}C).[3] ^{15}N NMR spectra were recorded in CD_2Cl_2 on Bruker Avance NEO 500 NMR operating at 50.7 MHz and acquisitions were referenced against nitromethane as external reference (380.5 ppm). ^1H NMR data are reported as follows: chemical shift (δ, ppm), multiplicity (s (singlet), d (doublet), t (triplet), m (multiplet), br (broad), integration. Solid-state MAS NMR data were collected with a Bruker Avance-NEO solid-state NMR spectrometer (400 MHz for ^1H nuclei) equipped with a standard three-channel 4-mm MAS probe head. A standard solid-echo pulse sequence with optimized echo delays of 0.000065 s and recycle time delays of 10 s was used to collect the ^2H MAS NMR spectrum with 46000 scans and at a spinning rate of 10 kHz. The proton-nitrogen cross-polarization ^{15}N MAS NMR spectrum was recorded with ^1H rf-pulses of 2.5 μs and contact times of 3.5 ms and 48000 scans at a spinning rate of 8 kHz and recycle time delays of 5 s. The external references in the ^{15}N and ^2H MAS NMR spectra were CH_3NO_2 and benzene-d_6 (δ of 7.1 ppm). Low-temperature solution-phase UV-vis spectra were recorded on a Cary 60 UV-vis spectrophotometer (175–900 nm) attached to TC-1 temperature controller from Quantum Northwest. Solution-phase spectra were blanked against the CH_2Cl_2. Solid-state IR spectra were recorded on a Bruker Vertex 70 Fourier transform IR (FTIR) spectrometer, were blanked against air, and were determined as the average of 64 scans. Solution phase IR spectra were recorded on a Bruker Tensor 37 Fourier transform IR (FTIR) using the CaF_2 cell with a 0.2 mm path length. Spectra were blanked against CD_2Cl_2 and determined as the average of 64 scans. Data are reported as follows: Wavenumber (cm^{-1}), peak intensity (s, strong; m, medium; w, weak). Variable-temperature IR spectra were recorded on a Mettler Toledo IC10 ReactIR spectrometer with a probe path length of ~13 μm. The photolysis at 77 K was monitored by collection of periodic UV-vis spectra using an Ocean Optics OCEAN SR spectrometer and DH-2000-BAL UV-vis-NIR light source. The spectra at 77K were blanked against a frozen glass (at 77 K) composed of 3:1mixture of DMB and TBB in a quartz EPR tube. The spectra were processed using the Savitzky-Golay smoothing function on OriginPro 2025. Combustion analysis was not performed on **2** or **3a**-**3c** because the weak binding of the azide ligands to Rh_2 in these complexes prevents access to solvent-free samples.

X-Ray Diffraction Details.

Routine Crystallography Crystallization details are included in the synthetic procedures for relevant compounds. Crystals suitable for X-ray diffraction were mounted on a MiTeGen dual-thickness micro-mount. The X-ray crystal structure of **2**, **3a**, **3b**, and **3c** were collected using a XtaLAB Synergy Dualflex HyPix 6000He diffractometer equipped with an Oxford Cryosystems low-temperature device operating at 100 K. Data were measured using Cu Kα radiation (K_α = 1.54184 Å). For compounds **2**, **3a**, **3b**, and **3c** the diffraction pattern was indexed, and the total number of runs and images was based on the strategy calculation from the program CrysAlisPro 1.171.42.101a (Rigaku OD, 2023). Data reduction, scaling, and absorption corrections were performed using CrysAlisPro 1.171.42.101a (Rigaku OD, 2023) using CrysAlisPro 1.171.42.101a (Rigaku Oxford Diffraction, 2023). Solutions were obtained using XT/XS in APEX III and refined in Olex2-1.5.[4, 5]

In situ Crytallography The X-ray crystal structures of **8a**, **8b**, and **8c** were collected using a XtaLAB Synergy Dualflex HyPix 6000He diffractometer equipped with an Oxford Cryosystems low-temperature device operating at 100 K. Data were measured using Cu Kα radiation (K_α = 1.54184 Å). were mounted on goniometer head. The crystals were photolyzed periodically using a 365 nm light (M365FP1) from ThorLabs and X-ray structures were collected periodically until the crystal degraded. For compounds **8a**, **8b**, and **8c** the diffraction pattern was indexed, and the total number of runs and images was based on the strategy calculation from the program CrysAlisPro 1.171.42.101a (Rigaku OD, 2023). Data reduction, scaling, and absorption corrections were performed using CrysAlisPro 1.171.42.101a (Rigaku OD, 2023) using CrysAlisPro 1.171.42.101a (Rigaku Oxford Diffraction, 2023). Solutions were obtained using XT/XS in APEX III and refined in Olex2-1.5.[4, 5]

SAFETY HN_3 is highly toxic and can decompose explosively. Appropriate safety precautions, including all standard personal protective equipment, a protective shield, low temperature, limited reaction scale, and *in situ* generation, should be taken.

B. Synthesis and Characterization

Generation of HN_3

SAFETY NOTE. HN_3 is highly toxic and can decompose explosively. Appropriate safety precautions, including all standard personal protective equipment, a protective shield, low temperature, limited reaction scale, and *in situ* generation, should be taken.

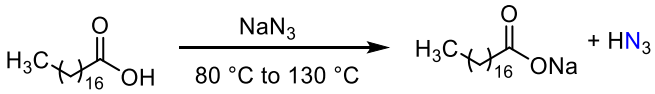

HN_3 was generated according to the following modification of literature methods; a photograph of the experimental apparatus is provided in Figure S1a.[6] Under an N_2 atmosphere, a 25-mL screw-capped Schlenk flask was charged with dry CD_2Cl_2 (0.60 mL). The solution was frozen at 77 K using liquid N_2. A 100-mL two-necked round bottom flask was charged with a magnetic stir bar, stearic acid (0.285g, 1.00 mmol, 2.00 equiv.), and sodium azide (NaN_3, 32.5 mg, 0.50 mmol, 1.00 equiv.). The two flasks were connected via a short-path distillation head. The entire assembly was evacuated and back-filled three times and kept under vacuum. With stirring, the stearic acid and sodium azide mixture was first heated to 80 °C for 30 min, then to 100 °C for 1 h, and then to 130 °C for 1.5 h (3 h total heating time). The generated HN_3 was condensed into Schlenk flask containing frozen CD_2Cl_2 (maintained at 77 K). After HN_3 generation was complete, the receiving flask was allowed to warm to–78 °C and kept at that temperature for 30 min. Subsequently, the temperature gradually raised to 23 °C.

Vacuum transfer of HN_3. A clean and dry J-Young tube was connected to the HN_3-containing Schlenk flask via a modified glass manifold (Figure S1b). The HN_3 solution was frozen at 77 K. The entire assembly was evacuated under active vacuum for 15 min. Under static vacuum, the J-Young tube was cooled to 77 K while the donor flask was gradually allowed to warm to 23 °C (Figure 1b). After the vacuum transfer was complete, the J-Young tube was allowed to warm to −78 °C, then to −20 °C, and finally to 23 °C. ^{1}H NMR (δ, 23 °C, CD_2Cl_2): 4.54(br, s, 1H). IR (CD_2Cl_2, cm^{-1}): 3280 (m), 2137 (s), 2073 (w), 1263 (m), 1157 (s). Spectral data are consistent previous literature reports.[7, 8]

Generation of [^{15}N]-HN_3. [^{15}N]-HN_3 was generated according to above procedures using stearic acid (0.143g, 0.50 mmol, 2.00 equiv.) and [^{15}N]-NaN_3 (16.5 mg, 0.25 mmol, 1.00 equiv.). ^{1}H NMR (δ, 23 °C, CD_2Cl_2): 4.57(br, s, 1H), ^{15}N NMR (δ, 23 °C, CD_2Cl_2): 55.7 (br, s), 208.0 (br, s). IR (CD_2Cl_2, cm^{-1}): 3275 (m), 2131 (s), 2115 (s) 2050 (w), 1259 (m), 1153 (s), 1141 (s).

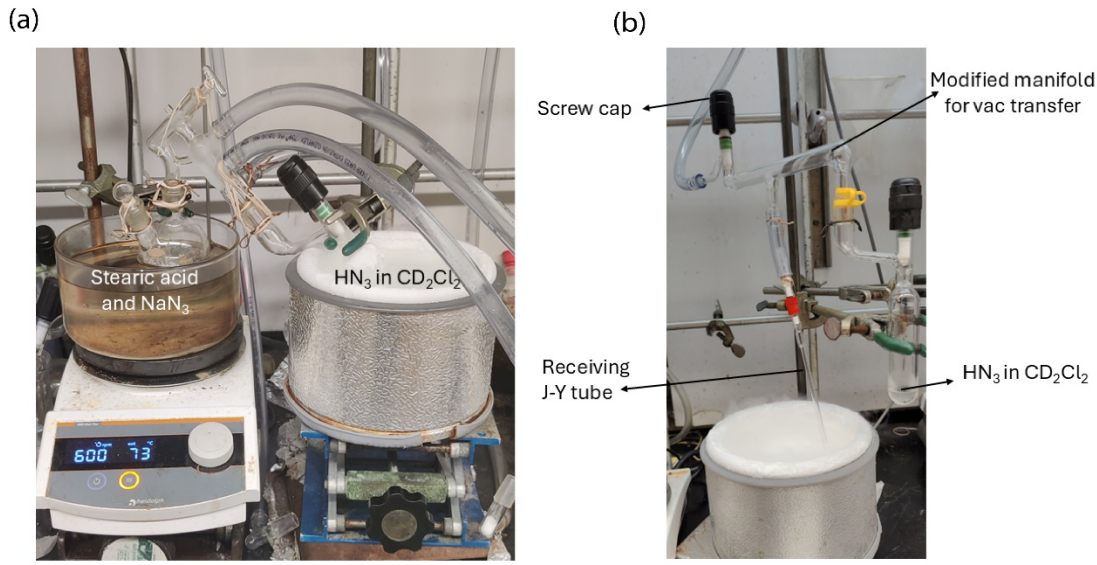

Figure S1. (a) Experimental set up for the generation of HN_3. (b) Experimental set up for the vacuum transfer of HN_3.

Synthesis of $Rh_2(esp)_2(HN_3)_2$ (2)

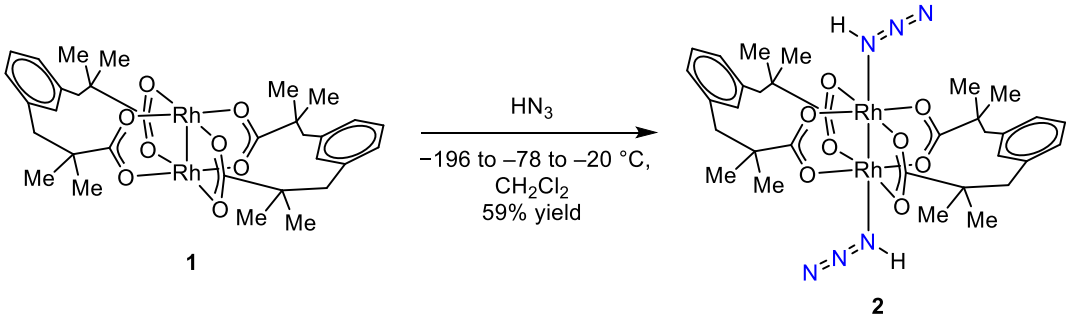

Under an N_2 atmosphere, a 25-mL screw-capped Schlenk flask was charged with $Rh_2(esp)_2$ (38.0 mg, 0.0501 mmol, 1.00 equiv.) and dry CH_2Cl_2 (5.0 mL). The solution was frozen at 77 K. A 100-mL two-necked round bottom flask was charged with a magnetic stir bar, stearic acid (0.571g, 2.01 mmol, 40.00 equiv.), and sodium azide (NaN_3, 65.0 mg, 1.00 mmol, 20.0 equiv.). The two flasks were connected via a short-path distillation head (reaction set-up pictured in Figure S2). Using the procedure described above (page S6), HN_3 was generated and directly condensed in the Rh-containing flask. After the vacuum transfer was complete, the reaction flask was warmed raised to −78 °C. The reaction solution was stirred for 1 h. The reaction solution was gradually warmed to –20 °C at which temperature it was kept for 1 d to afford dark green crystals. Under an N_2 atmosphere, the supernatant was decanted from the Schlenk flask. The supernatant was immediately quenched with saturated aqueous $NaHCO_3$. The Schlenk flask was transferred to an N_2-filled glove box. Complex **2** was dissolved in CH_2Cl_2 and transferred to a 20-mL scintillation vial. Complex **2** was recrystallized by cooling the CH_2Cl_2 solution to –20 °C to afford the title compound (25.1 mg, 59.4% yield). Isolated crystals were stored at −20 °C. ^{1}H NMR (δ, 23 °C, CD_2Cl_2) 7.05 (t, *J* = 7.5 Hz, 2H), 6.91–6.76 (m, 6H), 5.02 (br, s, 2H), 2.61 (s, 8H), 0.99(s, 24H). ^{13}C NMR (δ, 23 °C, CD_2Cl_2) 197.8, 138.5, 131.3, 128.3, 127.2, 47.4, 46.7, 25.9. IR (ATR, cm^{-1}): 3207 (w), 2970 (m), 2956 (m), 2923 (m), 2916 (m), 2943 (m), 2143 (s), 1570 (s), 1475 (s), 1407 (s), 1377 (m), 1361 (m), 1265 (m), 1244 (m), 1199 (w), 1176 (s), 1132 (w), 925 (m), 902 (m), 883 (m), 823 (m), 777 (m), 729 (s) , 705 (s), 636 (s). UV-vis (CH_2Cl_2, 243 K), λ_{max} (nm, ε ($M^{-1}cm^{-1}$)) 419 (160), 640 (240). HR-ESI-MS : $[(M+H)–2HN_3]^+$ 759.0911 (calc.); 759.0882 (expt).[a]

Synthesis of $Rh_2(esp)_2([^{15}N]\text{-}HN_3)_2$ ($[^{15}N]$-2). $[^{15}N]$-**2** was synthesized according to the above procedure using $Rh_2(esp)_2$ (19.0 mg, 0.0251 mmol, 1.00 equiv.), dry CH_2Cl_2 (2.5 mL), stearic acid (0.289 g, 1.02 mmol, 40.0 equiv.), and $[^{15}N]$-NaN_3 (34.0 mg, 0.511 mmol, 20.00 equiv.). and following the same recrystallization procedure dark green crystals of compound $[^{15}N]$-**2** were obtained (13.2 mg, 62.4%)^{1}H NMR (δ, 23 °C, CD_2Cl_2) 7.05 (t, *J* = 7.5 Hz, 2H), 6.91–6.76 (m, 6H), 4.80 (d, *J* = 69.0 Hz, 2H), 2.61 (s, 8H), 0.97(s, 24H). (see Figure S6) $^{15}N\{^1H\}$ NMR (δ, 23 °C, CD_2Cl_2) 209.2 and 55.3. ^{15}N NMR (δ, 23 °C, CD_2Cl_2) 209.2(s), 55.3(d, *J* = 69.7 Hz). IR (ATR, cm^{-1}): 3195 (w), 2970 (m), 2956 (m), 2923 (m), 2916 (m), 2943 (m), 2143 (s), 2119(s) 1570 (s), 1475 (s), 1407 (s), 1377 (m), 1361 (m), 1263 (m), 1242 (m), 1199 (w), 1161 (s), 1132 (w), 925 (m), 902 (m), 883 (m), 823 (m), 777 (m), 746 (m), 729 (s) , 705 (s), 632 (s).

[a] HN_3 dissociation is observed in the mass spectrometer.

Synthesis of $Rh_2(esp)_2(DN_3)_2$ ([^{2}H]-2). [^{2}H]-**2** was synthesized according to the above procedure using $Rh_2(esp)_2$ (50.0 mg, 0.066 mmol, 1.00 equiv.), dry CH_2Cl_2 (6.0 mL), [D_1]-stearic acid (0.750 g, 2.63 mmol, 40.0 equiv.), and NaN_3 (85.0 mg, 1.40 mmol, 20.00 equiv.). Following the same recrystallization procedure, dark green crystals of compound [^{2}H]-**2** were obtained (35.5mg, 64.1%). IR (ATR, cm^{-1}): 3195 (w), 2970 (m), 2956 (m), 2923 (m), 2916 (m), 2943 (m) 2388 (m), 2143 (s), 2119(s) 1570 (s), 1475 (s), 1407 (s), 1377 (m), 1361 (m), 1263 (m), 1242 (m), 1199 (w), 1161 (s), 1132 (w), 925 (m), 902 (m), 883 (m), 823 (m), 777 (m), 746 (m), 729 (s) , 705 (s), 632 (s).

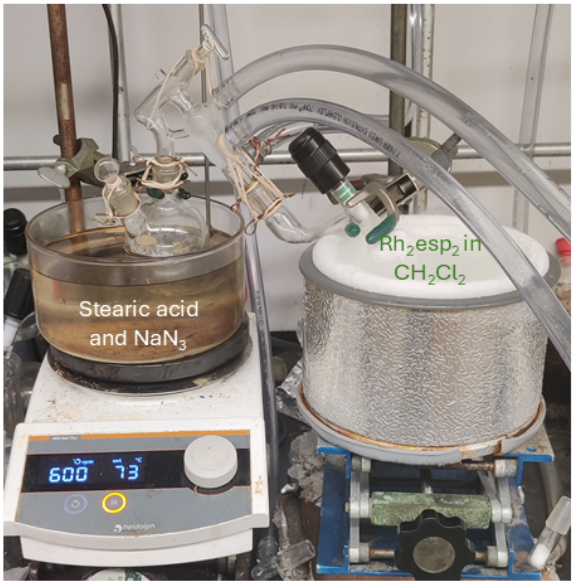

Figure S2. Set up for preparation $Rh_2(esp)_2(HN_3)_2$ (**2**).

General Synthesis of $Rh_2(esp)_2(ArN_3)_2$ (3)

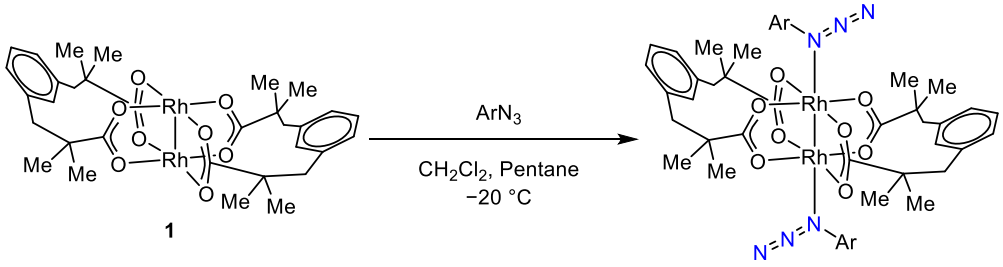

A 20-mL vial was charged with complex **1** (20.0 mg, 0.026 mmol, 1.00 equiv.), aryl azide (excess, ~10 equiv.), and CH_2Cl_2 or $CHCl_3$ (3.00 mL) inside a N_2-filled glovebox and the reaction mixture was stirred at 23° C for 1 h. The reaction mixture was layered with pentane and cooled to −20 °C at which temperature the mixture was maintained for 2 d to afford dark-green crystals.

Synthesis $Rh_2(esp)_2(PhN_3)_2$ (3a)

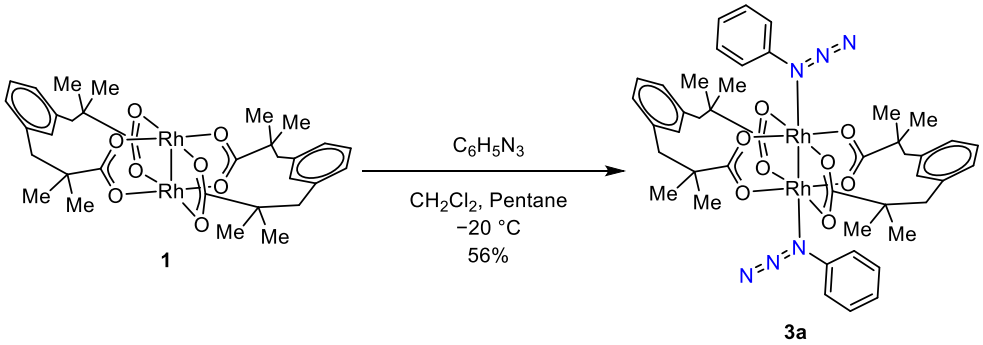

Following the general procedure, dark green crystals were obtained, the supernatant was decanted, and the crystals were washed with pentane and dried *in vacuo* at 23 °C to afford the title compound (**3a**, 18.4 mg, 56% yield). ^{1}H NMR (δ, 23 °C, CD_2Cl_2): 7.30 (t, J = 8.0 Hz, 4H), 7.11–7.04 (m, 6H), 6.99 (t, J = 7.5 Hz, 2H), 6.82 – 6.74 (m, 6H), 2.54 (s, 8H), 0.91 (s, 24H). ^{13}C NMR (δ, 23 °C, CD_2Cl_2): 196.8, 140.1, 138.1, 131.0, 129.9, 128.0, 126.9, 125.1, 119.3, 47.7, 46.4, 25.5, 13.9. IR (ATR): 2922(m), 2135(s), 2102(m), 1575(s), 1471(s), 1406(s), 1373(m), 1276(s), 1240(s), 1132(m), 827(m), 746(s). UV-vis (CH_2Cl_2, 298 K), λ_{max} (nm, ε ($M^{-1}cm^{-1}$)): 420 (356), 661 (570).

Synthesis $Rh_2(esp)_2(4\text{-}Me\text{-}C_6H_4N_3)_2$ (3b)

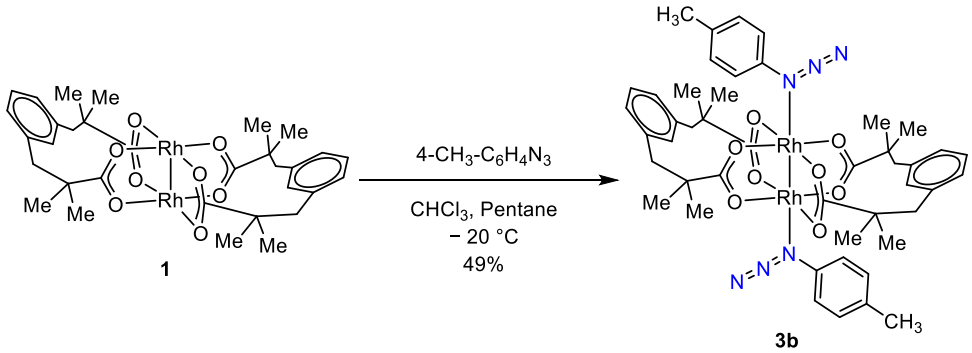

Following the general procedure, dark green crystals were obtained, the supernatant was decanted, and the crystals were washed with pentane and dried *in vacuo* at 23 °C to afford the title compound (**3b**, 16.3 mg, 49% yield). ^{1}H NMR (δ, 23 °C, CD_2Cl_2): 7.19 (d, *J* = 8.1 Hz, 4H), 7.09–7.05 (m, 6H), 6.88–6.84 (m, 6H), 2.61 (s, 8H), 2.34 (s, 6H), 0.96 (s, 24H) ^{13}C NMR (δ, 23 °C, CD_2Cl_2): 196.6, 138.0, 137.0, 135.0, 130.9, 130.2, 127.9, 126.7, 118.9, 46.9, 46.2, 25.4, 20.5 IR (ATR): 2721(m), 2160(s), 2140(m), 1905(m), 1379(s), 1309(s), 1272(s), 1203(s), 1172(s), 1064(s), 1037(s), 927(s). UV-vis (CH_2Cl_2, 298K), λ_{max} (nm, ε ($M^{-1}cm^{-1}$)): 416 (279), 663 (373).

Synthesis $Rh_2(esp)_2(4\text{-}CF_3\text{-}C_6H_4N_3)_2$ (3c)

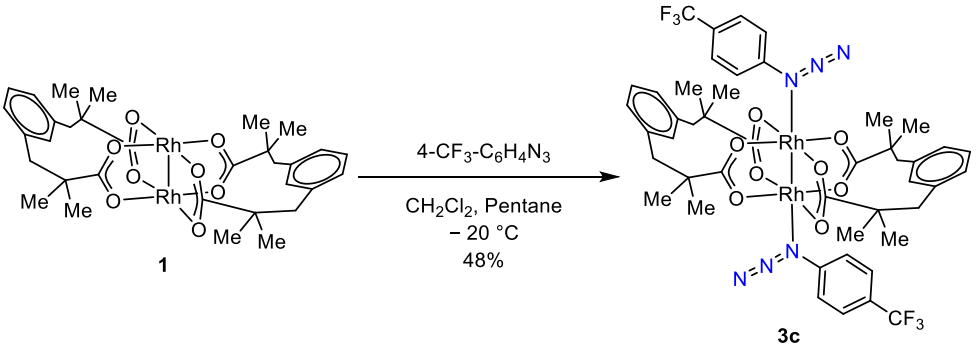

Following the general procedure dark green crystals were obtained, the supernatant was decanted, and the crystals were washed with pentane and dried *in vacuo* at 23 °C to afford the title compound (**3c**, 16.8 mg, 48% yield). ^{1}H NMR (δ, 23 °C, CD_2Cl_2): 7.65 (d, *J* = 8.5 Hz, 3H)[b], 7.27 (d, *J* = 8.25 Hz, 3H), 7.08 (t, *J* = 7.5 Hz, 2H), 6.86 (m, 6H), 2.61 (s, 8H), 0.98 (s, 24H).^{13}C NMR (δ, 23 °C, CD_2Cl_2): 197.1, 139.4, 131.1, 128.3, 127.1, 119.8, 47.3, 46.7, 29.9, 25.7. ^{19}F NMR (δ, 23 °C, CD_2Cl_2): -62.5 (s) IR (ATR): 2723(m), 2162(m), 2138(m), 1930(m), 1367(s), 1271(m), 1203(s), 1174(m), 1159(m), 1130(s), 1062(s), 1037(s), 958(s), 912(s), 864(s). UV-vis (CH_2Cl_2,), λ_{max} (nm, ε ($M^{-1}cm^{-1}$)): 415 (316), 663 (415, 298 K).

[b] During solvent removal *in vacuo*, partial loss of azide for compound **3c** was evident by ^{1}H NMR.

Supporting Data

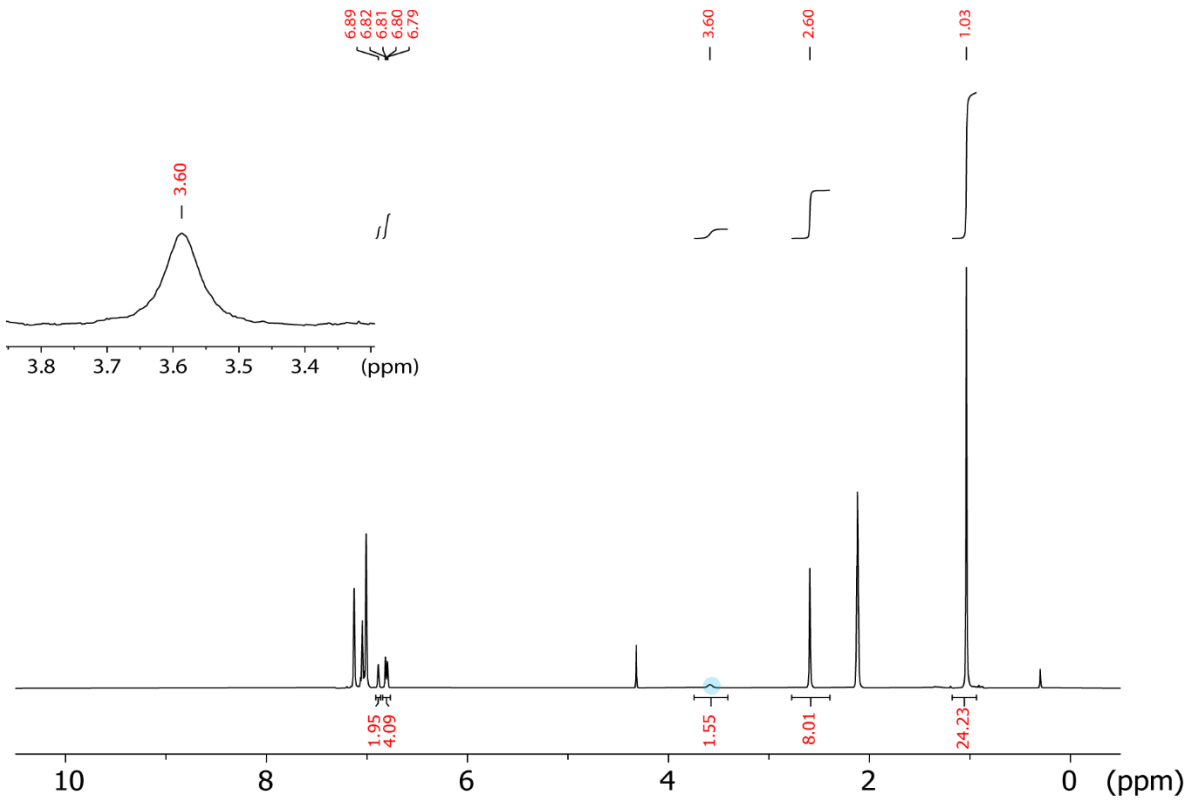

Figure S3. ^{1}H NMR spectrum of **2** recorded in d_8-toluene with an instrument operating at 500 MHz at 23 °C. Inset: Expansion of the spectral window between 3.4 to 3.8 ppm to highlight the resonance attributed to the N–H of coordinated HN_3 in toluene.

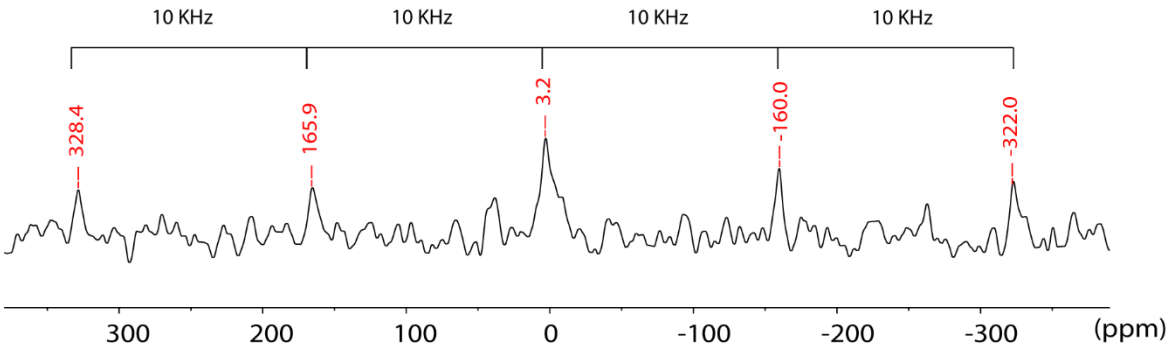

Figure S4. Solid-state ^{2}H NMR spectrum of compound [^{2}H]-**2** recorded in KBr powder with a solid-state NMR spectrometer (400 MHz for ^{1}H nuclei) equipped with a standard three-channel 4-mm MAS probe head at a spinning rate of 10 kHz. Benzene-d_6 was used as the external reference.

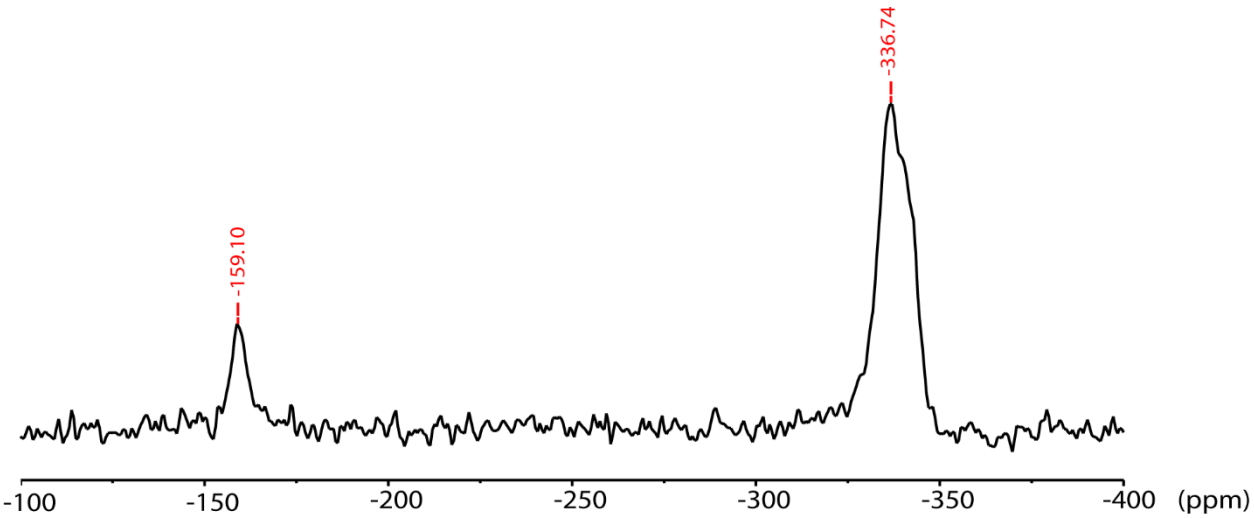

Figure S5. Solid state ^{15}N NMR spectrum of compound [^{15}N]-**2** recorded in KBr powder with a solid-state NMR spectrometer (400 MHz for ^{1}H nuclei) equipped with a standard three-channel 4-mm MAS probe head. The external references in the ^{15}N MAS NMR spectra were CH_3NO_2.

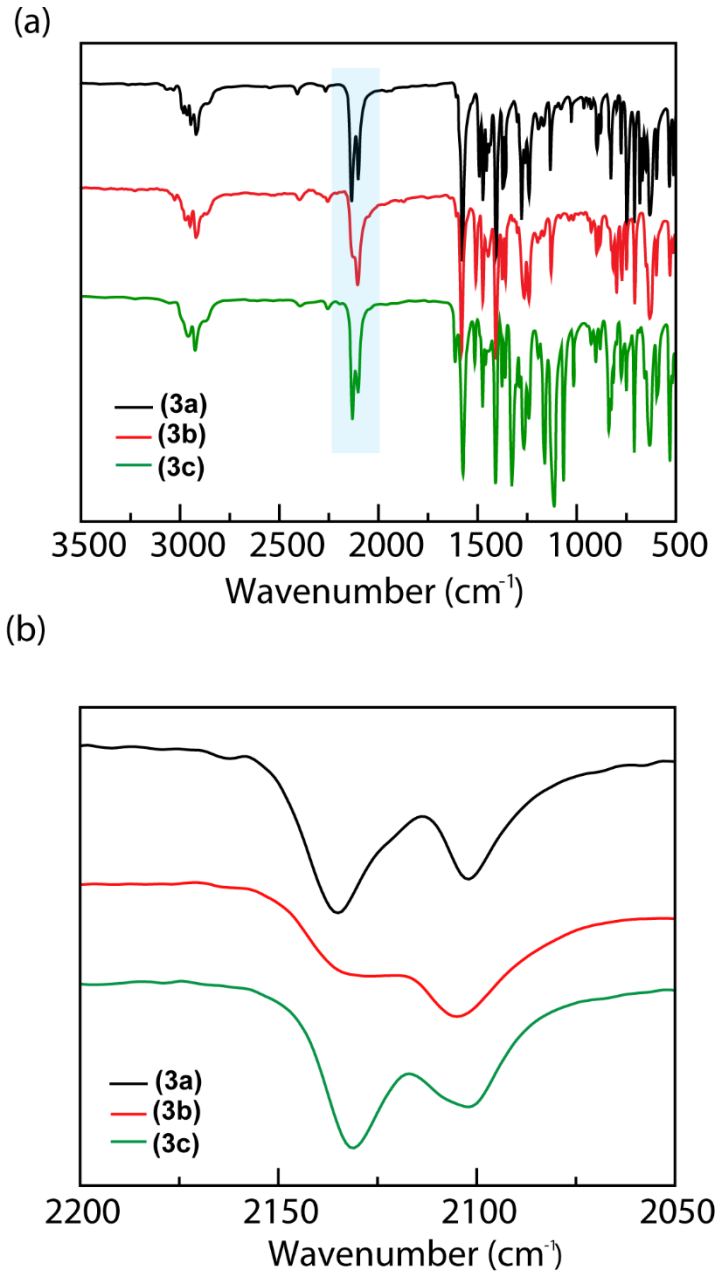

Figure S6. Solid-state IR spectra of **3a** (black trace), **3b** (red trace), and **3c** (green trace) plotted from 3500 cm^{-1} to 500 cm^{-1}. The blue shaded area compares azide stretches for compounds **3a**, **3b**, and **3c**.

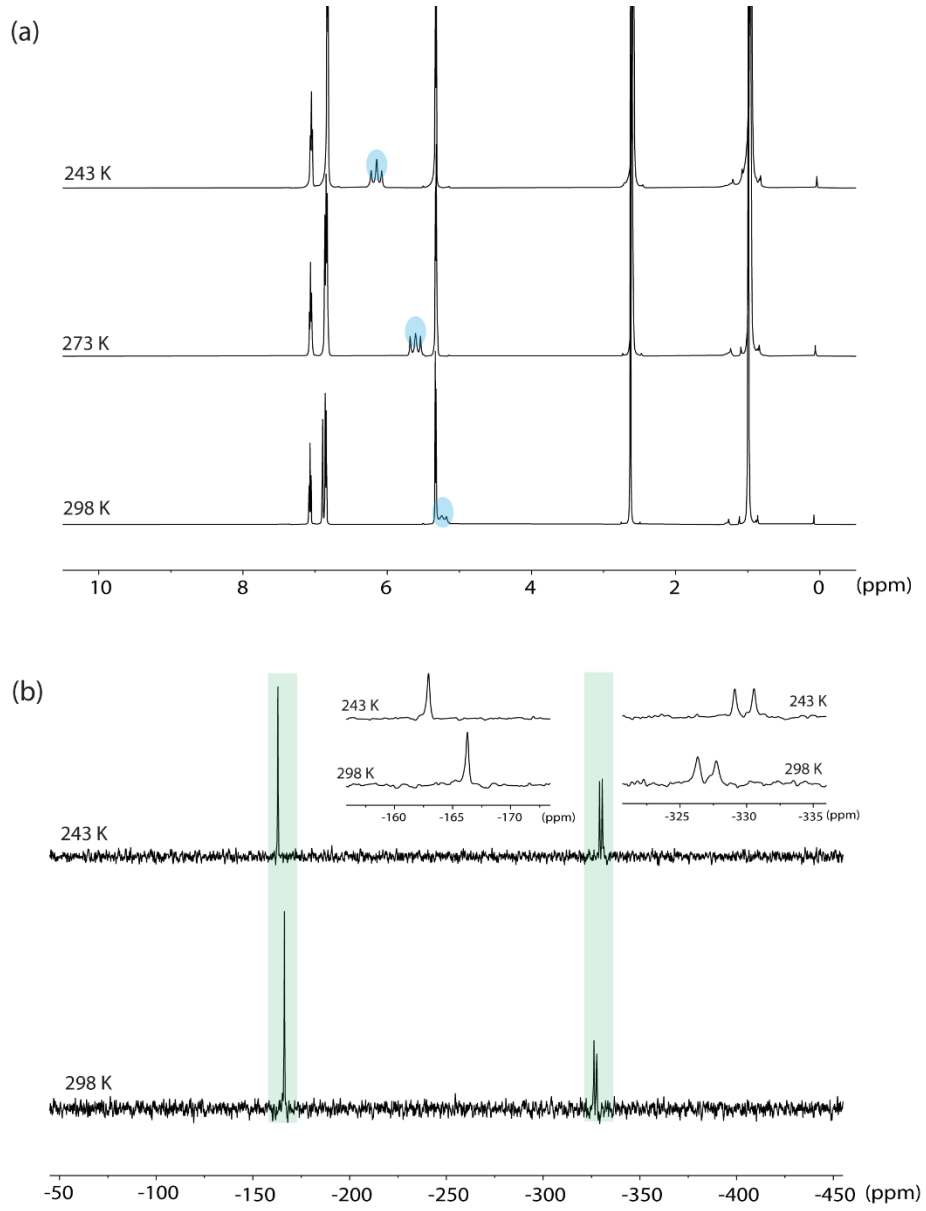

Figure S7. VT-NMR Spectroscopy of [^{15}N]-2. (a) Temperature-dependent ^{1}H NMR spectra of [^{15}N]-**2** recorded in CD_2Cl_2 with an instrument operating at 500 MHz recorded at 298 K, 273 K, and 243 K. The shaded blue bubbles highlight the downfield shift of the N–H peak and the peak sharpening with lowering of the temperature. (b) Temperature-dependent ^{15}N NMR spectra of [^{15}N]-**2** recorded in CD_2Cl_2 with an instrument operating at 50.7 MHz recorded at 298 K and 243 K. The shaded (green) area highlights the chemical shift of the ^{15}N peaks with lowering temperature.

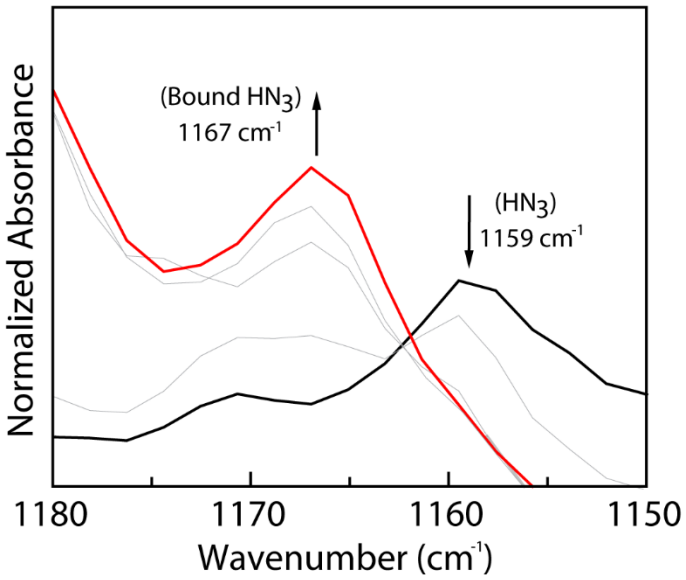

Figure S8. Solution phase IR of compound **2** depicting the temperature dependence of the symmetric azide stretch in the temperature range from 273 K (black) to 233 K (red).

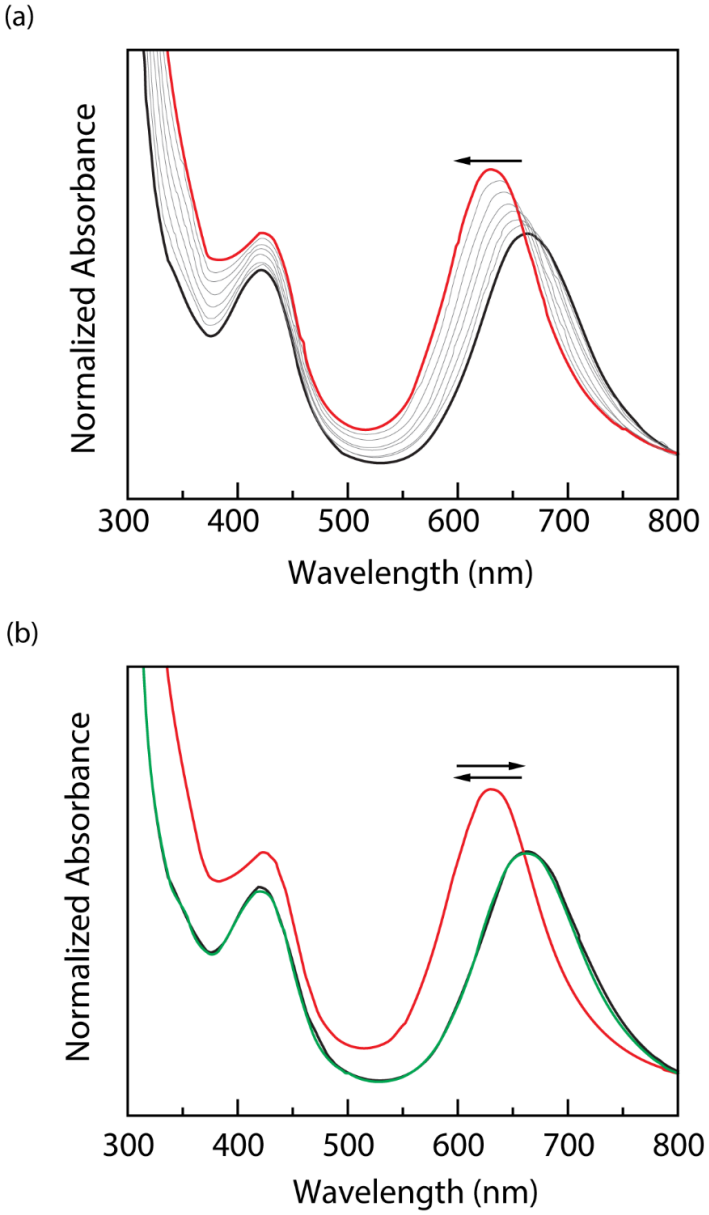

Figure S9. VT-UV-vis Spectroscopy for Compound 2. Temperature-dependent UV-vis spectra of a CH_2Cl_2 solution of $Rh_2(esp)_2(HN_3)_2$ (**2**). (a) Spectra of complex **2** with decreasing temperature from 298 K (black) to 223 K (red). (b) Spectra of compound **2** at 298 K (black), 223 K (red), and warming back to 298 K (green) showing the reversible temperature dependence. For comparison, VT-UV-vis of compound **1** performed under the same conditions showed 20 nm blue shift (665 nm to 645 nm) with decreasing temperature (Figure S44).

Determination of K_{eq} for HN_3 Complexation to $Rh_2(esp)_2$ (1)

A 4-mL scintillation vial was charged with **1** (15.2 mg, 0.0315 mmol) and CD_2Cl_2 (2.0 mL) to make a 15.8 mM stock solution. A modified NMR tube with a cap having rubber septa was charged with CD_2Cl_2 (0.50 mL) and HN_3 (0.0355 mmol, 1.00 equiv.). In this NMR titration, compound **1** was used as a titrant because addition of compound **1** is safer than adding the solution of HN_3.

The initial concentration of HN_3 was determined versus the concentration of residual solvent ($CDHCl_2$) in a ^1H NMR spectrum measured at 243 K; the concentration of residual proteo solvent was independently determined versus a 1,3,5-trimethoxybenzene (TMB) standard in CD_2Cl_2. To the solution of HN_3 in CD_2Cl_2, the stock solution of **1** was added portionwise (each portion: 20.0 μL, 0.316 μmol, 0.00890 equiv.). ^1H NMR spectra were recorded at 243 K after each increment added. After 20 incremental additions of compound **1** (Figure S10a, from lines b to u) the final ratio of 0.18 equivalents of **1** relative to HN_3 was reached. No further additions of compound **1** were possible, as crystals of complex **2** began to form—likely due to the solution being maintained at 243 K for an extended period (~5 hours) during the titration. The data obtained are compiled in Figure S10a.

During this titration, water was introduced due to ambient moisture and the repetitive injections made during the experiment (Figure S10a). To investigate potential water binding to **2**, we performed a UV-vis titration of complex **2** with an excess amount of water (~100 equiv.) at 243 K and observed no change in the UV-vis spectrum (Figure S10b). This experiment suggests that water does not compete with HN_3 to bind to Rh_2(II,II) at low temperature.

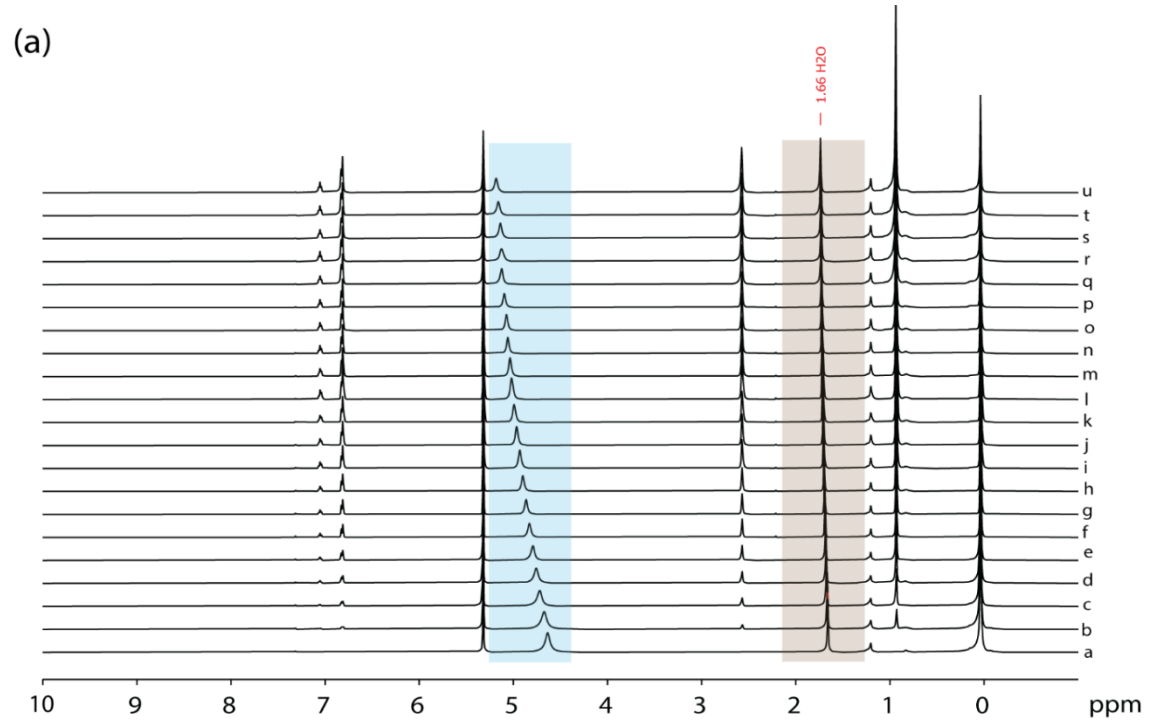

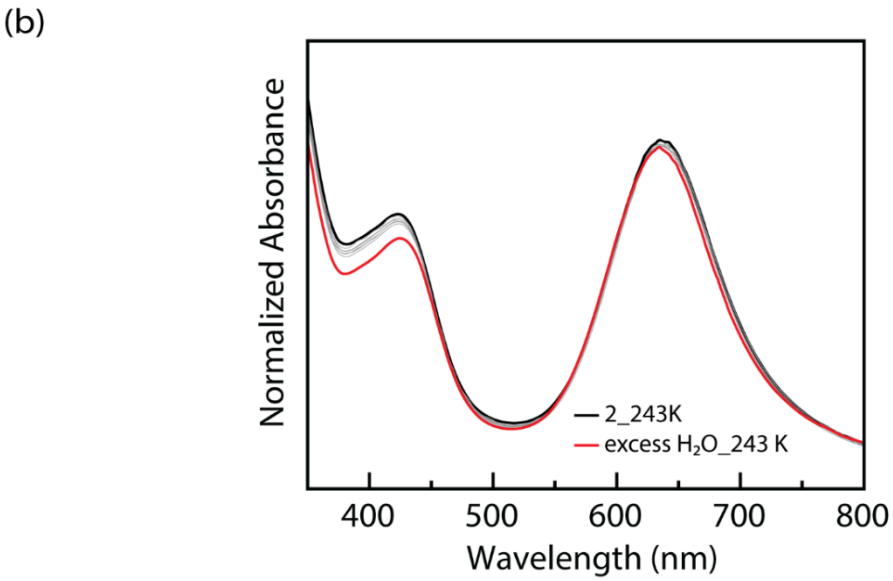

Figure S10. (a) ^{1}H NMR spectra obtained during titration of HN_3 with **1** at 243 K in CD_2Cl_2. Complex **1** added as a stock solution: (a) spectrum of HN_3, (b–u) 20–400 µL stock solution of **1** added. The blue shaded region highlights the chemical shift of HN_3 as a function of [**1**]. These data enabled determination of K_{eq} and ΔG of HN_3 binding to **1** (see below). The grey shaded area indicated the presence of water introduced via ambient moisture**.** (b) UV-vis spectra recorded during the titration of **2** (black) with excess water (red, after adding water) at 243 K. The lack of spectral change suggests water does not effectively compete with HN_3 at low temperature.

The equation for the equilibrium constant for adduct formation between HN_3 to $Rh_2(esp)_2$ (**1**) was derived using the Rose-Drago method.[9] For convenience, $Rh_2(esp)_2$ (**1**) is abbreviated as M, HN_3 is abbreviated as L, and $Rh_2(esp)_2(HN_3)_2$ (**2**) is abbreviated as ML_2. The following equations are then defined:

$$M + 2\,L \underset{}{\overset{K_{eq}}{\rightleftharpoons}} ML_2$$

$$K_{eq} = \frac{[ML_2]}{[M][L]^2} \quad \text{(S1)}$$

$$[M^0] = [M] + [ML_2] \quad \text{(S2)}$$

$$[L^0] = [L] + 2[ML_2] \quad \text{(S3)}$$

Where:
K_{eq} is the equilibrium constant
$[ML_2]$ is the concentration of $Rh_2(esp)_2(HN_3)_2$ (**2**) at equilibrium
[M] is the concentration of **1** at equilibrium
[L] is the concentration of HN_3 at equilibrium
$[M^0]$ is the initial concentration of **1**
$[L^0]$ is the initial concentration of HN_3

The average ^1H chemical shift of HN_3 is a weighted average between the chemical shift of free HN_3 and complexed HN_3 at equilibrium (Eqn S4), and we also define some parameters:

$$\delta_{obs} = N_L\delta_L + N_{ML_2}\delta_{ML_2} \quad \text{(S4)}$$

$$\Delta\delta_{obs} = \delta_{obs} - \delta_L$$

$$\Delta\delta_{max} = \delta_{ML_2} - \delta_L$$

Where:
δ_{obs} is the observed ^1H chemical shift of HN_3 in the presence of **1**
N_L is the mol fraction of free HN_3
δ_L is the ^1H chemical shift of free HN_3
N_{ML2} is the mol fraction of complexed HN_3
δ_{ML2} is the ^1H chemical shift of complexed HN_3
$\Delta\delta_{obs}$ is the difference between observed ^1H chemical shift of HN_3 in the presence of **1** and ^1H chemical shift of free HN_3
$\Delta\delta_{max}$ is the difference between ^1H chemical shift of complexed HN_3 and ^1H chemical shift of free HN_3

Equation S4 can be rewritten as:

$$\delta_{obs} = \frac{[L]}{[L^0]}\delta_L + \frac{2[ML_2]}{[L^0]}\delta_{ML_2}$$

$$\delta_{obs} - \delta_L = \frac{[L]}{[L^0]}\delta_L - \delta_L + \frac{2[ML_2]}{[L^0]}\delta_{ML_2}$$

$$\Delta\delta_{obs} = (-\frac{[L^0]-[L]}{[L^0]})\delta_L + \frac{2[ML_2]}{[L^0]}\delta_{ML_2}$$

$$\Delta\delta_{obs} = -\frac{2[ML_2]}{[L^0]}\delta_L + \frac{2[ML_2]}{[L^0]}\delta_{ML_2}$$

$$\Delta\delta_{obs} = \frac{2[ML_2]}{[L^0]}\left(\delta_{ML_2} - \delta_L\right)$$

$$\Delta\delta_{obs} = \frac{2[ML_2]\Delta\delta_{max}}{[L^0]}$$

$$[ML_2] = \frac{\Delta\delta_{obs}[L^0]}{2\Delta\delta_{max}} \quad \text{(S5)}$$

Substituting Equation S2 and Equation S3 into Equation S1, then substituting in Equation S5:

$$K_{eq} = \frac{[ML_2]}{([M^0]-[ML_2])([L^0]-2[ML_2])^2}$$

$$K_{eq} = \frac{\frac{\Delta\delta_{obs}[L^0]}{2\Delta\delta_{max}}}{\left([M^0]-\frac{\Delta\delta_{obs}[L^0]}{2\Delta\delta_{max}}\right)\left([L^0]-2\frac{\Delta\delta_{obs}[L^0]}{2\Delta\delta_{max}}\right)^2}$$

$$K_{eq} = \frac{\Delta\delta_{obs}[L^0]}{(2\Delta\delta_{max}[M^0]-\Delta\delta_{obs}[L^0])\left([L^0]\frac{\Delta\delta_{max}-\Delta\delta_{obs}}{\Delta\delta_{max}}\right)^2}$$

$$K_{eq} = \frac{\Delta\delta_{obs}\Delta\delta_{max}^2}{(2\Delta\delta_{max}[M^0]-\Delta\delta_{obs}[L^0])[L^0](\Delta\delta_{max}-\Delta\delta_{obs})^2} \quad \text{(S6)}$$

$\Delta\delta_{max}$ was determined by plugging in values for two measurements in Figure S10a into Equation S6, setting them equal, and then solving for $\Delta\delta_{max}$. This was repeated for multiple pairs of measurements to ensure the consistency of the value. $\Delta\delta_{max}$ was determined to be 2.87 ± 0.25 ppm. K_{eq} was then calculated individually for each titration point of **1**. It was found that at 243 K, K_{eq} = 1100 ± 100 M^{-2} and that ΔG = –3.37 ± 0.06 kcal/mol for HN_3 binding.

Thermodynamics for HN_3 Complexation to $Rh_2(esp)_2$ (1)

To determine ΔH^0 and ΔS^0 for coordination of HN_3 to $Rh_2(esp)_2$ (**1**), an NMR tube was charged with CD_2Cl_2 (0.50 mL) and crystals of $Rh_2(esp)_2(HN_3)_2$ (**2**). ^1H NMR spectra were then recorded at temperatures ranging from 203 K to 298 K. The resulting data are collected in Figure 5a.

The starting amount of $Rh_2(esp)_2(HN_3)_2$ (**2**) was determined by evaluating Equation S6 with the K_{eq}, $\Delta\delta_{obs}$, and $\Delta\delta_{max}$ determined at 243 K to calculate total [HN_3] concentration; the initial [**2**] is half total [HN_3]. The equilibrium constant K_{eq} at each temperature was determined using equation S6 with $\Delta\delta_{max}$ = 2.87 ppm (Table S1). The Van 't Hoff plot of ln(K_{eq}) plotted versus 1/T afforded a linear fit with slope of $-\Delta H^0/R$ = 2790 ± 70 K with an intercept of $\Delta S^0/R$ = −4.5 ± 0.3 with R^2 = 0.9951 (Figure S11). These were converted to ΔH^0 = −5.5 ± 0.1 kcal/mol and ΔS^0 = −9.0 ± 0.6 cal/K·mol. The data for T = 203 K and T = 273 K were not used in the calculations since the ^1H resonances of HN_3 overlap with those of complex **1** and $CDHCl_2$, respectively (Figure 5a).

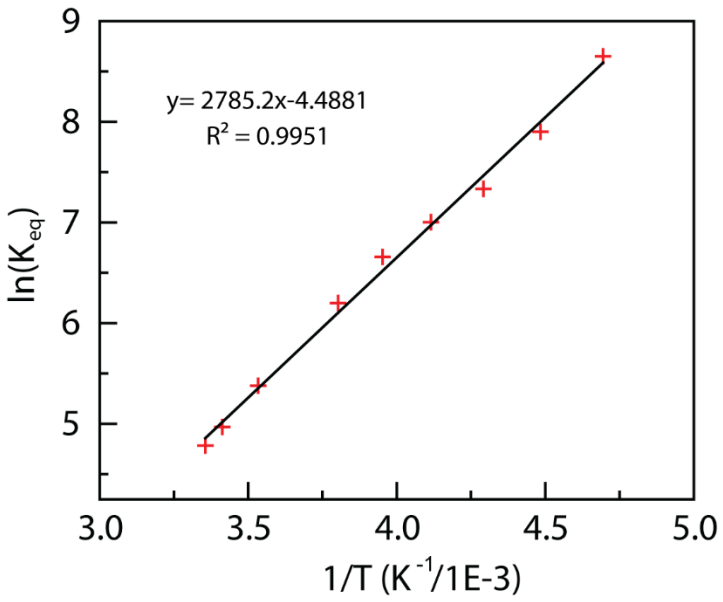

Figure S11. Plot of ln(K_{eq}) versus 1/T for complexation of HN_3 to **1**.

Table S1. Temperature dependence of K_{eq} for HN_3 binding to complex **1**

Entry	Temperature (K)	K_{eq} (M^{-2})
1	298	1.20×10^2
2	293	1.44×10^2
3	283	2.17×10^2
4*	273	3.02×10^2
5	263	4.93×10^2
6	253	7.79×10^2
7	243	1.1×10^3
8	233	1.53×10^3
9	223	2.69×10^3
10	213	5.72×10^3
11*	203	1.02×10^4

(*) K_{eq} for entry 4 and entry 11 are obtained from the equation in Figure S11

Determination of K_{eq} for PhN_3 Complexation to $Rh_2(esp)_2$ (1)

A 4-mL scintillation vial was charged with **1** (3.7 mg, 4.9 μmol) and CD_2Cl_2 (0.5 mL) to make a 9.8 mM stock solution. A modified NMR tube with a cap having rubber septum was charged with CD_2Cl_2 (0.50 mL) and PhN_3 (2.0 μL, 18 μmol, 1.00 equiv.).

To this NMR tube, the stock solution of **1** was added incrementally (each increment: 20.0 μL, 0.195 μmol, 0.00385 equiv.). ^1H NMR spectra were recorded at 243 K after each increment added. After 20 incremental additions of compound **1** (Figure S12a, from lines b to u) the final ratio of 0.134 equivalents of **1** relative to PhN_3 was reached. No further additions of compound **1** were possible, as crystals of complex $Rh_2(esp)_2(PhN_3)_2$ began to form—likely due to the solution being maintained at 243 K for an extended period (~6 hours) during the titration. The data obtained are compiled in Figure S12b and S12b.

During this titration, water was introduced due to ambient moisture (Figure S12a). To account for water binding to $Rh_2(esp)_2(PhN_3)_2$, we performed a UV-vis titration of complex $Rh_2(esp)_2(PhN_3)_2$ (**3a**) with an excess amount of water (~100 equiv.) at 243 K and observed no change in the UV-vis spectrum (Figure S12c). This experiment suggests that water does not compete with PhN_3 to bind to Rh_2(II,II) at low temperatures.

Similar to that for HN_3 binding, equation S6 was used to determine the equilibrium constant for adduct formation between PhN_3 and $Rh_2(esp)_2$ using the change in ^1H chemical shift of the ortho protons of PhN_3 during the titration of **1**. $\Delta\delta_{max}$ was determined by plugging in values for two measurements in Figure S12b into Equation S6, setting them equal, and then solving for $\Delta\delta_{max}$. This was repeated for multiple pairs of measurements to ensure the consistency of the value. $\Delta\delta_{max}$ was determined to be 0.48 ± 0.09 ppm. K_{eq} was then calculated individually for each titration point of **1**. It was found that at 243 K, K_{eq} = 11000 ± 3000 M^{-2} and that ΔG = –4.5 ± 0.2 kcal/mol for PhN_3 binding.

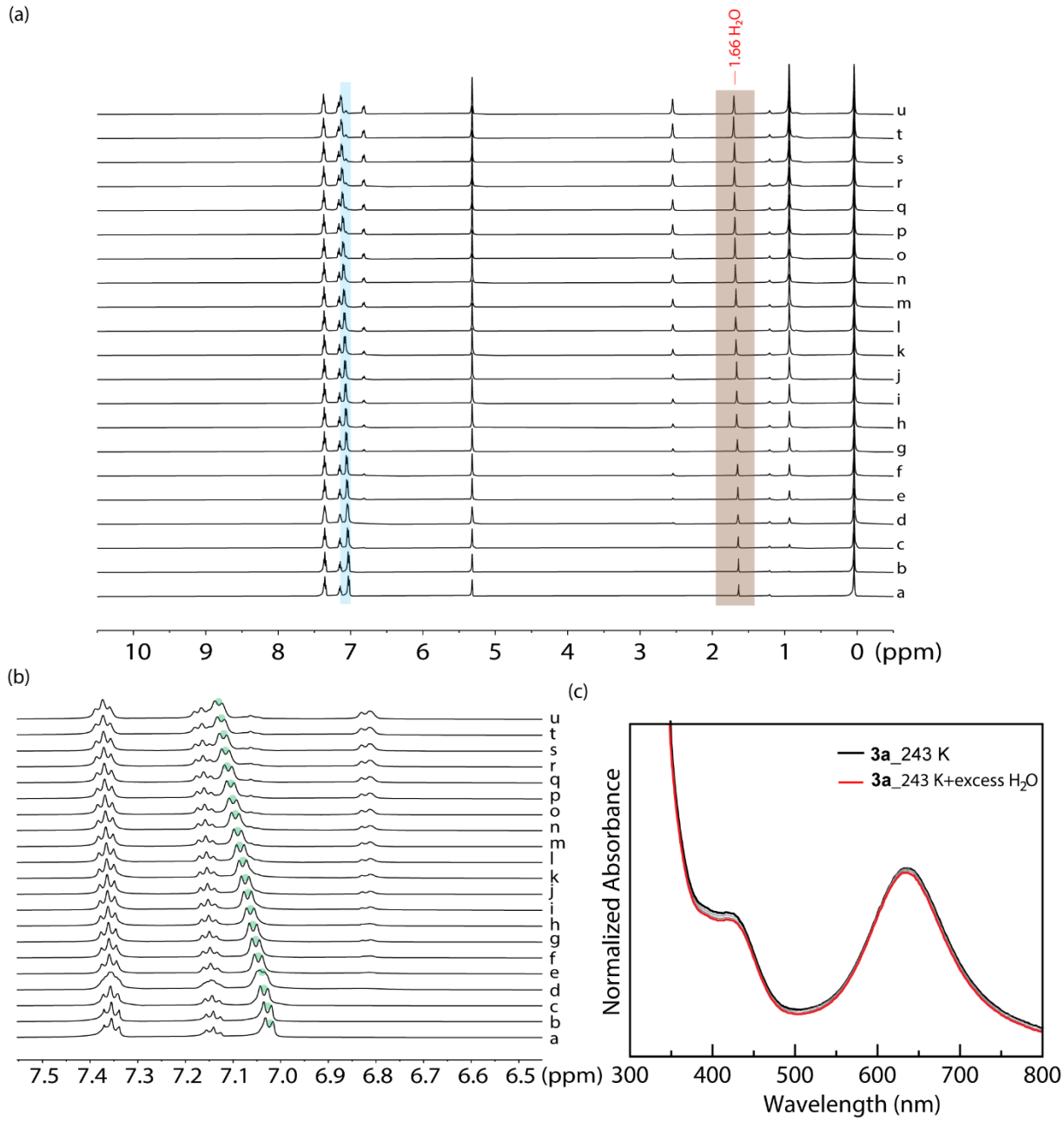

Figure S12. (a) ^{1}H NMR spectra of PhN_3 in the titration with **1** obtained at 243 K in CD_2Cl_2. Stock solution added: (a) 0 µL, (b–u) 20–400 µL at 20 µL increments. Monitoring the chemical shift as a function of [**1**] for the highlighted peak of the ortho protons of PhN_3 enabled the determination of K_{eq} and ΔG of PhN_3 complexation to **1** (see below). The grey shaded area indicated the presence of water introduced via ambient moisture**.** (b) Expansion of the spectral window from 6.5 ppm to 7.5 ppm depicting the downfield resonances of the ortho proton of PhN_3.(c) UV-vis spectra recorded during the titration of **3a** (black) with water (red, after adding water) at 243 K. The lack of spectral change suggests water does not effectively compete with HN_3 at low temperature.

Thermodynamics for PhN_3 Complexation to $Rh_2(esp)_2$ (1)

To determine the ΔH^0 and ΔS^0 for the complexation of HN_3 to $Rh_2(esp)_2$ (**1**) an NMR tube was charged with CD_2Cl_2 (0.50 mL) and crystals of $Rh_2(esp)_2(PhN_3)_2$. ^1H NMR spectra were then recorded at temperatures ranging from 203 K to 298 K. The resulting data are collected in Figure S8.

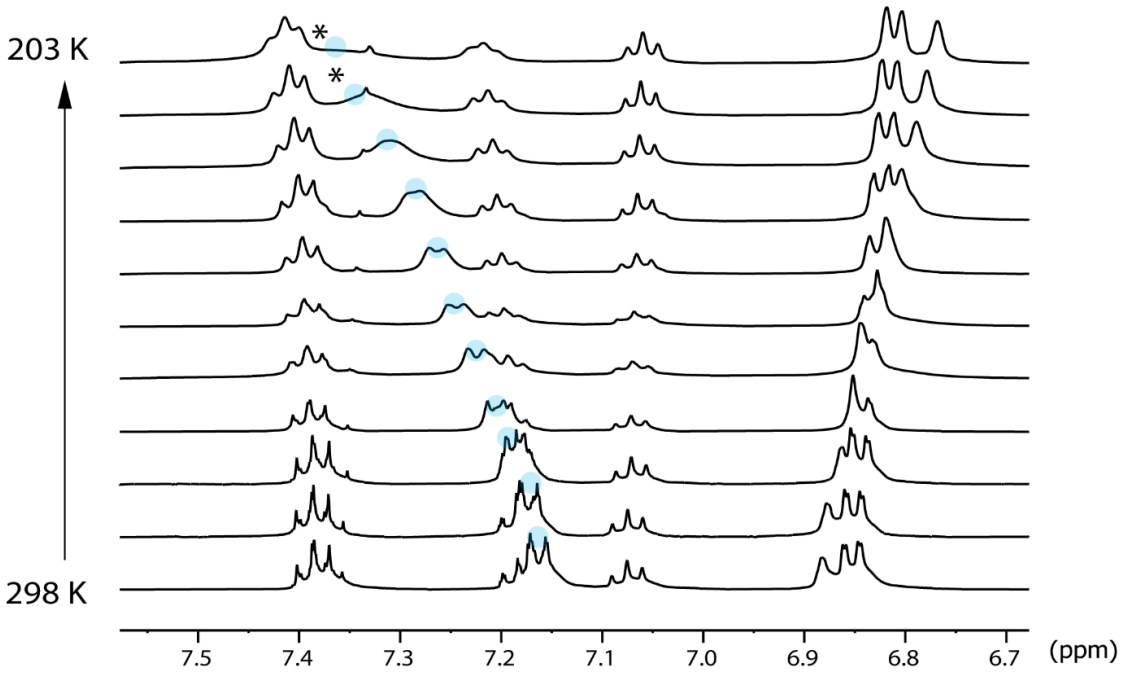

Figure S13. ^1H NMR spectra of $Rh_2(esp)_2(PhN_3)_2$ (**3a**) in CD_2Cl_2 at various temperatures. Monitoring the chemical shift as a function of temperature for the highlighted peak of the ortho protons of PhN_3 enabled determination of ΔH^0 and ΔS^0 of PhN_3 complexation to **1**.

To determine the concentration of $Rh_2(esp)_2$ and PhN_3, 1,3,5-trimethoxybenzene was added to the NMR tube and a ^1H NMR spectrum was taken at 298 K at the end of the experiment. The equilibrium constant K_{eq} at each temperature was determined using equation S6 with $\Delta\delta_{max}$ = 0.48 ppm (Table S2). The Van 't Hoff plot of $\ln K_{eq}$ plotted versus 1/T afforded a linear fit with slope of $-\Delta H^0/R$ = 2130 ± 30 K with an intercept of $\Delta S^0/R$ = 0.75 ± 0.12 with R^2 = 0.9986 (Figure S9). These were converted to ΔH^0 = −4.23 ± 0.06 kcal/mol and ΔS^0 = 1.5 ± 0.2 cal/K·mol. The data for T = 203 K and T = 213 K were not used in the calculations since the ^1H resonances of PhN_3 are too broad to be accurately discerned (Figure S8).

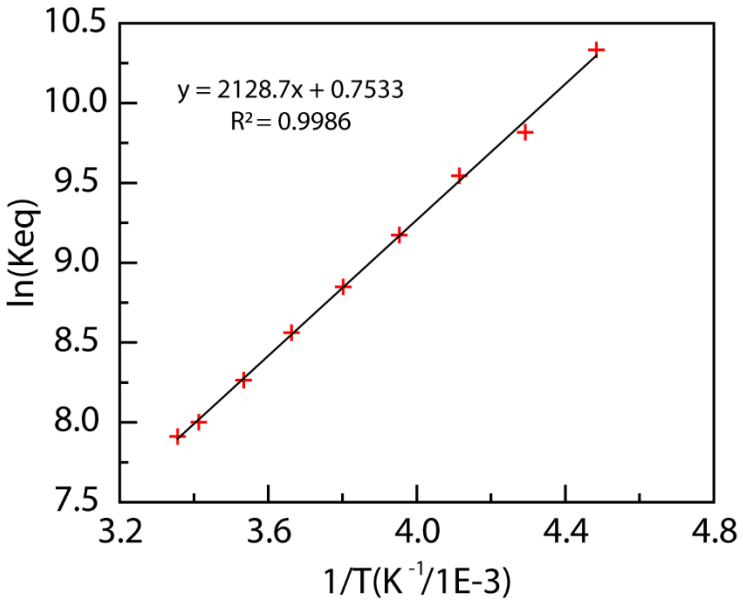

Figure S14. Plot of $\ln(K_{eq})$ versus 1/T for the thermodynamics of PhN_3 complexation to **1**.

Table S2. Temperature dependence of K_{eq} for PhN_3 binding to complex **1**.

Entry	Temperature (K)	K_{eq} (M^{-2})
1	298	2.72×10^3
2	293	2.98×10^3
3	283	3.88×10^3
4	273	5.23×10^3
5	263	6.96×10^3
6	253	9.63×10^3
7	243	1.39×10^4
8	233	1.83×10^4
9	223	3.07×10^4
10*	213	4.64×10^4
11*	203	7.60×10^4

(*) K_{eq} for entry 10 and entry 11 are obtained from the equation in Figure S14

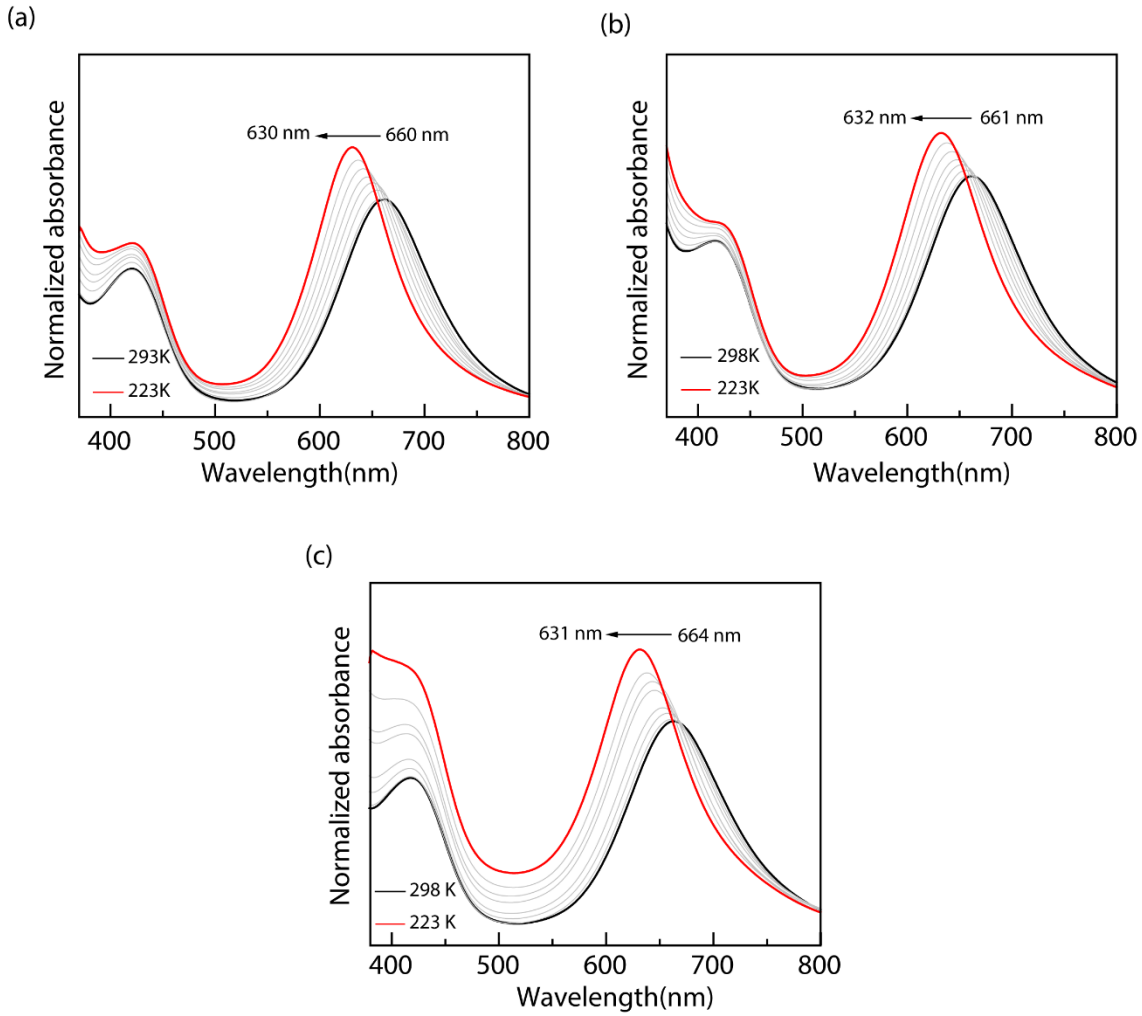

Figure 15. Temperature-dependent UV-vis spectra of a CH_2Cl_2 solution of $Rh_2(esp)_2(ArN_3)_2$ with decreasing temperature from 298 K (black) to 223 K (red) of (a) **3a**, (b) **3b**, and (c) **3c**.

Solution-Phase Photochemistry

Solution-Phase Photolysis of 2 in the Presence of 1-octene

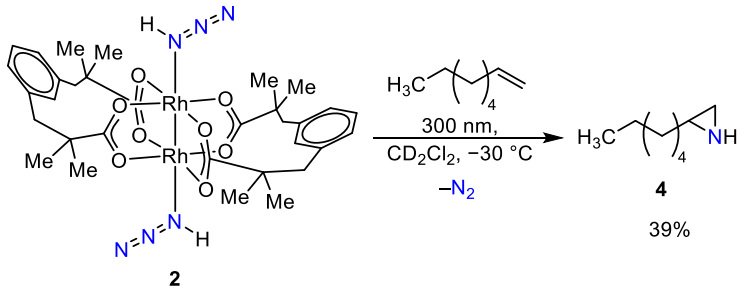

In an N_2-filled glovebox, a 4.0-mL scintillation vial was charged with the crystals of compound **2** (20.3 mg) in 2.5 mL of CD_2Cl_2 to prepare a stock solution. A J-Young NMR tube was charged with 0.50 mL of the stock solution of compound **2** and 0.01 mL (~2.5 equiv.) of 1-octene. Upon recording the ^{1}H NMR of the solution at t = 0 the solution was photolyzed for one hour in a 300 nm Rayonet photoreactor at –30 °C. The reaction temperature was maintained with a dry ice / *o*-xylene bath (–30 °C) in a finger dewar. Upon completion of the photolysis, the crude reaction mixture was analyzed via ^{1}H NMR and ESI-MS (Figure S16 and S17, respectively). The yield was calculated with an external standard of 1,3,5-trimethoxybenzene (TMB). Formation of **4** was indicated by diagnostic ^{1}NMR resonances at 2.0–1.96 ppm (m) and 1.65 ppm (d) and by HR-MS (128.1432 (expt); 128.1434 (calculated for $[C_8H_{18}N]^+$)). These data are consistent with previous reports of **4** measured in $CDCl_3$.[10]

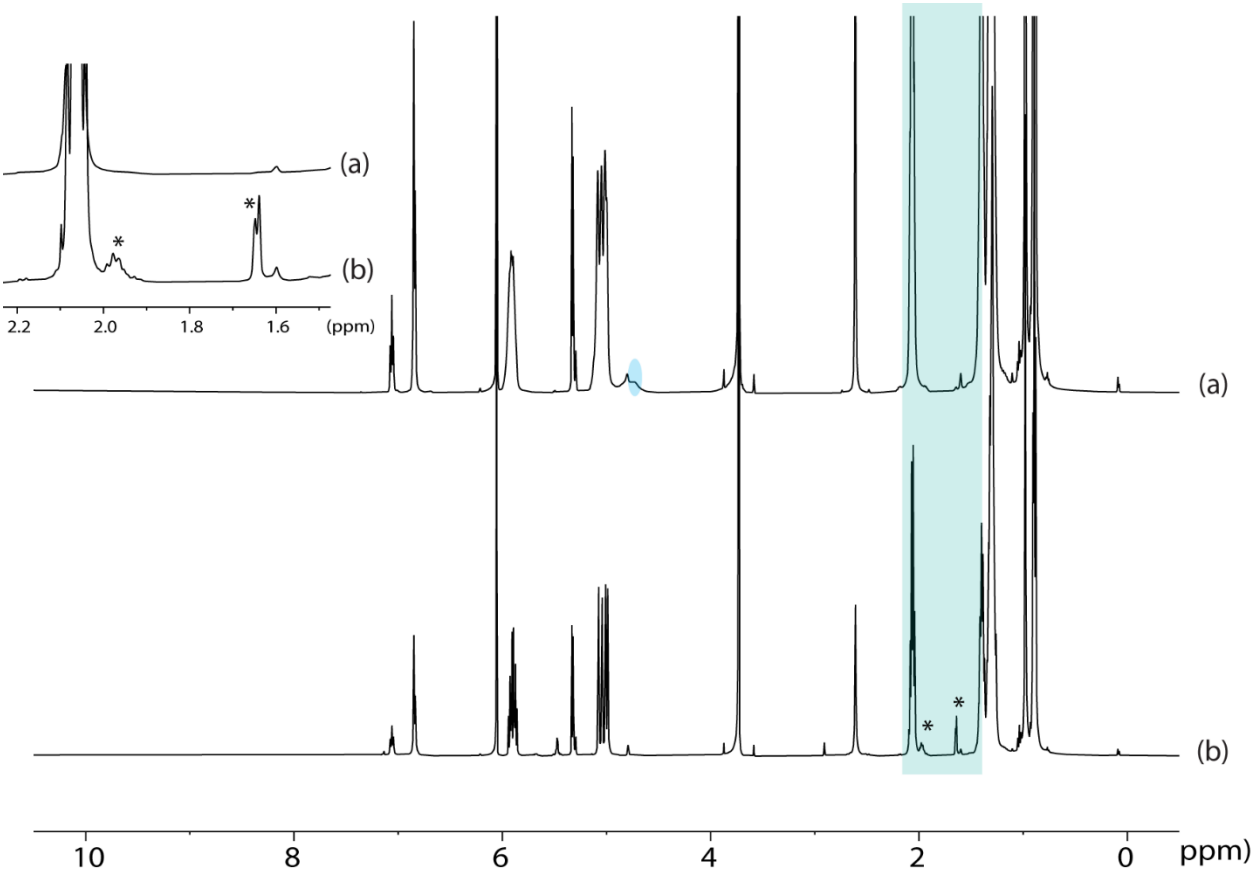

Figure S16. Photolysis (λ = 300 nm) of compound **2** at –30 °C in the presence of 1-octene in CD_2Cl_2 for 1 h results in the formation of compound **4**. (a) ^{1}H NMR spectrum of the crude mixture at t = 0; the N–H peak is highlighted in blue; (b) ^{1}H NMR spectrum of the crude mixture after 1 h photolysis; the green shaded area indicates the aziridination of 1-octene. Expansion of the green shaded area, * at 1.99–1.95 ppm (m, 1H) and 1.64 ppm (d, 1H) are diagnostic of **4**.

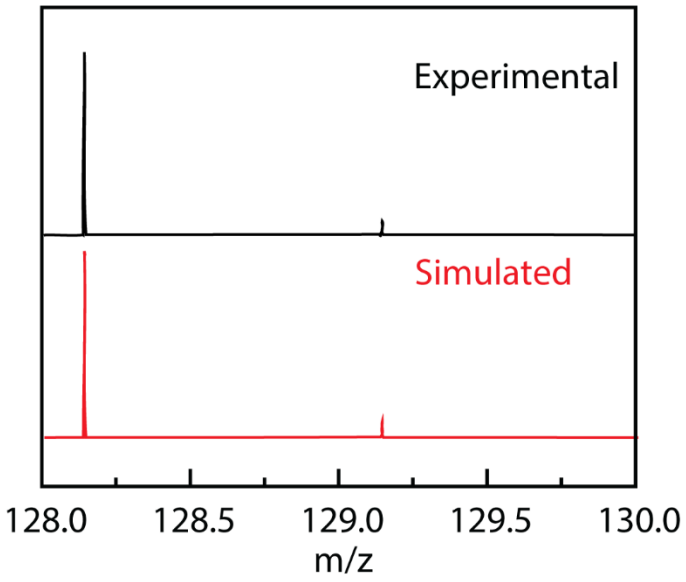

Figure S17. ESI-MS(+) of the crude photolysis mixture indicating the formation of **4** from 1-octene. Black: experimental; red: simulation. 128.1432 (expt); 128.1434 (calculated for $[C_8H_{18}N]^+$)

Solution-Phase Photolysis of [^{15}N]-2 in the presence of 1-octene

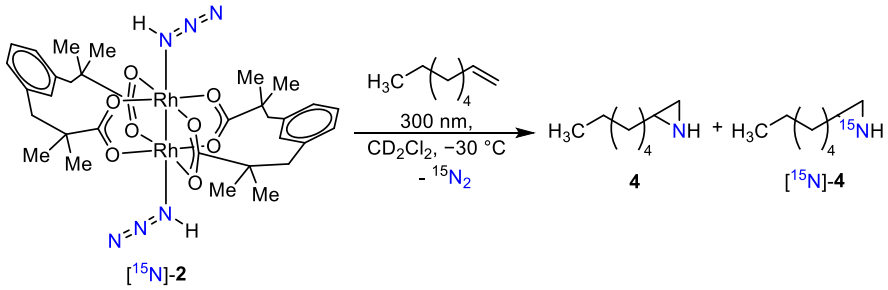

In an N_2-filled glovebox, a J-Young NMR tube was charged with crystals of compound [^{15}N]-**2** (~10 mg) and 0.50 mL CD_2Cl_2. A 4-mL scintillation vial was charged with 0.10 ml of 1-octene and 0.5. mL of CD_2Cl_2 to make a stock solution. An aliquot of 0.10 mL of the stock solution was added to reaction mixture in the J-Y tube. Upon recording the ^{1}H NMR of the solution at t = 0 the solution was photolyzed for an hour in a 300 nm Rayonet photoreactor at –30 °C. The reaction temperature was maintained with a dry ice / *o*-xylene bath (–30 °C) in a finger dewar. Upon completion of the photolysis, the crude reaction mixture was analyzed via ^{1}H NMR and ESI-MS (Figure S18 and S19, respectively). The yield was calculated with an external standard of 1,3,5-trimethoxybenzene (TMB). Formation of **4** was indicated by diagnostic ^{1}H NMR resonances at 1.99–1.95 ppm (m) and 1.64 ppm (d) and formation of both **4** and [^{15}N]-**4** by HR-MS (128.1434 (expt); 128.1434 (calculated for $[C_8H_{18}N]^+$) and 129.1404 (expt); 129.1403 (calculated for [^{15}N]-$[C_8H_{18}N]^+$)). These data are consistent with previous reports of **4** measured in $CDCl_3$.[10]

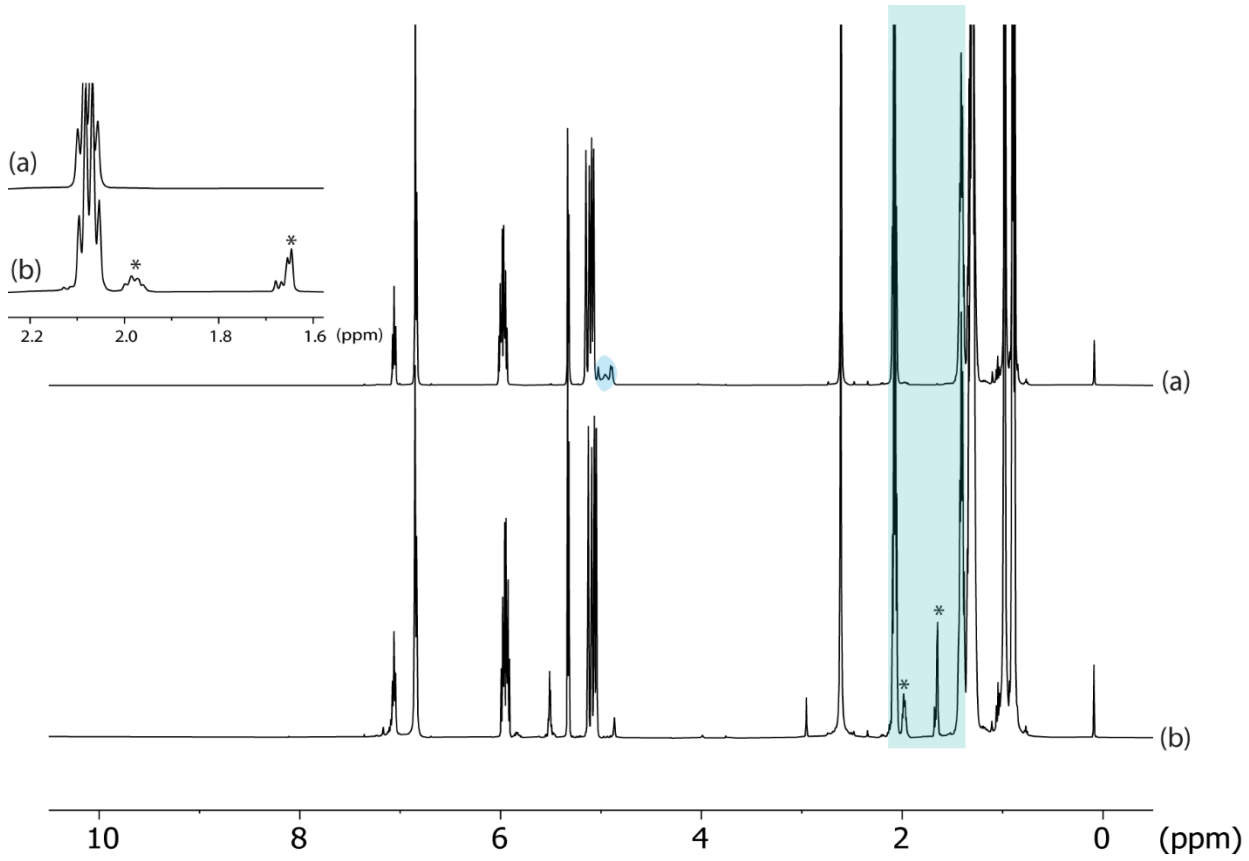

Figure S18. Photolysis (λ = 300 nm) of compound [^{15}N]-**2** at –30 °C with 1-octene in CD_2Cl_2 for 1 h results in the formation of compound **4** and [^{15}N]-**4**. (a) ^{1}H NMR of the crude mixture at t = 0, N–H peak highlighted in blue; (b) NMR of the crude mixture after 1 h photolysis, green shaded area indicates the aziridination of 1-octene. Expansion of the green shaded area, * at [1.99–1.95 ppm (m,1H) and 1.64 ppm (d, 1H)] indicates the formation of **4** and [^{15}N]-**4**.

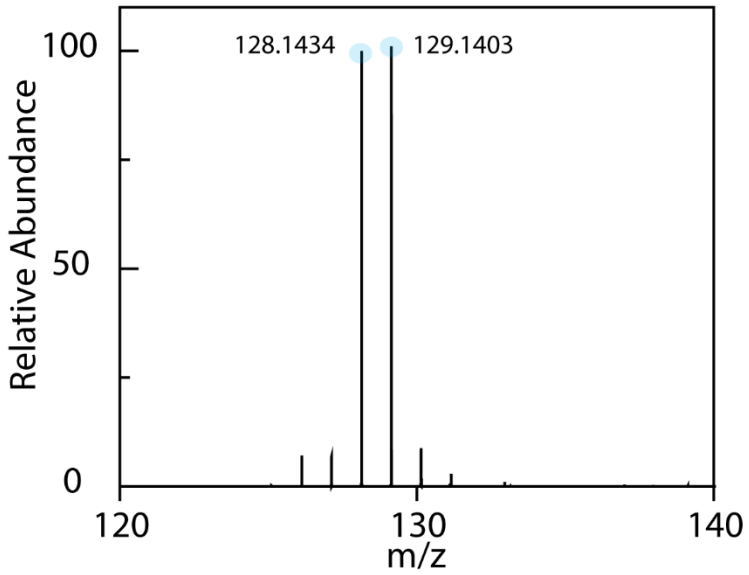

Figure S19. The ESI-MS(+) of the crude reaction mixture after photolysis in the range of 120 to 140 which depicts that the m/z and (m+1)/z peaks are of compounds **4** and [^{15}N]-**4**, respectively, in a 1:1 ratio.

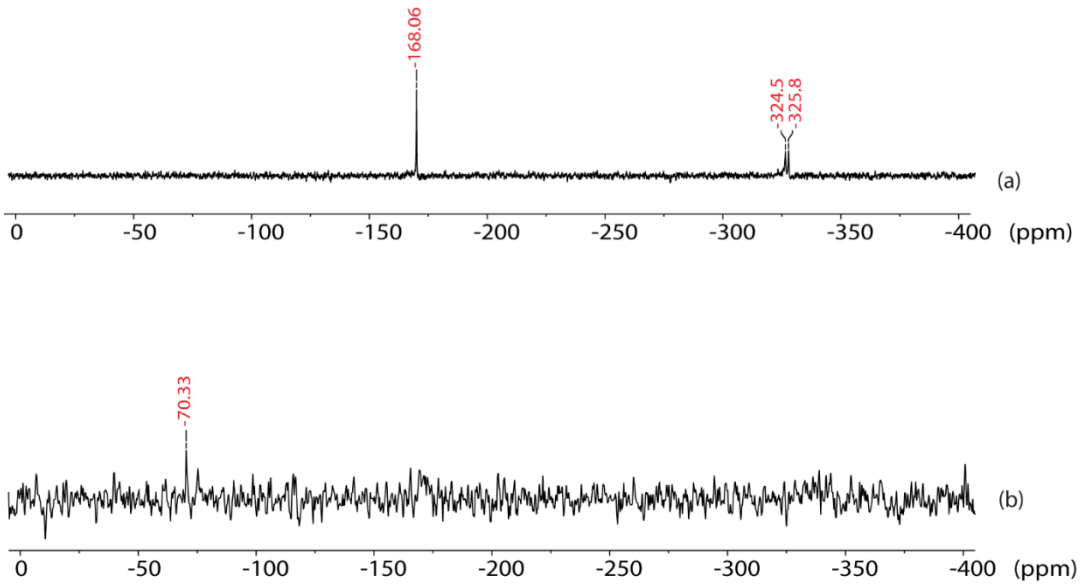

Figure S20. (a) ^{15}N NMR spectrum of [^{15}N]-**2**. (b) ^{15}N NMR spectrum of the crude reaction mixture following photolysis (300 nm, 1h) of compound [^{15}N]-**2** at 243 K**.** The peak at –70.33 ppm indicates the formation of dissolved [^{15}N]-N_2 after completion of the reaction. The spectra were recorded in CD_2Cl_2 at 243 K with an instrument operating at 50.7 MHz.

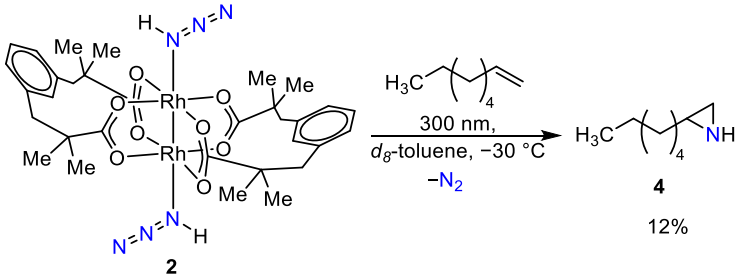

In an N_2-filled glovebox, a 4.0-mL scintillation vial was charged with the crystals of compound **2** (20.3 mg) in 2.5 mL of d_8-toluene to prepare a stock solution. A J-Young NMR tube was charged with 0.50 mL of the stock solution of compound **2**, 0.01 mL (~2.5 equiv.) of 1-octene. Upon recording the ^{1}H NMR of the solution at t = 0 the solution was photolyzed for one hour in a 300 nm Rayonet photoreactor at –30 °C. The reaction temperature was maintained with a dry ice / *o*-xylene bath (–30 °C) in a finger dewar. Upon completion of the photolysis, the crude reaction mixture was analyzed via ^{1}H NMR and ESI-MS (Figure S21). The yield was calculated with an external standard of 1,3,5-trimethoxybenzene (TMB). Formation of **4** was indicated by diagnostic ^{1}NMR resonance at 1.64 ppm (d) and by HR-MS (128.1432 (expt); 128.1434 (calculated for $[C_8H_{18}N]^+$)) which are consistent with the previous HR-MS data.

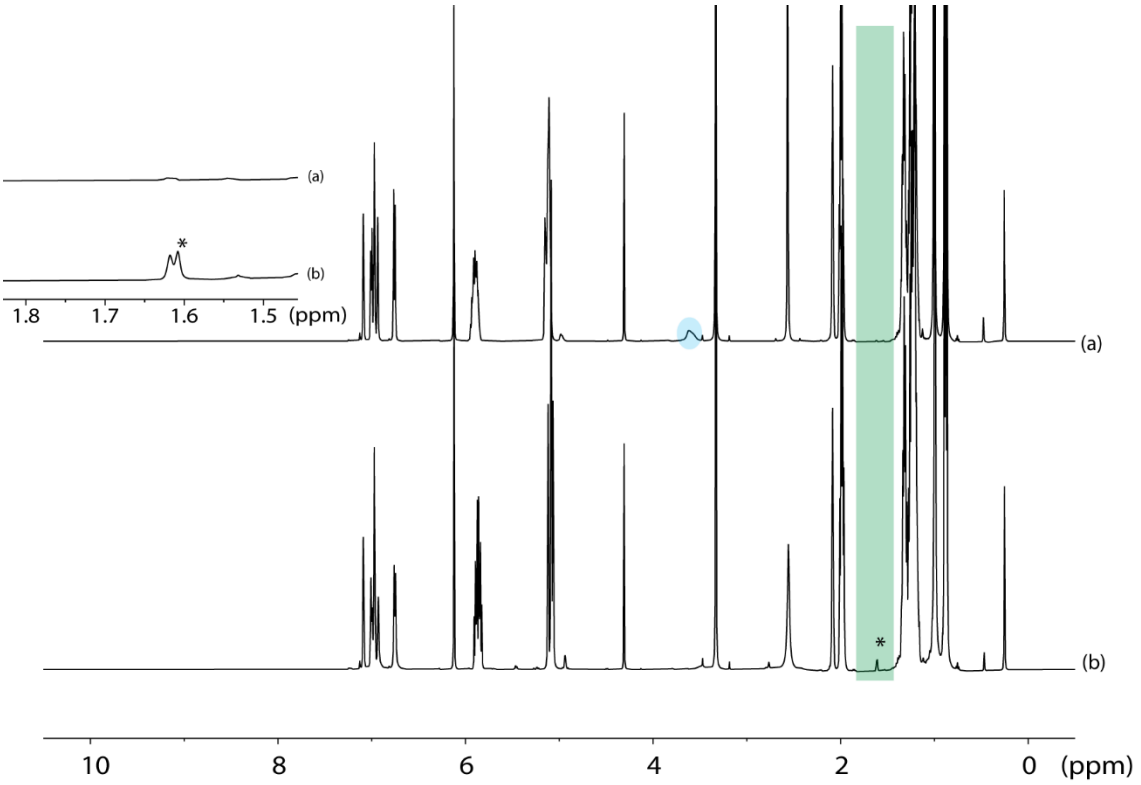

Figure S21. Photolysis (λ = 300 nm) of compound **2** at –30 °C in the presence of 1-octene in d_8-toluene for 1 h results in the formation of compound **4**. (a) ^{1}H NMR spectrum of the crude mixture at t = 0; the N–H peak is highlighted in blue; (b) ^{1}H NMR spectrum of the crude mixture after 1 h photolysis; the green shaded area indicates the aziridination of 1-octene. Expansion of the green shaded area, * 1.65 ppm (d, 1H) is diagnostic of **4**.

Photolysis of HN_3 in the Presence of 1-Octene

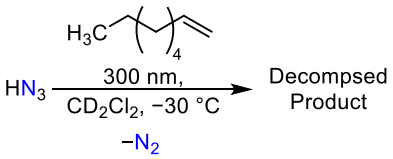

HN_3 was generated according to above procedures using stearic acid (0.143g, 0.50 mmol, 2.00 equiv.) and NaN_3 (16.5 mg, 0.25 mmol, 1.00 equiv.) and vacuum transferred to a Schlenk tube containing 0.5 mL CD_2Cl_2. A clean and dry J-Young tube was charged with 10µL 1-octene. The J-Young tube connected to the HN_3-containing Schlenk flask via a modified glass manifold (Figure S1b). The HN_3 solution was frozen at 77 K. The entire assembly was evacuated under active vacuum for 15 min. Under static vacuum, the J-Young tube was cooled to 77 K while the donor flask was gradually allowed to warm to 23 °C (Figure 1b). After the vacuum transfer was complete, the J-Young tube was allowed to warm to −78 °C, then to −20 °C, and finally to 23 °C. Upon recording the ^{1}H NMR of the solution at t = 0 the solution was photolyzed for an hour in a 300 nm Rayonet photoreactor at −30 °C. The reaction temperature was maintained with a dry ice / *o*-xylene bath (−30 °C) in a finger dewar. Upon completion of the photolysis, the crude reaction mixture was analyzed via ^{1}H NMR (Figure S22) which shows no NH-azidirination of 1-octene in absence of compound **1**.

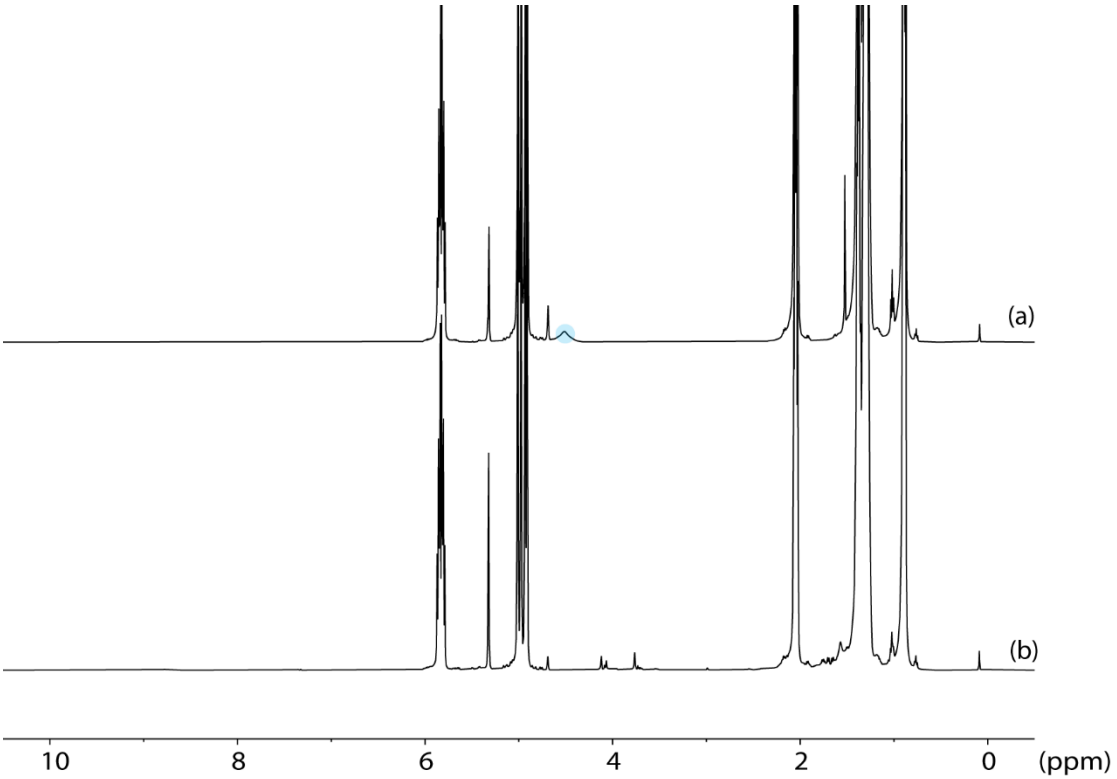

Figure S22. Photolysis (λ = 300 nm) of compound HN_3 at –30 °C with 1-octene in CD_2Cl_2 for 1 h. (a) ^1H NMR of the crude mixture at t = 0, N–H peak highlighted in blue; (b) NMR of the crude mixture after 1 h photolysis.

Photolysis of 2 in the presence of norbornene

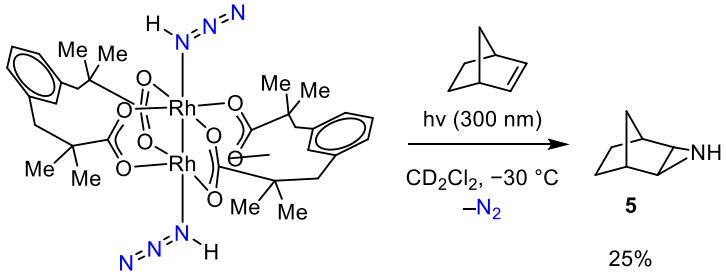

In an N_2-filled glovebox, a 4-mL scintillation vial was charged with the crystals of compound **2** (20.3 mg) in 2.5 mL of CD_2Cl_2 to prepare a stock solution. A J-Young NMR tube was charged with 0.50 mL of the stock solution of compound **2**, 0.01 mL (from the stock solution of ~10.0 mg norbornene in 0. mL CD_2Cl_2) of norbornene. Upon recording the ^{1}H NMR of the solution at t = 0 the solution was photolyzed for one hour in a 300 nm Rayonet photoreactor at –30 °C. The reaction temperature was maintained with a dry ice / *o*-xylene bath (–30 °C) in a finger dewar. Upon completion of the photolysis, the crude reaction mixture was analyzed via ^{1}H NMR and ESI-MS (Figure S23 and S24, respectively). The yield was calculated with an external standard of 1,3,5-trimethoxybenzene (TMB). Formation of **5** was indicated by diagnostic ^{1}NMR resonances at 2.18 (s, 2H),1.57–1.47 ppm (d, 2H), and 1.21-1.14 ppm (m, 2H) and by HR-MS (110.0967 (expt); 110.0964 (calculated for $[C_7H_{12}N]^+$)). These data are consistent with previous reports of **5** measured in $CDCl_3$.[10]

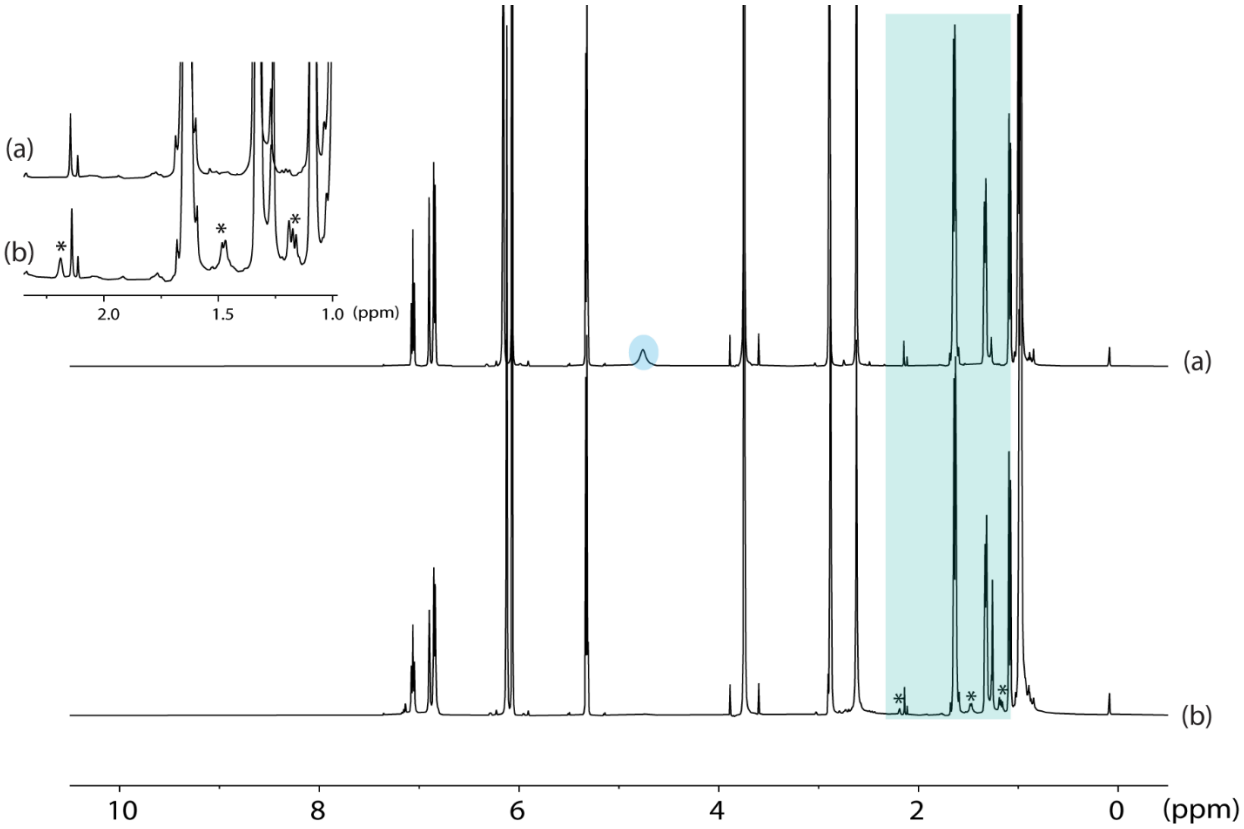

Figure S23. Photolysis (λ = 300 nm) of compound **2** at –30 °C with norbornene in CD_2Cl_2 for 1 h results in the formation of compound **5**. (a) ^1H NMR of the crude mixture at t = 0, N–H peak highlighted in blue; (b) NMR of the crude mixture after 1 h photolysis, green shaded area indicates the aziridination of norbornene; (c) Expansion of the green shaded area; * at 2.18 (s, 2H), 1.57–1.47 ppm (d, 2H), and 1.21–1.14 ppm (m, 2H) indicates the formation of compound **5**.

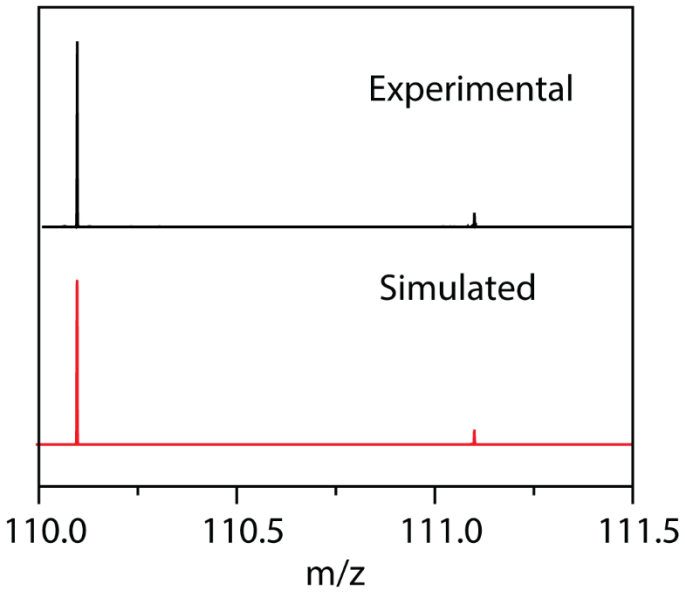

Figure S24. ESI-MS(+) of the crude photolysis mixture indicating the formation of the aziridine product $[C_7H_{12}N]^+$ (**5**) from norbornene; black: experimental; red: simulation. 110.0967 (expt); 110.0964 (calculated for $[C_8H_{17}N]^+$).

Photolysis of 2 in the presence of *cis*-4-octene

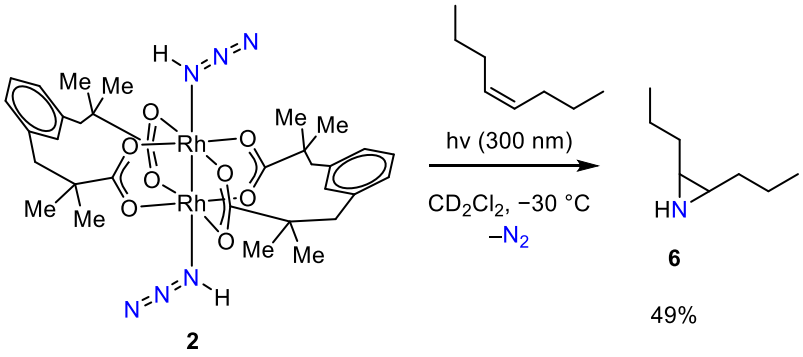

In an N_2-filled glovebox, a J-Young NMR tube was charged with crystals of compound **2** and 0.50 mL CD_2Cl_2. A 4-mL scintillation vial was charged with 0.10 ml of *cis*-4-octene and 0.50 mL of CD_2Cl_2 to make a stock solution. An aliquot of 0.20 mL of the stock solution was added to the reaction mixture in the J-Young tube. Upon recording the ^{1}H NMR of the solution at t = 0 the solution was photolyzed for an hour in a 300 nm Rayonet photoreactor at –30 °C. The reaction temperature was maintained with a dry ice / *o*-xylene bath (–30 °C) in a finger dewar. Upon completion of the photolysis, the crude reaction mixture was analyzed via ^{1}H NMR and ESI-MS (Figure S25 and S26, respectively). The yield was calculated with an external standard of 1,3,5-trimethoxybenzene (TMB). Formation of **6** was indicated by diagnostic ^{1}NMR resonances at 1.98–1.95 (m, 2H) and by HR-MS (128.1436 (expt); 128.1434 (calculated for $[C_8H_{18}N]^+$)). These data are consistent with previous reports of **6** measured in $CDCl_3$.[10]

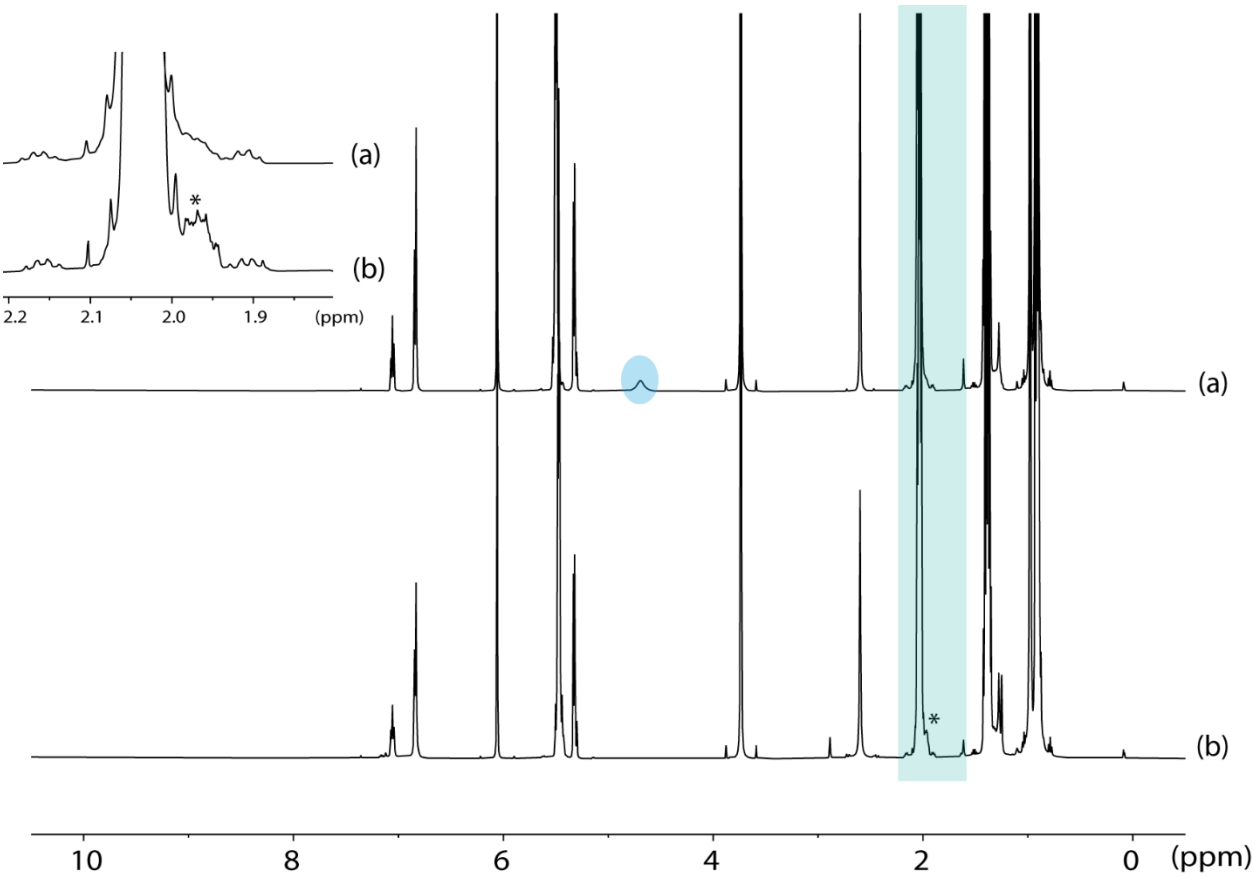

Figure S25. Photolysis (λ = 300 nm) of compound **2** at –30 °C with *cis*-4-octene in CD_2Cl_2 for 1 h results in the formation of compound **6**. (a) ^1H NMR of the crude mixture at t = 0, the N–H peak is highlighted in blue; (b) NMR of the crude mixture after 1 h photolysis, green shaded area indicates the aziridination of *cis*-4-octene; (c) Expansion of the green shaded area; * at 1.98–1.95 (m, 2H) indicates the formation of compound **6.**

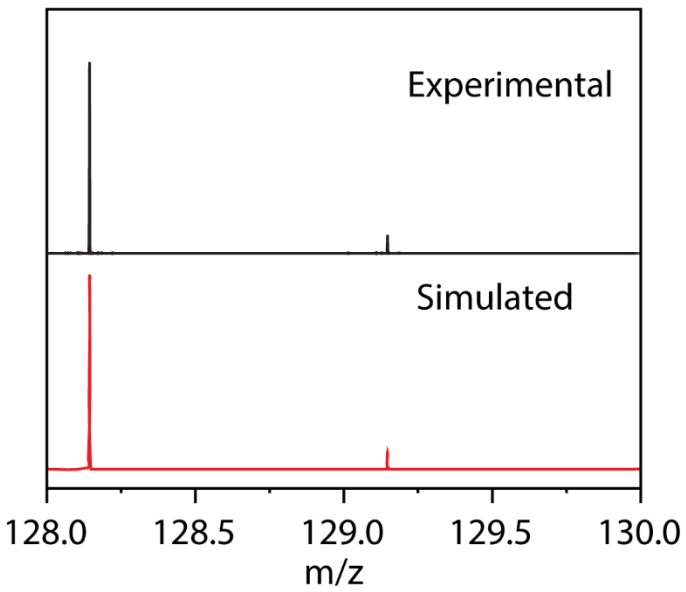

Figure S26. ESI-MS(+) of the crude photolysis mixture indicating the formation of the aziridine **6** ($[C_8H_{18}N]^+$) from *cis*-4-octene; black: experimental; red: simulation. (128.1436 (expt); 128.1434 (calculated for $[C_8H_{18}N]^+$)).

^{1}H NMR Monitoring of the Photolysis Complex 2 with 1-octene at 243 K

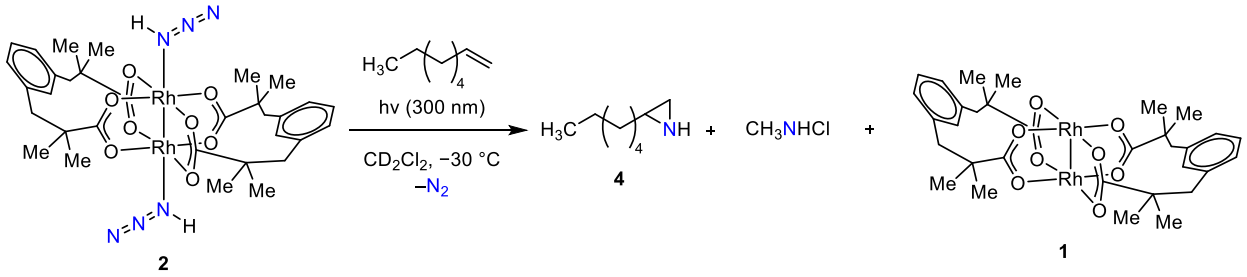

In an N_2-filled glovebox, a 4-mL scintillation vial was charged with the crystals of compound **2** (20.3 mg) in 2.5 mL of CD_2Cl_2 to prepare a stock solution. A J-Young NMR tube was charged with 0.50 mL of the stock solution of compound **2** and 0.01 mL (~2.5 equiv.) of 1-octene. Upon recording the ^{1}H NMR of the solution at t = 0 at 298 K the solution was photolyzed in a 300 nm Rayonet photoreactor at –30 °C for until the N–H peak disappears (for the spectral evolution see Figure S27). Periodic ^{1}H NMR were recorded at 298 K to monitor the spectral evolution The growing peaks at 2.9 ppm (s) and at 3.9 ppm (br, s) indicates the formation of *N*-chloromethylamine. See Figures S28 and S29 for the ^{1}H and ^{13}C NMR after the completion of the reaction.

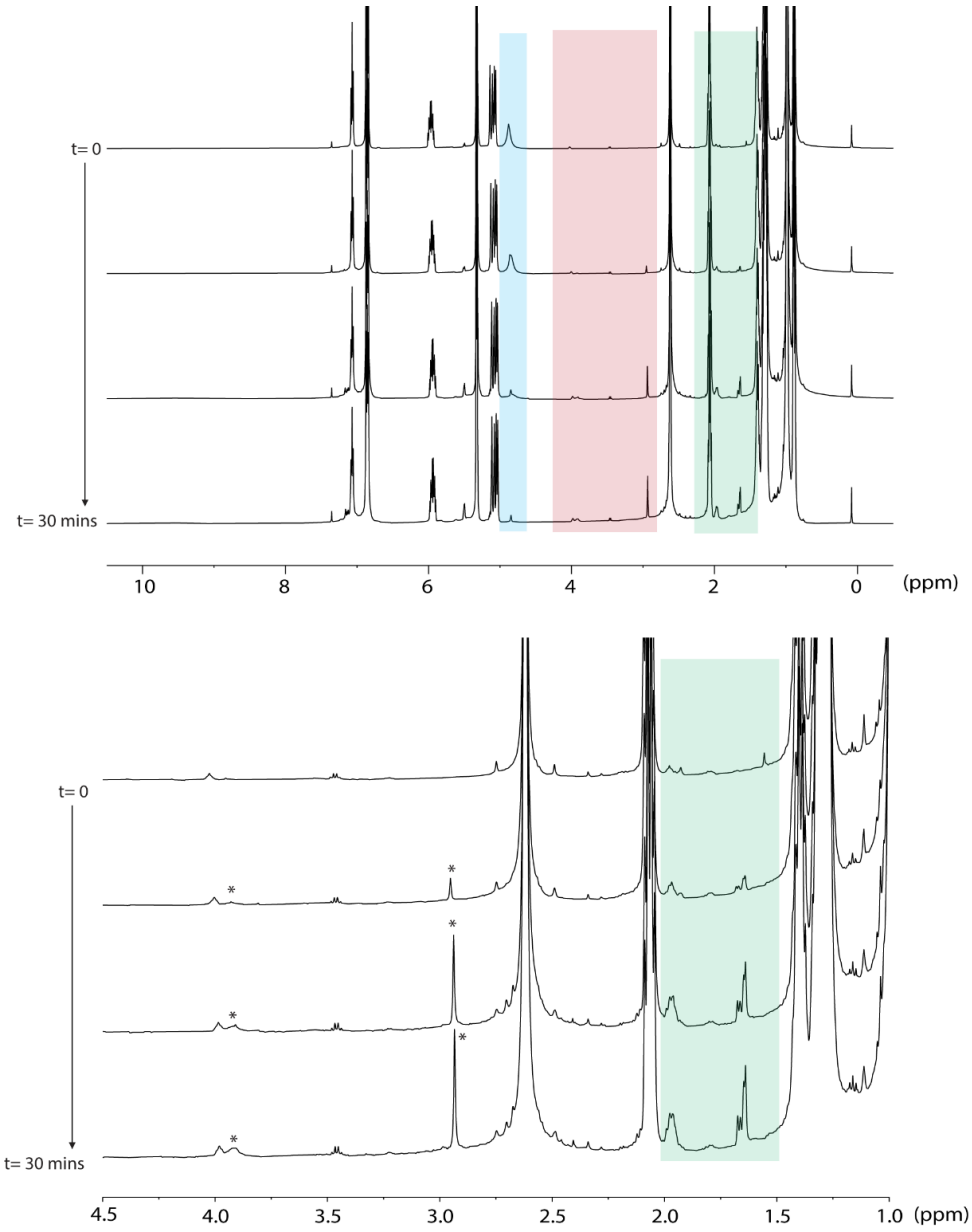

Figure S27. ^{1}H Spectra obtained during the photolysis (λ=300 nm) of **2** with 1-octene at −30 °C. Spectra were recorded at 298 K with instrument operating at 500 MHz. (a) The shaded area (blue) highlights the depletion of the N–H peak, the shaded area (orange) highlights the peaks appearance at the 4.2 ppm to 2.8 ppm. The shaded area (green) highlights the formation of **4.** (b) Expansion of the spectral window (4.5 to 1.0 ppm); * sign indicates the growth of peaks at 3.92 ppm (br, s) and the at 2.93 ppm (s) that *N*-chloromethylamine.

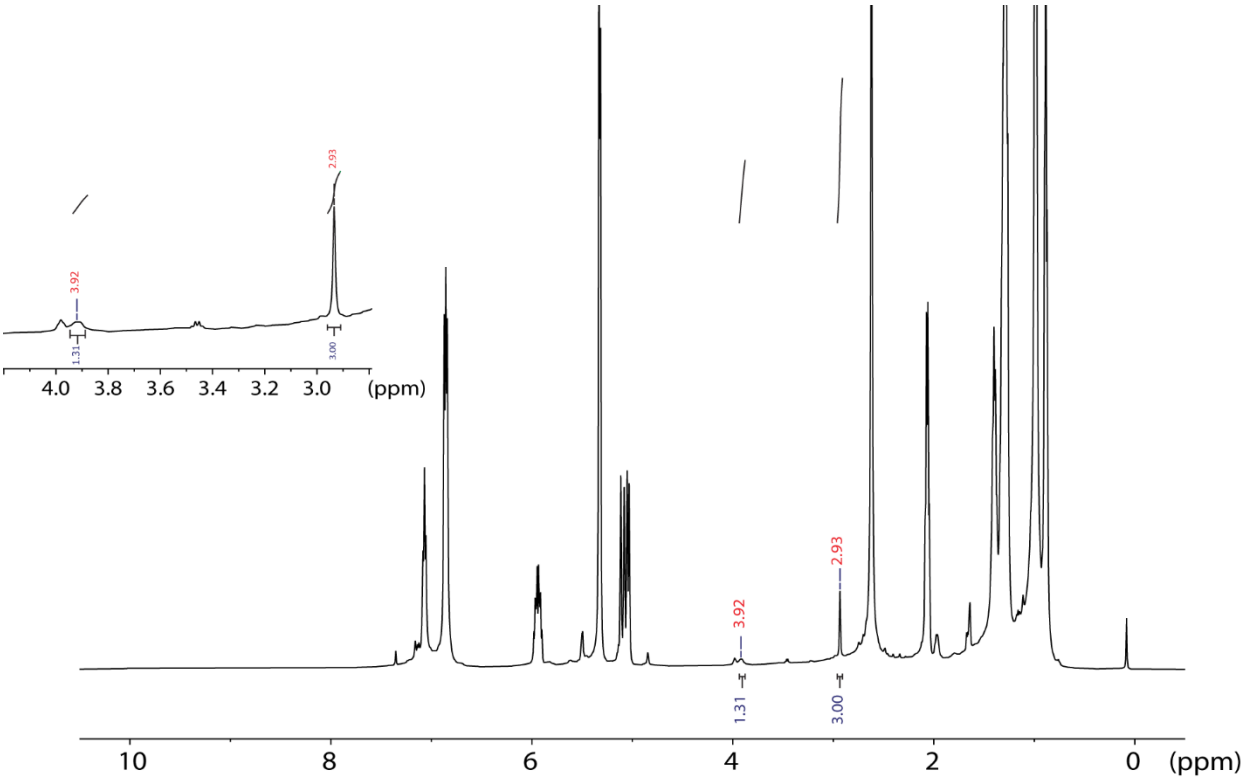

Figure S28. The ^{1}H NMR spectrum recorded after photolysis of **2** in presence of 1-octene. The peaks at 2.93 (s) and 3.92 (br, s) have the relative integration of 3:1. The NMR spectrum was recorded at 298 K with instrument operating at 500 MHz. Inset: Expansion of the spectral window from 2.7 to 4.3 ppm.

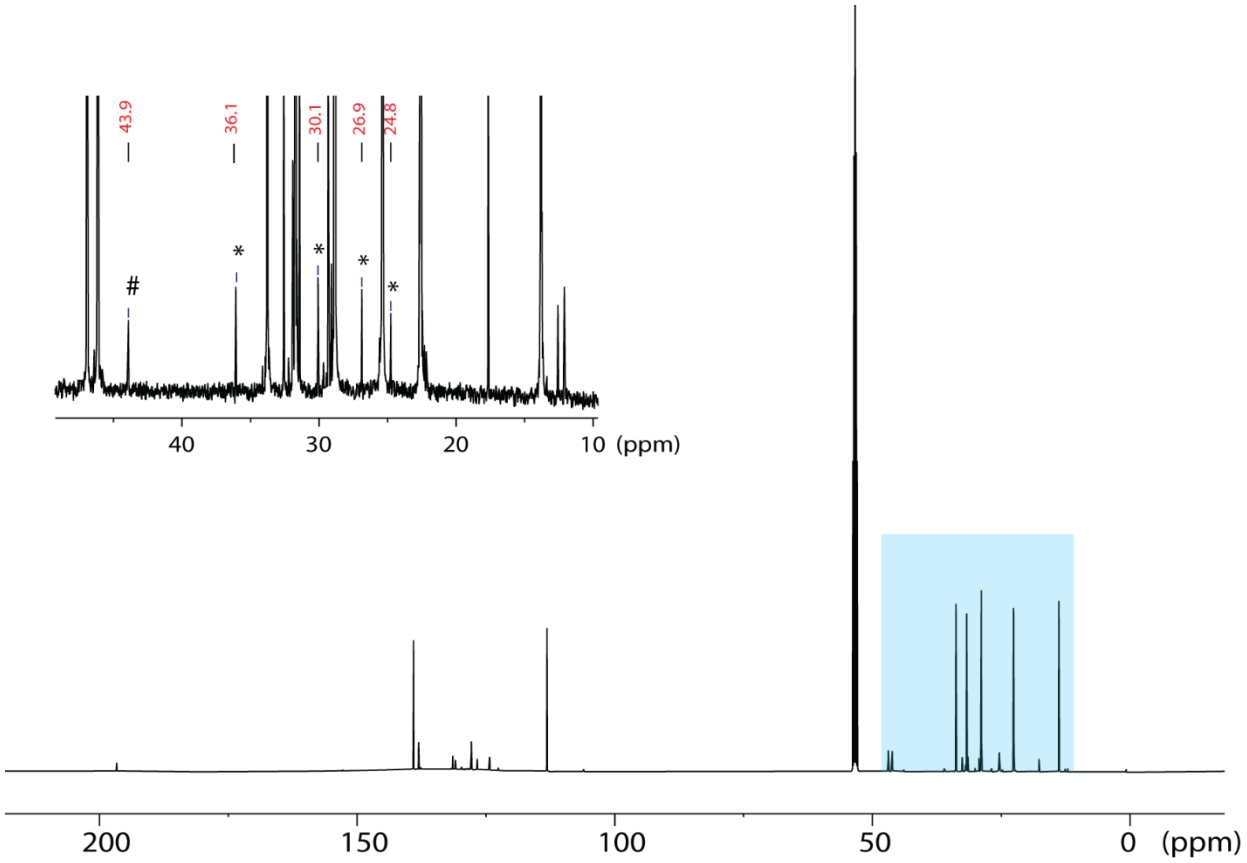

Figure S29. The ^{13}C NMR spectrum recorded after photolysis of **2** in presence of 1-octene. Inset: Expansion of the blue shaded area highlights the formation of **4** (*) and CH_3NHCl (#). The NMR spectrum was recorded in CD_2Cl_2 with an instrument operating at 125.6 MHz at 23 °C

Photolysis of Complex 2 in the Glassy Solvent Matrix at 77 K

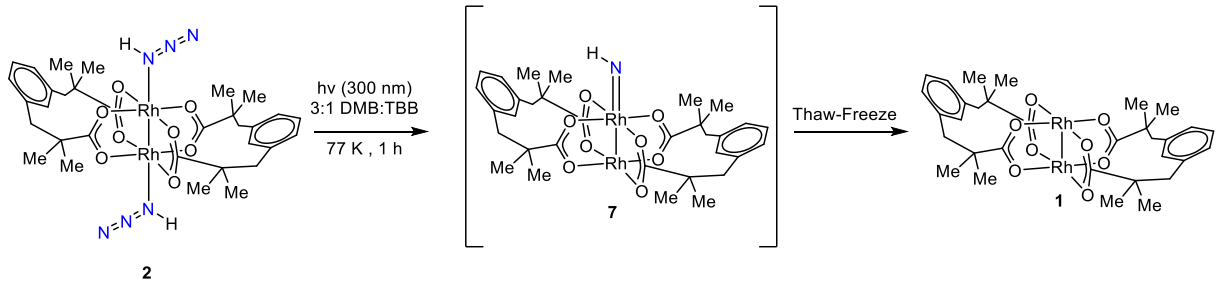

In an N_2-filled glovebox, a 4-ml scintillation vial was charged with 2.4 mL 2,2-dimethylbutane (DMB) and 0.8 mL *tert*-butylbenzene (TBB) to make a stock solution of the glassy solvent mixture. In a separate 4-mL scintillation vial, ~5.0 mg of the crystals of **2** were dissolved in 1.0 mL of the glassy solvent mixture. A modified EPR tube with J-Young manifold was charged with the solution of compound **2**. The solution in EPR tube was frozen at 77 K to make a transparent glass of complex **2**. The UV-vis spectrum was measured. The sample was photolyzed (λ = 300 nm) for 1 h at 77 K (−196 °C) and the UV-vis spectrum was periodically collected (Figure S29). After 1 h of photolysis, the reaction mixture was warmed to 298 K (25 °C). After 5 minutes, the solution was cooled to 77 K and the final UV-vis spectrum was collected which overlaid with compound **1** dissolved in glassy solvent mixture at 77K (Figure S31).

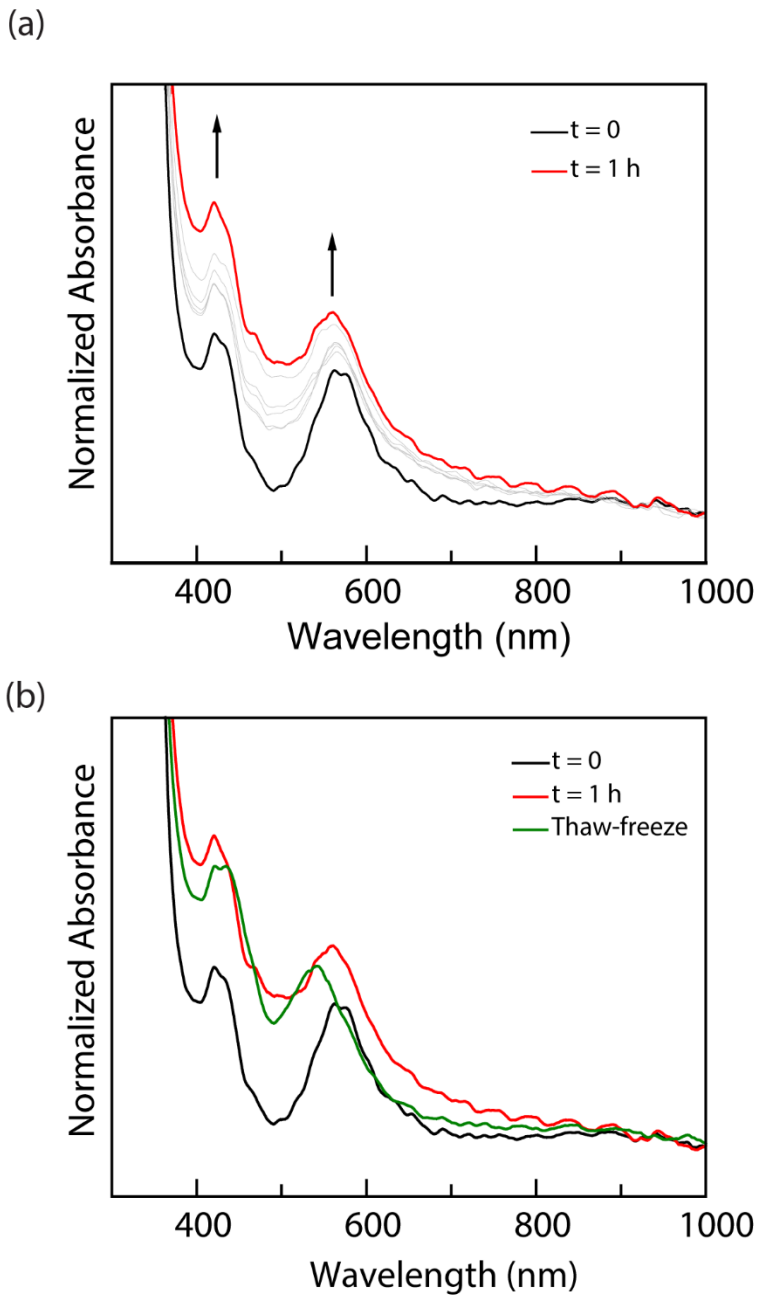

Figure S30. (a) UV-vis spectra recorded during the cryogenic photolysis (λ = 300 nm) of **2** at 77 K. The spectral evolution from t = 0 (black) to t = 1h (red) indicates the conversion of **2** to **7.** comparison of spectra recorded at t = 0, t = 1h (red) and after thaw-freeze at 77 K (green).

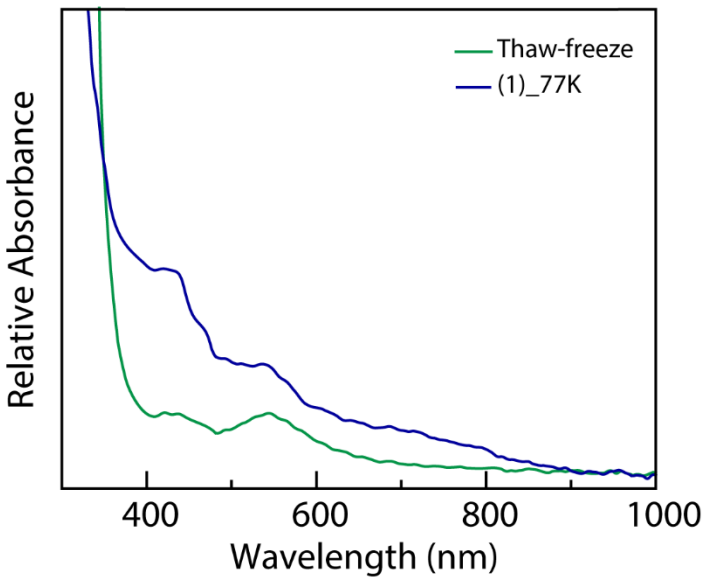

Figure S31. UV-vis comparison of compound **1** (blue) with spectrum recorded after the thaw-freeze of the photolysis (300 nm) of compound **2** at 77 K (green).

Photolysis of Complex [^{15}N]-2 in the Glassy Solvent Matrix at 77 K in Presence of 1-Octene

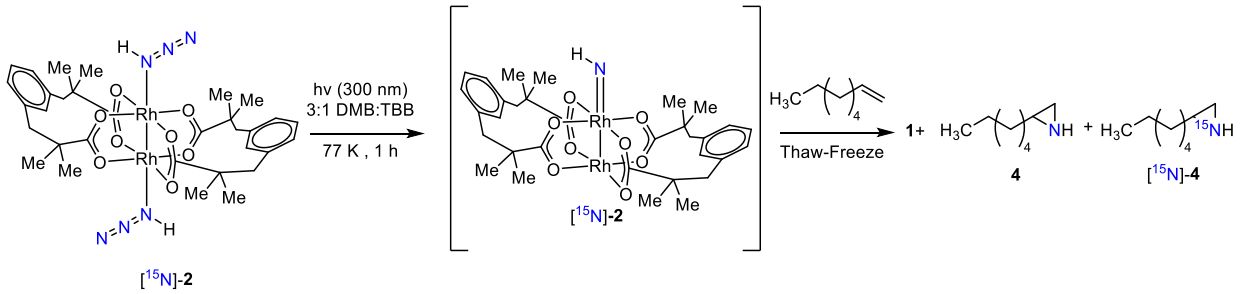

In an N_2-filled glovebox, a 4-ml scintillation vial was charged with 2.4 mL 2,2-dimethylbutane (DMB) and 0.8 mL *tert*-butylbenzene (TBB) to make a stock solution of the glassy solvent mixture. In a separate 4-mL scintillation vial, ~5.0 mg of the crystals of [^{15}N]-**2** were dissolved in 1.0 mL of the glassy solvent mixture. A modified EPR tube with J-Young manifold was charged with the solution of compound [^{15}N]-**2**. The solution in EPR tube was frozen at 77 K to make a transparent glass of complex [^{15}N]-**2**. The UV-vis spectrum was measured. The sample was photolyzed (λ = 300 nm) for 1 h at 77 K (−196 °C) and the UV-vis spectrum was periodically collected (Figure S32). After 80 mins of photolysis, the reaction mixture was warmed to 298 K (25 °C). After 5 minutes, the solution was cooled to 77 K and the final UV-vis spectrum was collected. The formation of **4** and [^{15}N]-**4** was determined by the ESI-MS(+) analysis of the crude reaction mixture (see Figure S33).

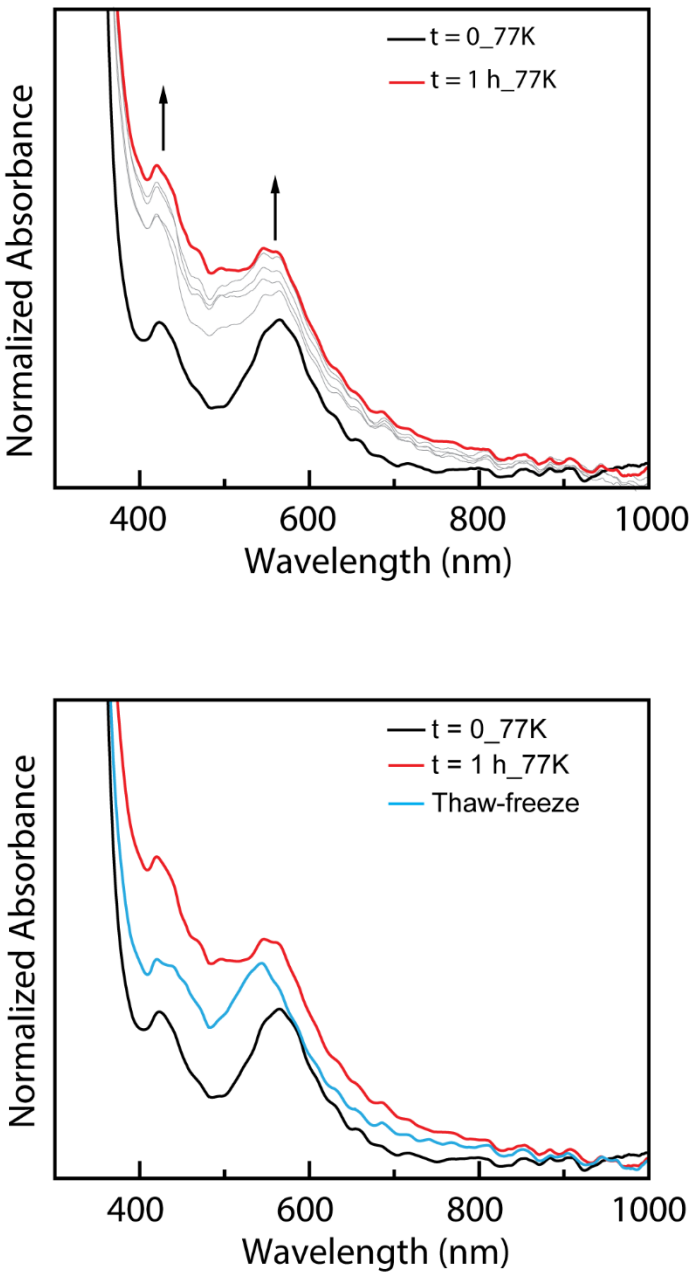

Figure S32. (a) UV-vis spectra recorded during the cryogenic photolysis (λ = 300 nm) of [^{15}N]-**2** in presence of 1-octene at 77 K. The spectral evolution from t = 0 (black) to t = 1h (red) indicates the conversion of [^{15}N]-**2** to **7.** (b) UV-vis comparison of spectra recorded at t = 0, t = 1h (red) and after thaw-freeze at 77 K (sky blue).

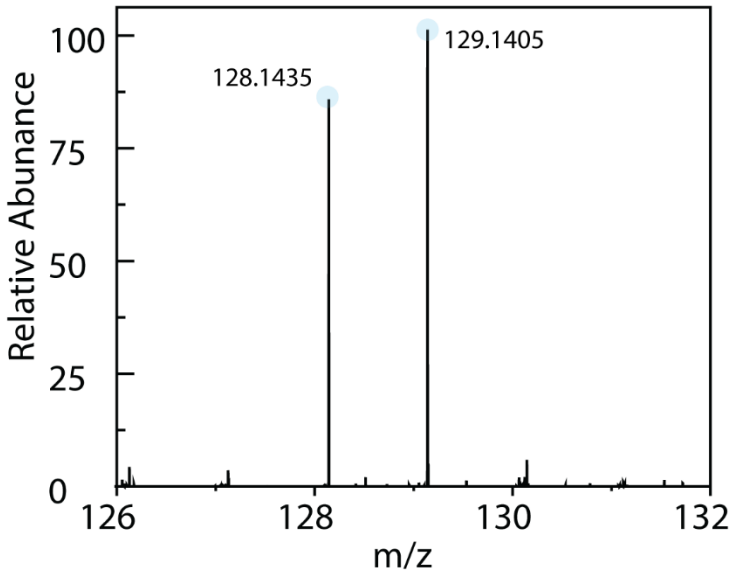

Figure S33. The ESI-MS(+) of the crude reaction mixture after photolysis in the glassy solvent mixture at 77 K in the range of 126 to 132 which depicts that the m/z and (m+1)/z peaks are of compounds **4** and [^{15}N]-**4**, respectively, in a 1:1 ratio.

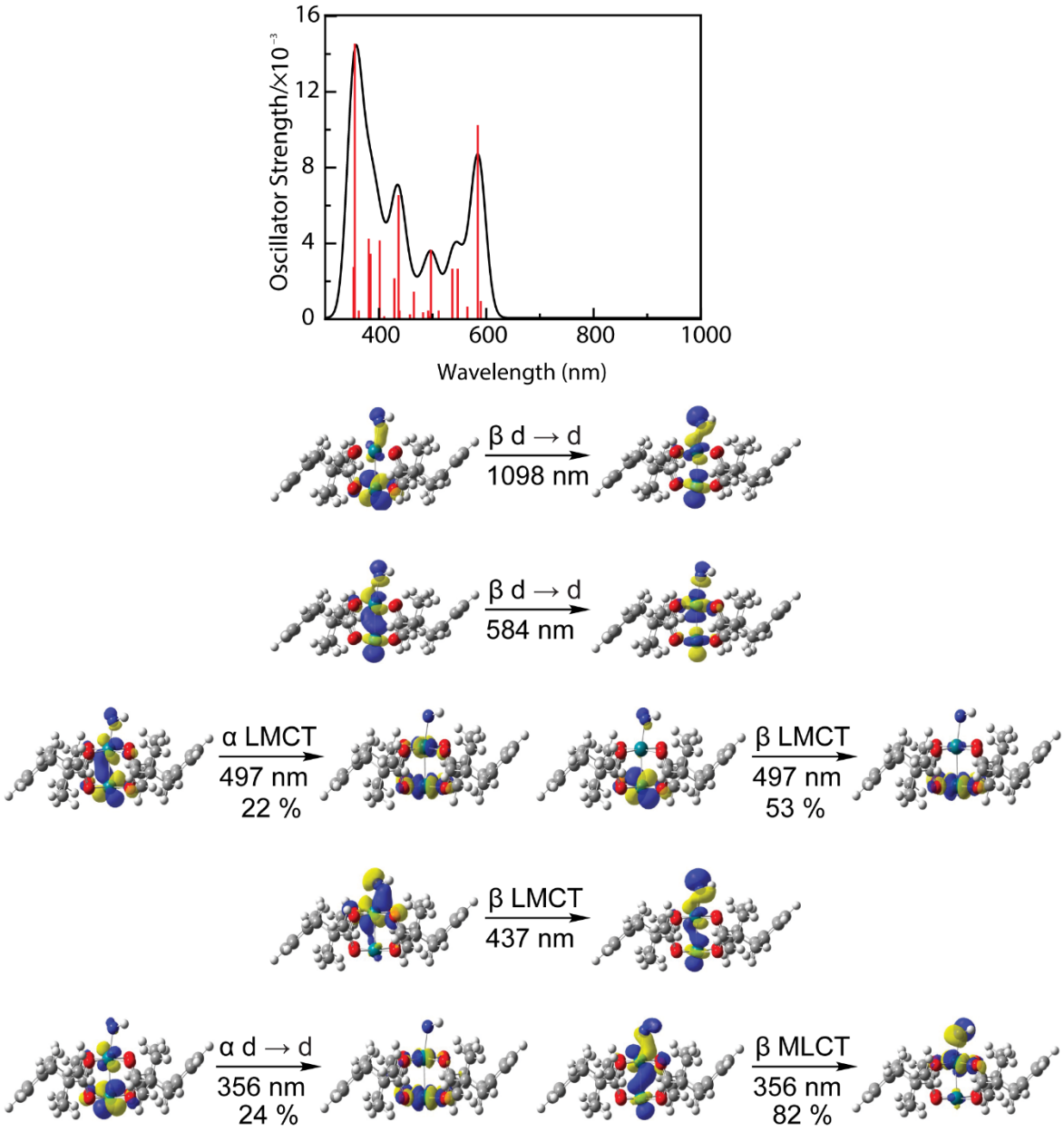

Figure S34. TD-DFT and NTO analysis of ^{3}**7**. Vertical excitations in red and simulated spectrum in black.

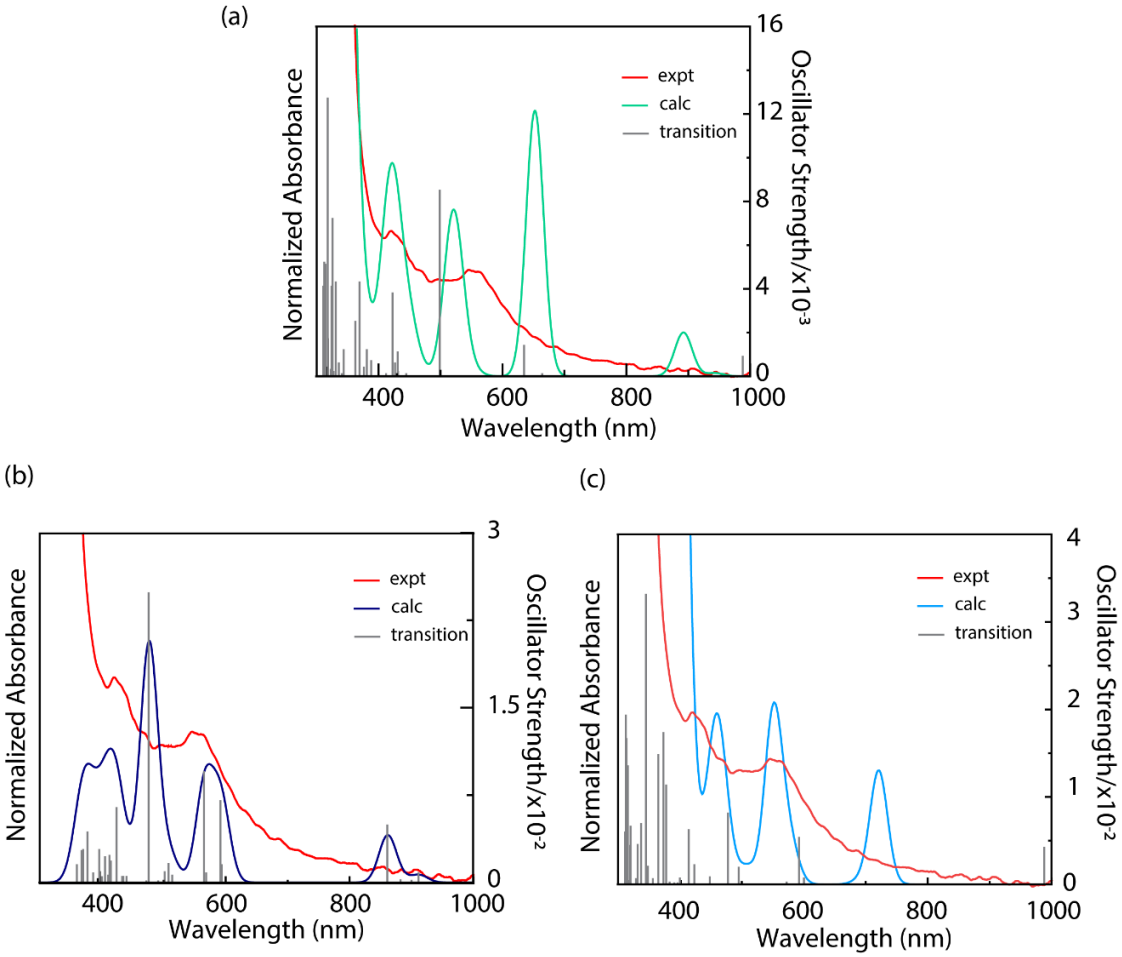

Figure S35 (a) Comparison of UV-vis spectrum of **7** at 77 K (red) with the simulated spectrum (green) of $^{1}[Rh_2(esp)_2NH]$ (^{1}[**7**]) based on the TD-DFT calculation by PBE0-BS1 method. Vertical transition pictured in grey. (b) Comparison of UV-vis spectrum of **7** at 77 K (red) with the simulated spectrum (dark blue) of $^{3}[Rh_2(esp)_2(NH)(HN_3)]$ based on the TD-DFT calculation by PBE0-BS1 method. Vertical transition pictured in grey. (c) Comparison of UV-vis spectrum of **7** at 77 K (red) with the simulated spectrum (sky blue) of $^{1}[Rh_2(esp)_2(NH)(HN_3)]$ based on the TD-DFT calculation by PBE0-BS1 method. Vertical transitions are pictured in grey.

Photolysis of Complex 3a in the Glassy Solvent Matrix at 77 K

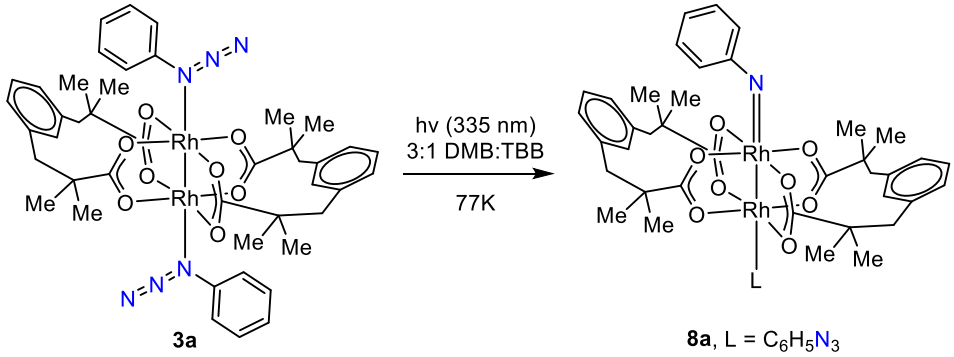

In an N_2-filled glovebox, a 4-mL scintillation vial was charged with 2.4 mL 2,2-dimethylbutane (DMB) and 0.8 mL *tert*-butylbenzene (TBB) to make a stock solution of the glassy solvent mixture. In a separate 4-mL scintillation vial, ~5.0 mg of the crystals of compound **3a** were dissolved in 1.0 mL of the glassy solvent mixture. A modified EPR tube with J-Young manifold was charged with the solution of compound **3a**. The solution in EPR tube was frozen at 77 K to make a transparent glass of complex **3a**. Upon recording the UV-vis spectrum of the initial time-point, the mixture was photolyzed (λ = 335 nm) for 80 mins at 77 K (−196 °C) and the photolysis was monitored by collection of periodic UV-vis spectra (see Figure S35). After 1 h of photolysis, the reaction mixture was warmed to 298 K (25 °C). After 5 minutes, the solution was cooled to 77 K and the final UV-vis spectrum was collected (Figure S36).

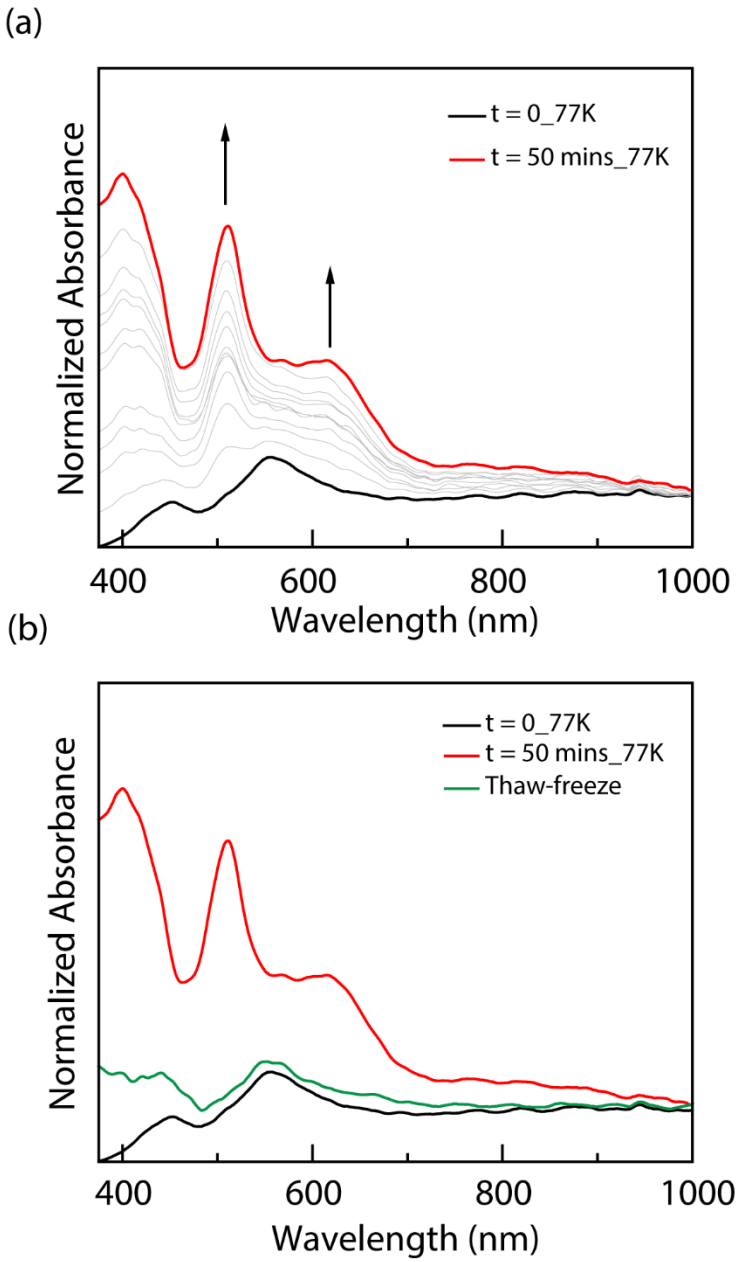

Figure S36. (a) UV-vis spectra recorded during the cryogenic photolysis (λ = 335 nm) of **3a** at 77 K. The spectral evolution from t = 0 (black) to t = 50 mins (red) indicates the conversion of **3a** to **8a**. (b) UV-vis spectra of **3a** (black), **8a** (i.e., after 50 mins photolysis, red), and after thermal annealing (green) collected at 77 K.

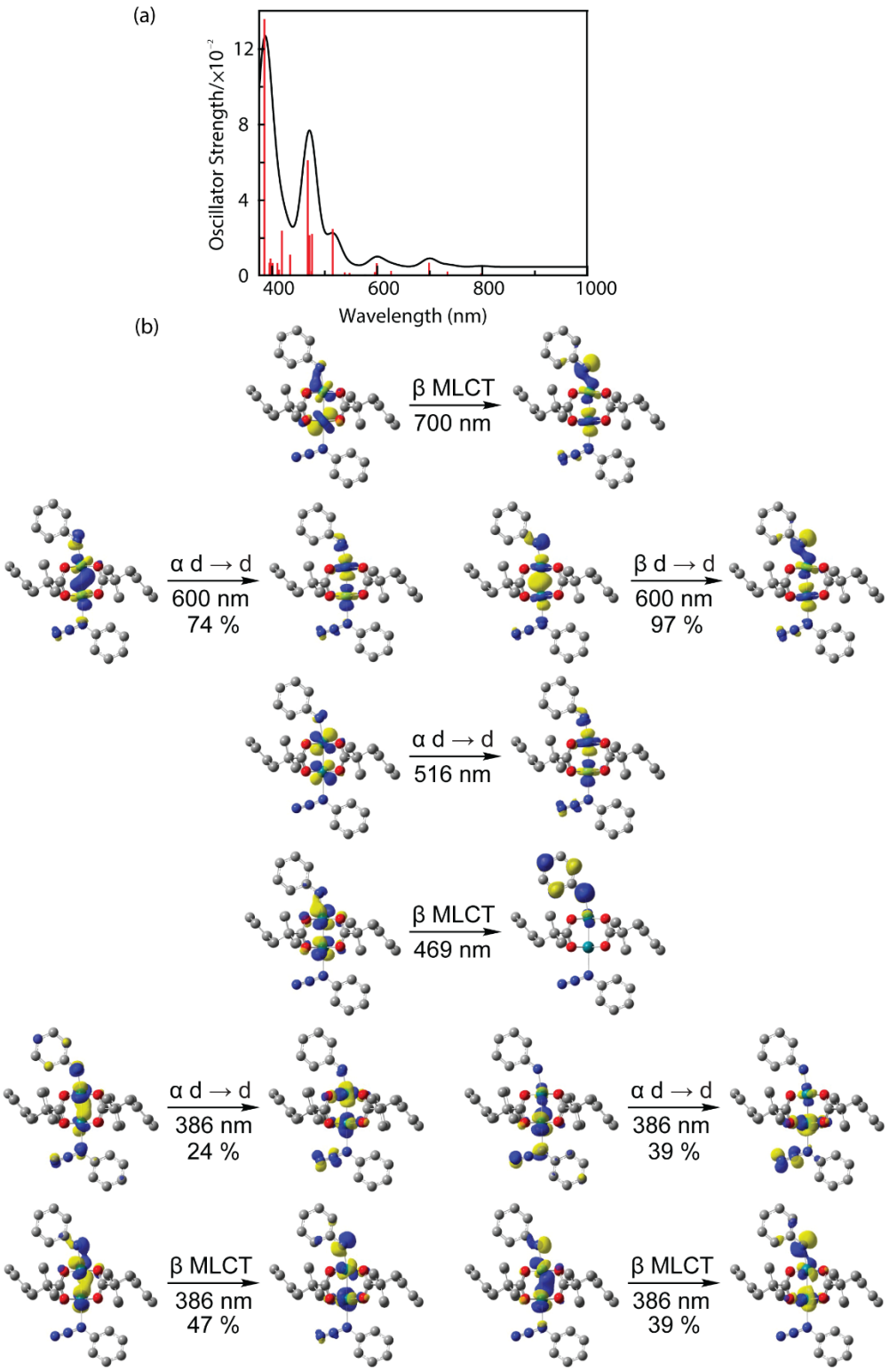

Figure S37. (a) TD-DFT simulated spectrum(black) of ^{3}[**8a**] along with corresponding the vertical excitations (red). (b) NTO analysis of ^{3}[**8a**].

Photolysis of complex 3b in the Glassy Solvent Matrix at 77 K

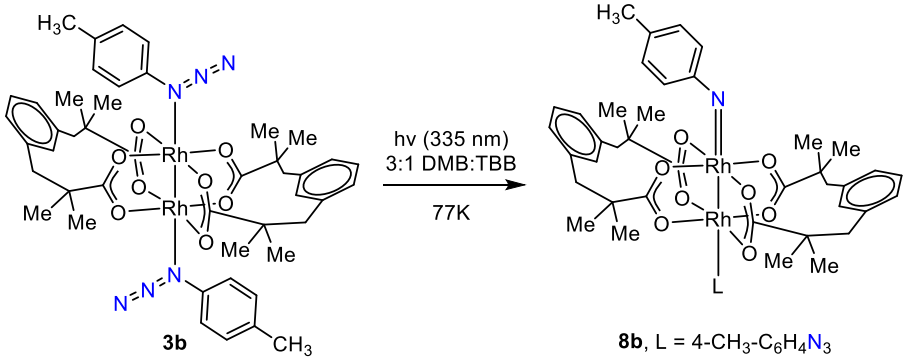

In an N_2-filled glovebox, a 4-mL scintillation vial was charged with 2.4 mL 2,2-dimethylbutane (DMB) and 0.8 mL *tert*-butylbenzene (TBB) to make a stock solution of the glassy solvent mixture. In a separate 4-mL scintillation vial, ~5.0 mg of the crystals of compound **3b** were dissolved in 1.0 mL of the glassy solvent mixture. A modified EPR tube with J-Young manifold was charged with the solution of compound **3b**. The solution in EPR tube was frozen at 77 K to make a transparent glass of complex **3b**. Upon recording the UV-vis spectrum of the initial time-point, the mixture was photolyzed (λ = 335 nm) for 20 mins at 77 K (−196 °C) and the photolysis was monitored by collection of periodic UV-vis spectra (see Figure S37). After 1 h of photolysis, the reaction mixture was warmed to 298 K (25 °C). After 5 minutes, the solution was cooled to 77 K and the final UV-vis spectrum was collected (Figure S38).

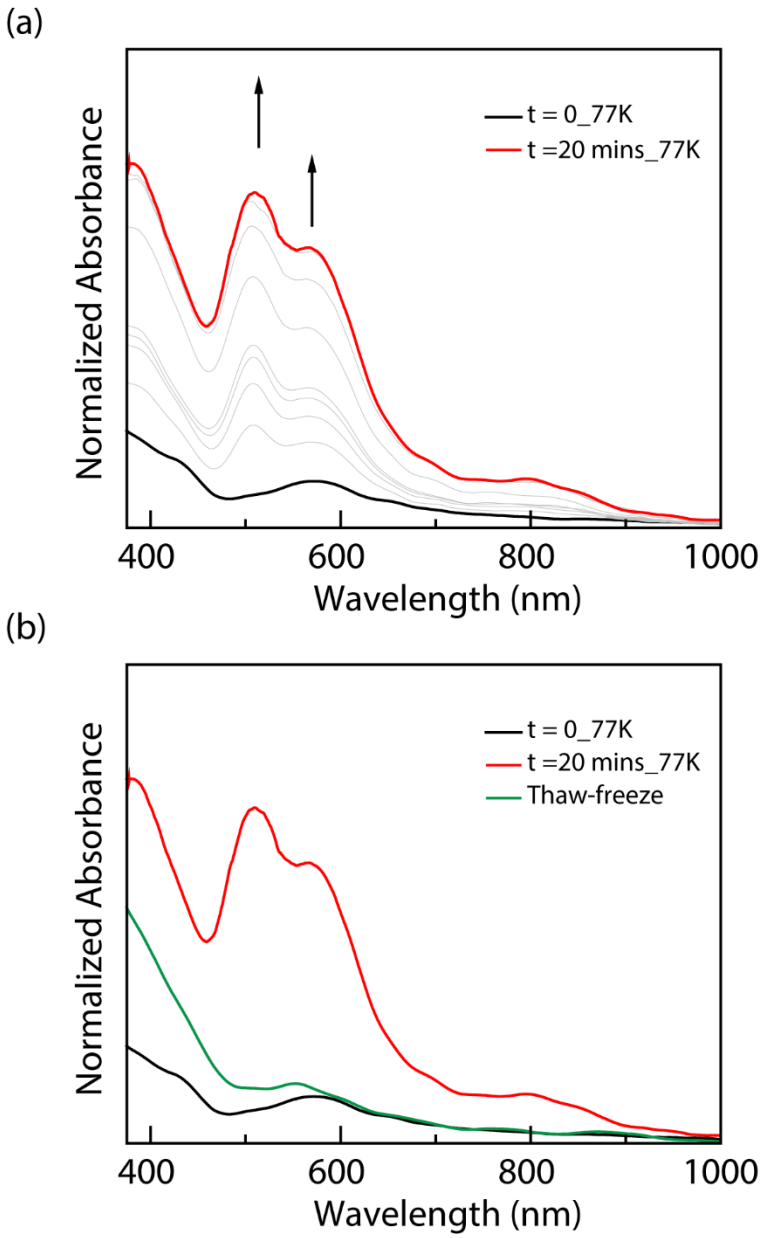

Figure S38. (a) UV-vis spectra recorded during the cryogenic photolysis (λ = 335 nm) of **3b** at 77 K. The spectral evolution from t = 0 (black) to t = 20 mins (red) indicates the conversion of **3b** to **8b**. (b) UV-vis spectra of **3b** (black), **8b** (i.e., after 20 mins photolysis, red), and after thermal annealing (green) collected at 77 K.

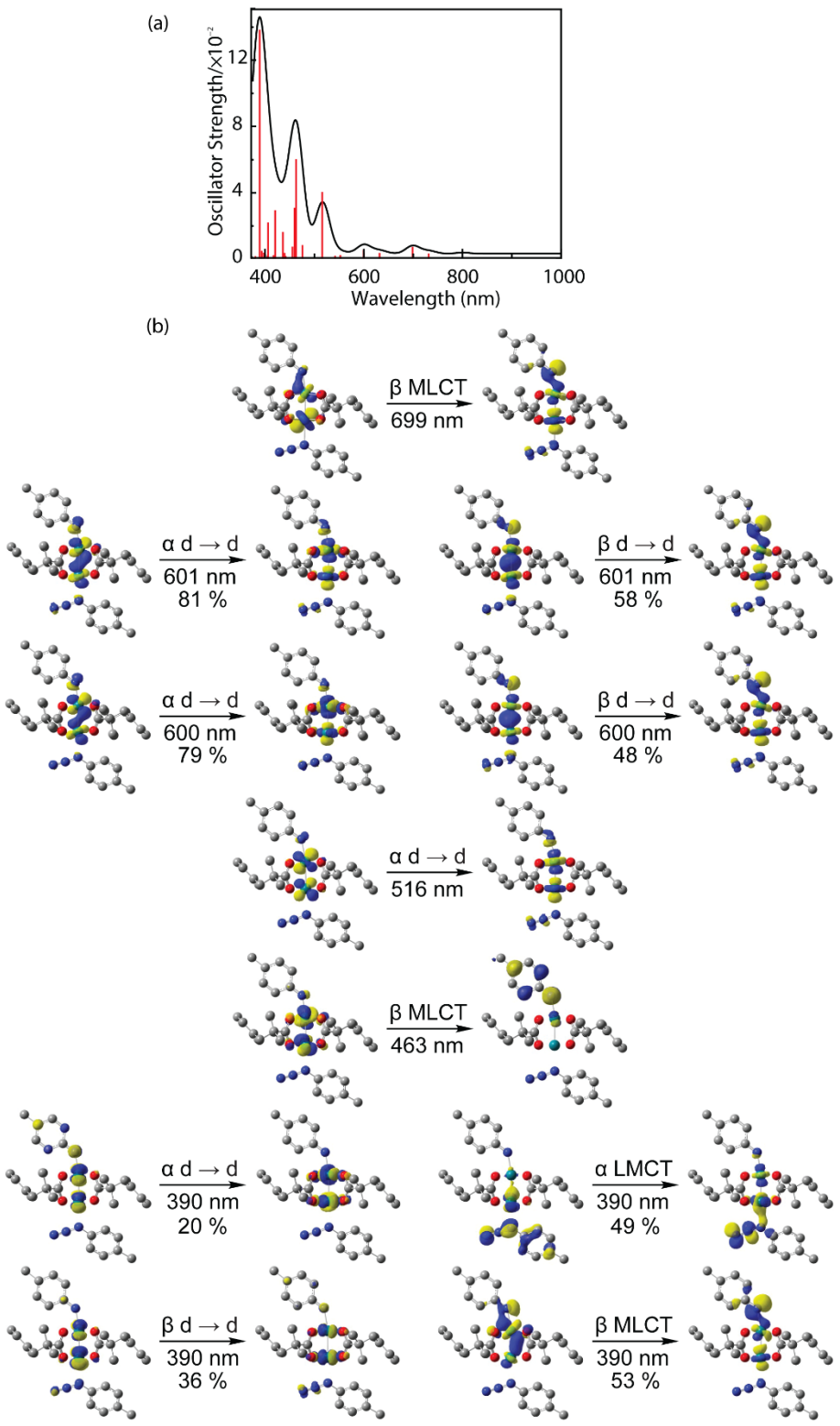

Figure S39. (a) TD-DFT simulated spectrum (black) of ^{3}[**8b**] along with corresponding the vertical excitations (red). (b) NTO analysis of ^{3}[**8b**].

Photolysis of Complex 3c in the Glassy Solvent Matrix at 77 K

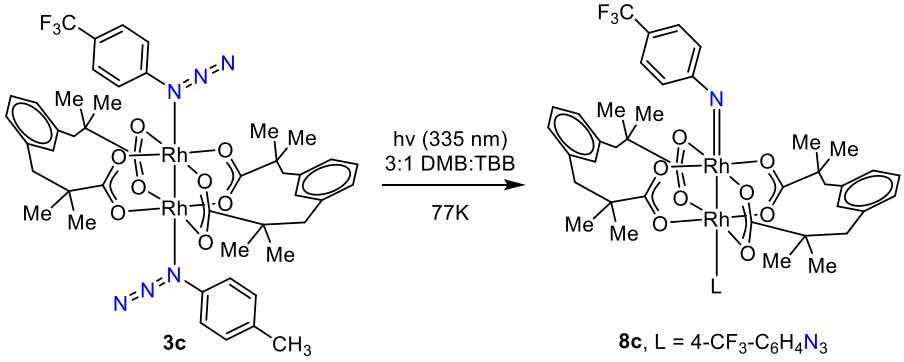

In an N_2-filled glovebox, a 4-mL scintillation vial was charged with 2.4 mL 2,2-dimethylbutane (DMB) and 0.8 mL *tert*-butylbenzene (TBB) to make a stock solution of the glassy solvent mixture. In a separate 4-mL scintillation vial, ~5.0 mg of the crystals of compound **3c** were dissolved in 1.0 mL of the glassy solvent mixture. A modified EPR tube with J-Young manifold was charged with the solution of compound **3c**. The solution in EPR tube was frozen at 77 K to make a transparent glass of complex **3c**. Upon recording the UV-vis spectrum of the initial time-point, the mixture was photolyzed (λ = 335 nm) for 20 mins at 77 K (−196 °C) and the photolysis was monitored by collection of periodic UV-vis spectra (see Figure S39). After 1 h of photolysis, the reaction mixture was warmed to 298 K (25 °C). After 5 minutes, the solution was cooled to 77 K and the final UV-vis spectrum was collected (Figure S40).

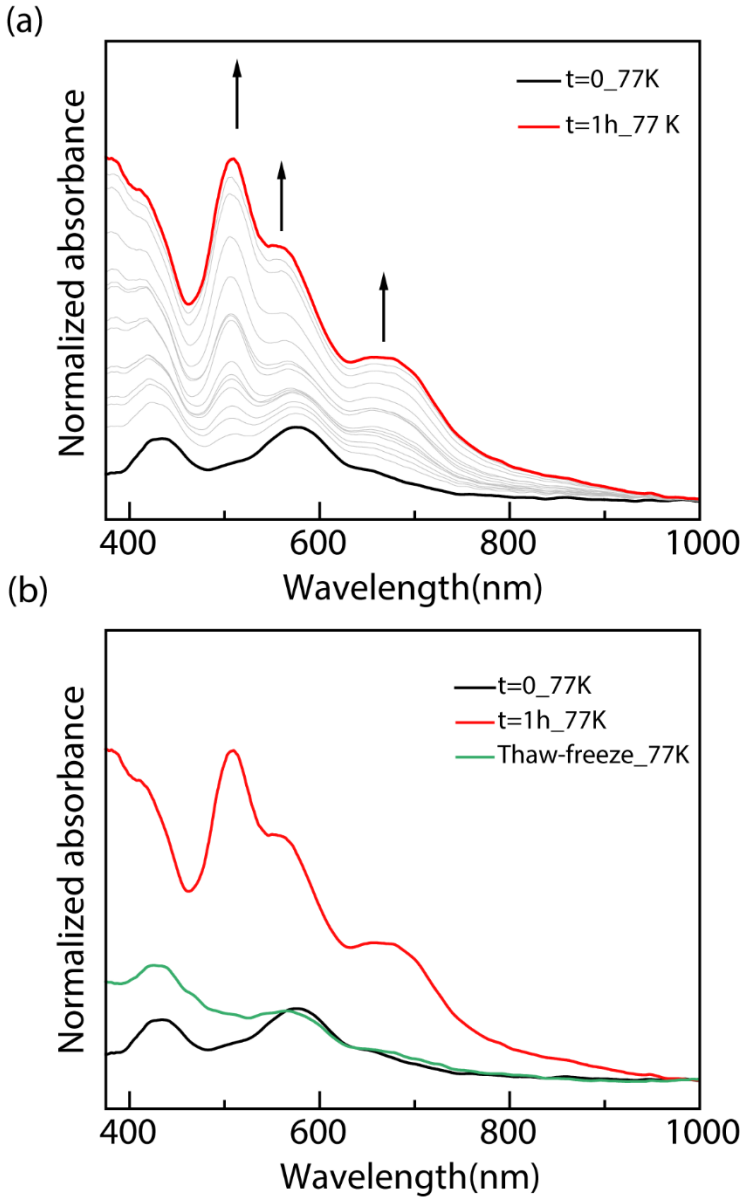

Figure S40. (a) UV-vis spectra recorded during the cryogenic photolysis (λ = 335 nm) of **3c** at 77 K. The spectral evolution from t = 0 (—) to t = 20 mins (—) indicates the conversion of **3c** to **8c**. (b) UV-vis spectra of **3c** (black), **8c** (i.e., after 20 mins photolysis, red), and after thermal annealing (green) collected at 77 K.

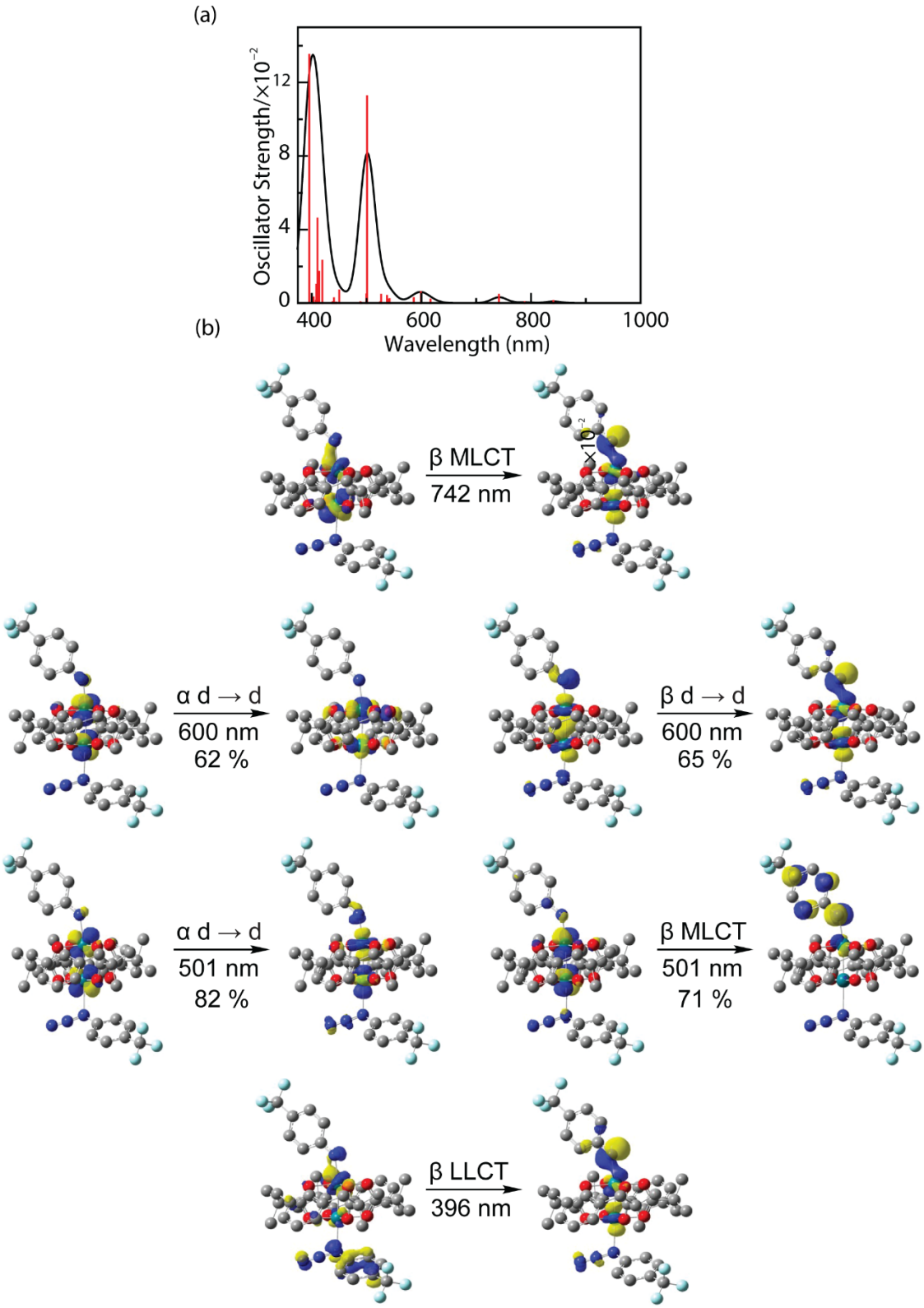

Figure S41. (a) TD-DFT simulated spectrum (black) of ^{3}[**8c**] along with corresponding the vertical excitations (red). (b) NTO analysis of ^{3}[**8c**].

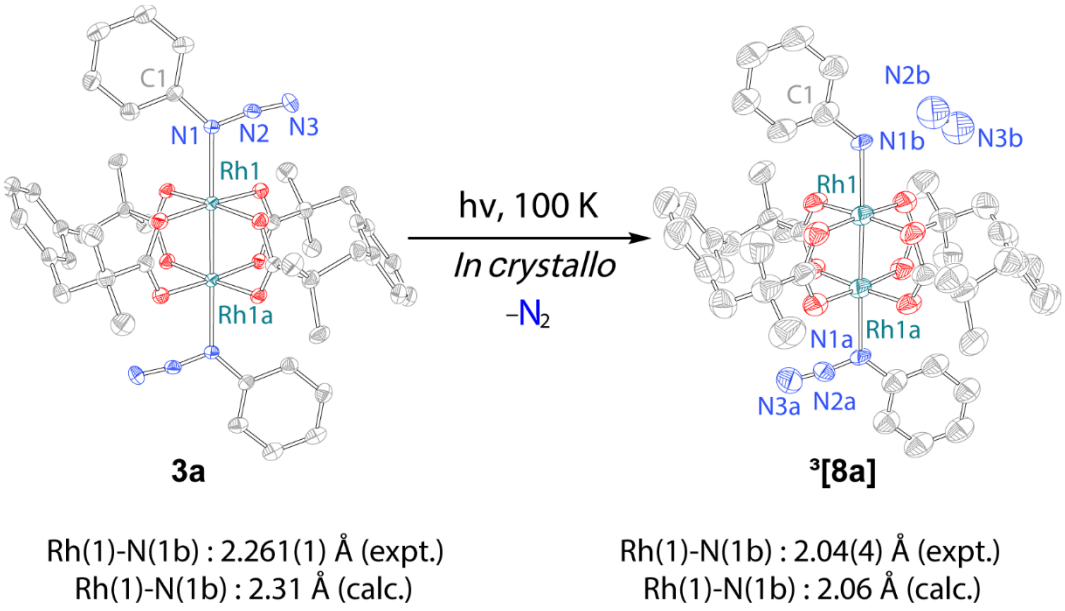

3a

Rh(1)-N(1b) : 2.261(1) Å (expt.)
Rh(1)-N(1b) : 2.31 Å (calc.)

^{3}[8a]

Rh(1)-N(1b) : 2.04(4) Å (expt.)
Rh(1)-N(1b) : 2.06 Å (calc.)

Figure S42. *In crystallo* characterization of ^{3}[**8a**], upon photo-extrusion of N_2 molecule from **3a** with 35% photoconversion.

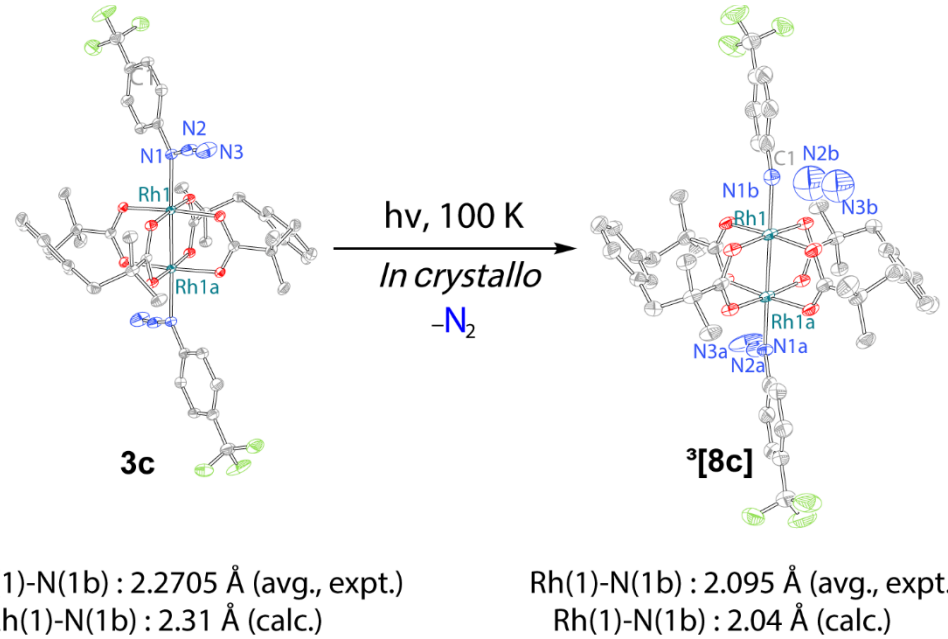

Figure S43. *In crystallo* characterization of ^{3}[**8c**], upon photo-extrusion of N_2 molecule from **3c** with 35% photoconversion.

D. Additional Supporting Data

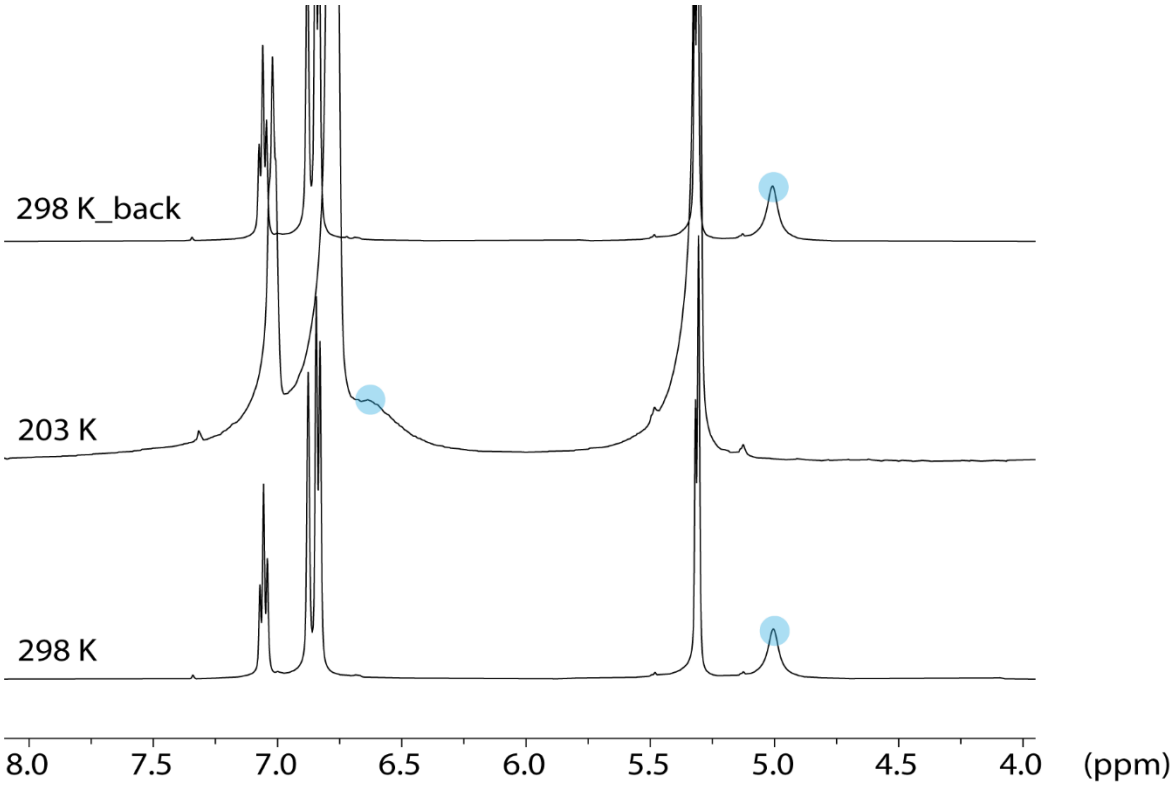

Figure S44. Temperature dependent reversibility of 2. ^{1}H NMR spectra of complex **2** at 298 K, 203 and warming back to 298 K. The shaded highlights (blue) highlight the reversible temperature dependence of N–H peak of the complex (**2**). For comparison, VT-NMR of the free HN_3 performed under the same conditions showed the sharpening of N–H peak with decreasing temperature accompanied by only a 0.20 ppm downfield shift (Figure S45).

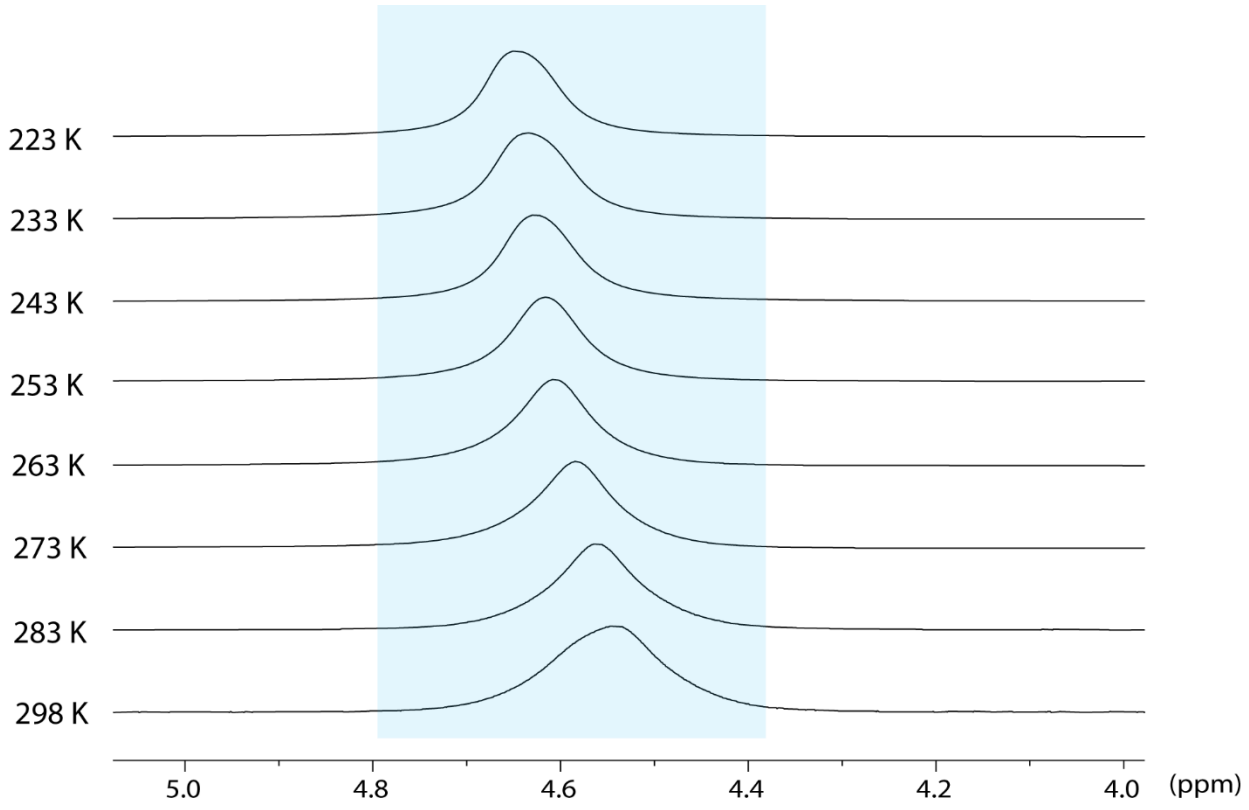

Figure S45. VT-NMR Spectroscopy of HN_3. Temperature-dependent ^1H NMR spectra of HN_3 recorded in CD_2Cl_2 with an instrument operating at 500 MHz. The shaded (blue) area highlights the peak sharpening of the N–H proton of HN_3 upon cooling from 298 K to 223 K.

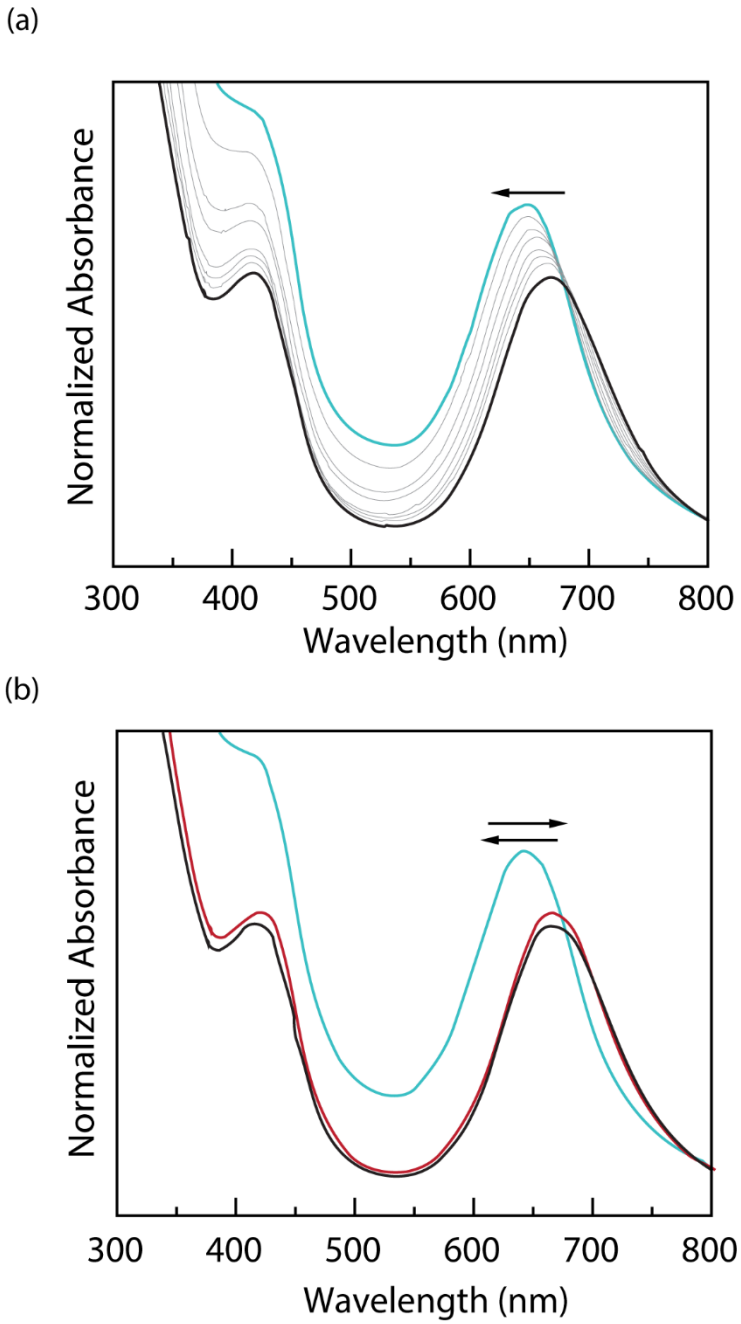

Figure S46. VT-UV-vis Spectroscopy of Compound 1. Temperature-dependent UV-vis spectra of a CH_2Cl_2 solution of $Rh_2(esp)_2$ (**1**). (a) Spectra of complex **1** with decreasing temperature from 298 K (black) to 223 K (sky blue). (b) Spectra of compound (**1**) at 298 K (black), 223 K (sky blue), and warming back to 298 K (brown) showing the reversible temperature dependence.

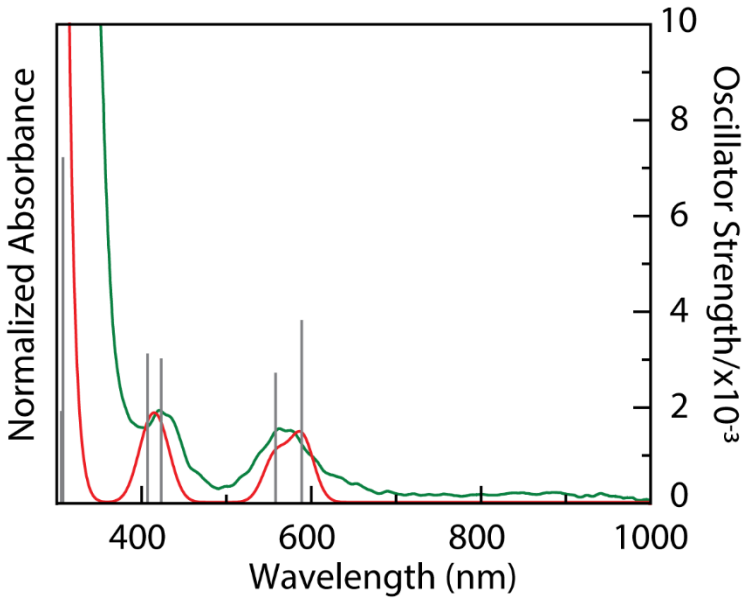

Figure S47. Comparison of the experimental UV-vis spectrum (red) of compound **2** (77 K) with the simulated spectrum (green) for compound **2** based on the vertical excitations (grey) calculated by TD-DFT (PBE0-BS1).

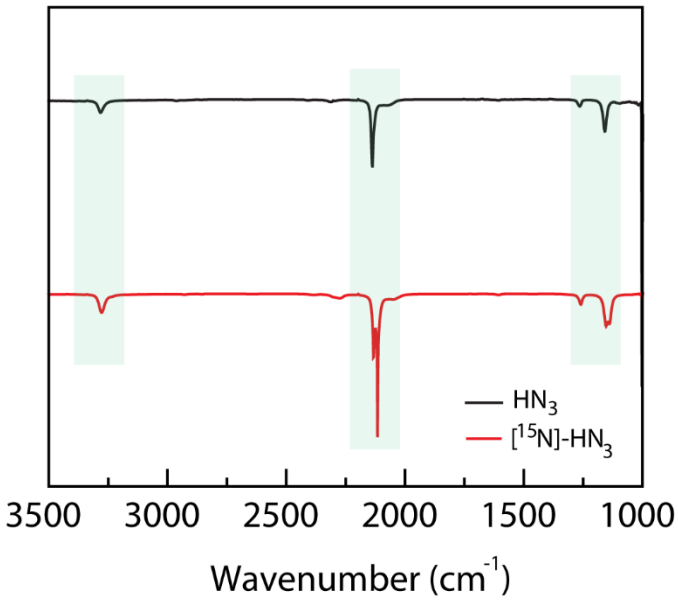

Figure S49. Solution phase IR spectra of HN_3 and [^{15}N]-HN_3 in the spectral range 3500 cm^{-1} to 1000 cm^{-1} at 23 °C. The shaded area highlights the characteristic red shift of peaks attributed to [^{15}N]-HN_3 in comparison to HN_3. For HN_3 (black) the peaks are at 3280 cm^{-1} (N–H stretch), 2137 cm^{-1} (N_3 asymmetric stretch), 2073 cm^{-1}, 1263 cm^{-1}, and 1157 cm^{-1} (N_3 symmetric stretch). For [^{15}N]-HN_3 (red) the peaks are at 3275 cm^{-1} (N–H stretch), 2115 cm^{-1} (N_3 asymmetric stretch), 2050 cm^{-1}, 1259 cm^{-1}, and 1141 cm^{-1} (N_3 symmetric stretch).

E. Computation Details.

All computations were carried out using Revision C.01 of Gaussian 16 suite of programs,[11] All geometries were optimized using the PBE0[12] functional in conjunction with Grimme's D3 empirical dispersion[13] and Becke-Johnson damping[14] the basis set combination (BS1) of the Couty and Hall modification (mod-LANL2DZ) to the basis set of LANL2DZ+ECP combination for Rh[15] and for C, H, N, O basis set of 6–31G(d,p).[16-18] All minima were confirmed by analytical frequency computations. The SMD solvation model was employed for all optimizations using parameters consistent with dichloromethane as the solvent.[19] UV–vis absorption spectra were simulated using TD-DFT[20] single points employing SMD(tert-butylbenzene) on the SMD(DCM)-PBE0-D3BJ/BS1-optimized geometries (SMD(tert-butylbenzene)- TD-DFT//SMD(DCM)-PBE0-D3BJ/BS1). The first 30 vertical excitations were solved iteratively. The simulated spectra were generated using an in-house coded Fortran program using 20nm broadening on a Gaussian line-shape..[21] All orbital images were generated using GaussView6[22] with an isovalue of 0.05. Singlet-triplet gaps (ΔE_{ST}) for the singlet and triplet nitrenes were calculated from single points employing the SMD(DCM)-PBE0 functional in conjunction with Grimme's D3 empirical dispersion and Becke-Johnson damping using the basis set of Def2-TZVP[23] for all atoms with the corresponding ECP on Rh[24] on the previously optimized geometries (SMD-PBE0-D3BJ/Def2-TZVP//SMD-PBE0-D3BJ/BS1) To further corroborate the assignment of a triplet spin ground state for the nitrenes, singlet points were calculated with Orca (Version 6.1.1)[25] utilizing domain based local pair natural orbital coupled cluster method with single-, double-, and perturbative triple excitations[26-28] with def2-TZVP and De2-TZVP/C auxiliary basis sets[29] (DLPNO-CCSD(T)/Def2-TZVP).

Table S3. Optimized coordinates of $^{1}Rh_2(esp)_2(HN_3)_2$ (^{1}[**2**])

Rh	0.065662	0.002324	-1.194299
O	1.489104	-1.466116	-1.053656
O	1.38017	1.453822	1.20604
O	1.384378	-1.459353	1.197355
O	1.490008	1.476281	-1.044756
N	0.324064	-0.001633	-3.483977
N	1.442637	-0.386182	-3.846426
C	1.839333	-1.878429	0.095144
C	2.889168	-2.986696	0.122522
C	1.837209	1.880148	0.107427
C	2.887171	2.988692	0.150948
C	4.142921	2.514646	-0.626422
H	3.865826	2.40123	-1.679387
H	4.88245	3.321441	-0.565773
C	4.264138	0.00616	-0.616358
H	3.495889	0.010363	-1.383437
C	4.737631	1.225562	-0.125148
C	3.236833	3.351139	1.590302
H	2.353435	3.705317	2.128609
H	3.984901	4.151313	1.594616
H	3.64247	2.496096	2.136272
C	3.242813	-3.366867	1.556207
H	3.6487	-2.518187	2.111955
H	3.991961	-4.165913	1.548731
H	2.361135	-3.72999	2.0916
C	4.142015	-2.501988	-0.653591
H	4.882131	-3.309049	-0.605123
H	3.860685	-2.375998	-1.704076
C	4.737359	-1.21869	-0.138599
N	2.459403	-0.836376	-4.048563
C	5.74105	-1.210647	0.835142
H	6.1369	-2.152619	1.206922
C	5.741096	1.206705	0.848585
H	6.136723	2.144429	1.23115
C	6.242046	-0.00465	1.319971
H	7.030132	-0.008797	2.068458
C	2.299414	4.210759	-0.565717
H	2.033037	3.970654	-1.598663
H	3.032141	5.024654	-0.574498

H	1.401093	4.569563	-0.051351
C	2.299611	-4.198942	-0.609464
H	1.403067	-4.565815	-0.097657
H	3.033057	-5.011859	-0.632331
H	2.029792	-3.943417	-1.637766
H	-0.044244	0.721732	-4.103438
Rh	-0.065662	-0.002324	1.194299
O	-1.489104	1.466116	1.053656
O	-1.38017	-1.453822	-1.20604
O	-1.384378	1.459353	-1.197355
O	-1.490008	-1.476281	1.044756
N	-0.324064	0.001633	3.483977
N	-1.442637	0.386182	3.846426
C	-1.839333	1.878429	-0.095144
C	-2.889168	2.986696	-0.122522
C	-1.837209	-1.880148	-0.107427
C	-2.887171	-2.988692	-0.150948
C	-4.142921	-2.514646	0.626422
H	-3.865826	-2.40123	1.679387
H	-4.88245	-3.321441	0.565773
C	-4.264138	-0.00616	0.616358
H	-3.495889	-0.010363	1.383437
C	-4.737631	-1.225562	0.125148
C	-3.236833	-3.351139	-1.590302
H	-2.353435	-3.705317	-2.128609
H	-3.984901	-4.151313	-1.594616
H	-3.64247	-2.496096	-2.136272
C	-3.242813	3.366867	-1.556207
H	-3.6487	2.518187	-2.111955
H	-3.991961	4.165913	-1.548731
H	-2.361135	3.72999	-2.0916
C	-4.142015	2.501988	0.653591
H	-4.882131	3.309049	0.605123
H	-3.860685	2.375998	1.704076
C	-4.737359	1.21869	0.138599
N	-2.459403	0.836376	4.048563
C	-5.74105	1.210647	-0.835142
H	-6.1369	2.152619	-1.206922
C	-5.741096	-1.206705	-0.848585
H	-6.136723	-2.144429	-1.23115

C	-6.242046	0.00465	-1.319971
H	-7.030132	0.008797	-2.068458
C	-2.299414	-4.210759	0.565717
H	-2.033037	-3.970654	1.598663
H	-3.032141	-5.024654	0.574498
H	-1.401093	-4.569563	0.051351
C	-2.299611	4.198942	0.609464
H	-1.403067	4.565815	0.097657
H	-3.033057	5.011859	0.632331
H	-2.029792	3.943417	1.637766
H	0.044244	-0.721732	4.103438

Electronic energy = -2391.894452

Sum of electronic and zero-point energies = -2391.168621

Sum of electronic and thermal energy = -2391.118532

Sum of electronic and thermal enthalpy = -2391.118532

Sum of electronic and free energy = -2391.251042

Table S4. Optimized coordinates of $^{3}Rh_2(esp)_2(NH)$ (^{3}**7**)

Rh	-0.036785	-0.006516	-1.278302
O	1.383636	-1.484043	-1.294079
O	1.451561	1.477696	1.001025
O	1.459579	-1.438741	0.957618
O	1.389418	1.468955	-1.252533
C	1.822784	-1.880113	-0.174665
C	2.870272	-2.98918	-0.192655
C	1.820922	1.891539	-0.139329
C	2.864085	3.004217	-0.182023
C	4.06742	2.514916	-1.030738
H	3.725121	2.390117	-2.062879
H	4.809718	3.321074	-1.025363
C	4.196733	0.006741	-1.013348
H	3.395606	0.005156	-1.74665
C	4.688781	1.230179	-0.550993
C	3.303804	3.396043	1.224627
H	2.456029	3.759816	1.811525
H	4.046997	4.197959	1.162159
H	3.748121	2.554129	1.760639
C	3.296426	-3.362757	1.223233
H	3.732304	-2.512959	1.753709
H	4.043267	-4.162321	1.17801
H	2.44389	-3.72391	1.805113
C	4.081145	-2.502005	-1.032006
H	4.824463	-3.307024	-1.015199
H	3.748716	-2.383064	-2.068138
C	4.695451	-1.214141	-0.551538
C	5.742251	-1.198186	0.375471
H	6.157555	-2.136981	0.733576
C	5.736184	1.219188	0.37552
H	6.147125	2.159933	0.733443
C	6.261291	0.011822	0.830214
H	7.083268	0.013951	1.541209
C	2.224282	4.208748	-0.884067
H	1.892511	3.947225	-1.892392
H	2.953423	5.022355	-0.95648
H	1.361125	4.576781	-0.31887
C	2.244784	-4.204552	-0.888345
H	1.376232	-4.56994	-0.329741

H	2.978586	-5.015349	-0.94178
H	1.924468	-3.956653	-1.903704
Rh	0.021716	0.015977	1.139448
O	-1.397088	1.477426	1.132831
O	-1.483135	-1.455344	-1.156223
O	-1.473364	1.451471	-1.117164
O	-1.403531	-1.459768	1.097255
N	0.388766	-0.202282	3.04673
C	-1.840985	1.884351	0.010477
C	-2.886206	2.992768	0.059203
C	-1.845653	-1.874827	-0.021121
C	-2.890317	-2.984953	0.040843
C	-4.074208	-2.504011	0.920875
H	-3.708591	-2.38611	1.945775
H	-4.815495	-3.311089	0.926422
C	-4.20198	0.00442	0.916766
H	-3.383123	0.002942	1.630168
C	-4.707595	-1.216979	0.463624
C	-3.360559	-3.361908	-1.359943
H	-2.526881	-3.725654	-1.966755
H	-4.107088	-4.160021	-1.289359
H	-3.810429	-2.512526	-1.879309
C	-3.344995	3.361743	-1.347547
H	-3.790241	2.509355	-1.865973
H	-4.09251	4.159677	-1.287124
H	-2.506596	3.723049	-1.949328
C	-4.076832	2.513088	0.93106
H	-4.816727	3.321394	0.93096
H	-3.718827	2.395213	1.958718
C	-4.708832	1.227135	0.468699
C	-5.778887	1.215053	-0.431491
H	-6.200161	2.155441	-0.778304
C	-5.77807	-1.202129	-0.436063
H	-6.199065	-2.141442	-0.786086
C	-6.312478	0.00711	-0.874562
H	-7.15211	0.008106	-1.564638
C	-2.236186	-4.197098	0.716657
H	-1.886183	-3.947236	1.721818
H	-2.963104	-5.012327	0.79311
H	-1.383292	-4.557701	0.131346

C	-2.239248	4.208692	0.735111
H	-1.382641	4.568274	0.154706
H	-2.968523	5.022557	0.802194
H	-1.896242	3.964015	1.743916
H	1.197971	-0.796675	3.289349

Electronic energy = -2117.83543924

Sum of electronic and zero-point energies = -2117.14489

Sum of electronic and thermal energy = -2117.101784

Sum of electronic and thermal enthalpy = -2117.10084

Sum of electronic and free energy = -2117.2172

Table S5. Optimized coordinates of $^{3}Rh_2(esp)_2(NH)(HN_3)$

Rh	0.024546	0.151795	-1.370123
O	1.425385	-1.331686	-1.461264
O	1.513652	1.413292	1.091811
O	1.474549	-1.482278	0.786897
O	1.475143	1.59755	-1.156733
N	-0.232824	0.622071	-3.280302
C	1.844162	-1.832226	-0.369561
C	2.870942	-2.954064	-0.488497
C	1.898175	1.916778	-0.002176
C	2.954829	3.017265	0.048404
C	4.162817	2.583736	-0.82319
H	3.833849	2.552953	-1.866607
H	4.917695	3.373781	-0.738552
C	4.25322	0.082026	-1.021507
H	3.462792	0.157283	-1.762643
C	4.756908	1.252331	-0.447439
C	3.383054	3.290444	1.486376
H	2.531833	3.612845	2.092358
H	4.133411	4.08808	1.496867
H	3.815153	2.403857	1.956402
C	3.270815	-3.468881	0.890267
H	3.713776	-2.681413	1.504527
H	4.003978	-4.274681	0.778605
H	2.403455	-3.867092	1.424303
C	4.101732	-2.412677	-1.263398
H	4.83385	-3.226878	-1.309022
H	3.787058	-2.195592	-2.28907
C	4.726535	-1.182394	-0.661265
C	5.758513	-1.264568	0.278927
H	6.154369	-2.237729	0.559032
C	5.789472	1.143513	0.489473
H	6.209934	2.042667	0.933217
C	6.288849	-0.107418	0.844788
H	7.099738	-0.180788	1.564776
C	2.336789	4.281926	-0.560781
H	2.013376	4.105586	-1.590076
H	3.075101	5.090551	-0.560639
H	1.471208	4.613637	0.023076
C	2.234228	-4.085535	-1.304771

H	1.352536	-4.487485	-0.793744
H	2.954704	-4.900672	-1.428853
H	1.930383	-3.734907	-2.294564
H	-0.829295	1.456694	-3.407815
Rh	0.054611	-0.021198	1.055275
O	-1.35382	1.461283	1.173669
O	-1.4328	-1.294586	-1.365415
O	-1.398922	1.604483	-1.075774
O	-1.38476	-1.467501	0.881299
N	0.139684	-0.445372	3.296597
N	-0.618089	-1.347427	3.681045
C	-1.774263	1.951409	0.083533
C	-2.814614	3.063332	0.186115
C	-1.812535	-1.795948	-0.267049
C	-2.861072	-2.90275	-0.307319
C	-4.056876	-2.478152	0.58592
H	-3.707509	-2.44073	1.622789
H	-4.804987	-3.276168	0.518215
C	-4.167553	0.024411	0.772267
H	-3.364293	-0.038706	1.500461
C	-4.670729	-1.15444	0.215339
C	-3.308225	-3.178265	-1.738664
H	-2.463651	-3.494739	-2.356846
H	-4.053647	-3.980538	-1.739095
H	-3.75159	-2.294022	-2.202566
C	-3.236184	3.546711	-1.197477
H	-3.672914	2.741592	-1.792964
H	-3.98034	4.343364	-1.093017
H	-2.380649	3.948075	-1.747763
C	-4.029875	2.523761	0.986212
H	-4.766738	3.33367	1.032147
H	-3.698321	2.322385	2.009809
C	-4.655986	1.28221	0.408771
N	-1.412203	-2.112003	3.924998
C	-5.704338	1.348204	-0.514358
H	-6.11123	2.315931	-0.797341
C	-5.719813	-1.061452	-0.704644
H	-6.139043	-1.96737	-1.135501
C	-6.235404	0.182384	-1.061147
H	-7.058087	0.243519	-1.768709

C	-2.222056	-4.161031	0.294638
H	-1.884347	-3.97889	1.318629
H	-2.953471	-4.975759	0.307625
H	-1.363067	-4.486582	-0.302214
C	-2.18064	4.217524	0.972516
H	-1.308418	4.617321	0.443884
H	-2.907706	5.028112	1.087651
H	-1.863065	3.890096	1.966054
H	1.033455	-0.472465	3.791247

Electronic energy = -2282.45956148

Sum of electronic and zero-point energies = -2281.745249

Sum of electronic and thermal energy = -2281.697722

Sum of electronic and thermal enthalpy = -2281.696778

Sum of electronic and free energy = -2281.823552

Table S6. Optimized coordinates of $^1[Rh_2(esp)_2(PhN_3)_2]$ (**3a**)

Rh	-0.619213	0.961457	0.346267
O	1.920919	-0.566286	1.182437
O	0.479711	2.086192	-0.97077
O	0.763465	1.251019	1.840572
O	1.648095	0.27465	-1.621877
N	-1.812154	2.850028	0.932133
N	-1.082999	3.84644	0.950097
C	1.718096	0.421502	1.944954
C	2.701764	0.641598	3.091049
N	-0.308161	4.672332	0.976748
C	2.121629	2.372046	-2.673721
C	1.3585	1.504642	-1.677051
C	3.37072	2.02834	2.896457
C	3.249041	2.769844	0.503511
C	-3.216004	3.028429	0.803298
C	-3.992129	1.86894	0.840593
C	3.745527	-0.470233	3.127472
C	-3.806019	4.282224	0.635838
C	-5.371691	1.973227	0.704735
C	2.88449	3.464734	-1.878039
C	1.099834	3.055195	-3.589519
C	1.909376	0.658803	4.402855
C	3.769362	2.933122	-0.782681
C	3.080595	1.525981	-3.504981
C	4.005718	2.230843	1.546948
C	5.874617	2.043939	0.018359
C	5.332598	1.871748	1.290354
C	-5.975766	3.218201	0.536159
C	5.099025	2.566761	-1.014426
C	-5.188622	4.367574	0.504289
Rh	0.619316	-0.961118	-0.345272
O	-1.920793	0.566623	-1.181435
O	-0.479639	-2.085867	0.971743
O	-0.763364	-1.250689	-1.83957
O	-1.648004	-0.274326	1.622876
N	1.811745	-2.849818	-0.931278
N	1.082265	-3.845963	-0.949889
C	-1.717998	-0.421166	-1.943942
C	-2.701676	-0.641265	-3.090026

N	0.307196	-4.671636	-0.976786
C	-2.121638	-2.37178	2.674595
C	-1.358447	-1.504329	1.678012
C	-3.370396	-2.028145	-2.895619
C	-3.248739	-2.769707	-0.502689
C	3.215745	-3.028813	-0.805106
C	3.992072	-1.86939	-0.840459
C	-3.745622	0.470402	-3.126242
C	3.805779	-4.283206	-0.642153
C	5.371832	-1.97435	-0.707153
C	-2.884219	-3.464625	1.87886
C	-1.099891	-3.054743	3.590588
C	-1.909325	-0.65815	-4.40186
C	-3.769146	-2.933231	0.783435
C	-3.080847	-1.525805	3.505667
C	-4.00548	-2.230914	-1.546188
C	-5.874627	-2.044774	-0.017814
C	-5.332517	-1.87231	-1.289734
C	5.975917	-3.219914	-0.543046
C	-5.098969	-2.567364	1.015039
C	5.188576	-4.369205	-0.513099
H	0.391846	3.654234	-3.010845
H	1.616963	3.71186	-4.297043
H	0.535097	2.314231	-4.165865
H	1.417818	-0.305049	4.574816
H	2.586299	0.847816	5.242731
H	1.143436	1.438652	4.389807
H	4.118264	2.139209	3.690359
H	2.607468	2.797242	3.053942
H	2.220054	3.060746	0.695644
H	-3.510421	0.905211	0.963371
H	4.314628	-0.524221	2.196769
H	4.442287	-0.289927	3.9532
H	3.272126	-1.443576	3.284959
H	-3.198231	5.18276	0.606607
H	2.144171	4.144833	-1.444067
H	3.474598	4.037573	-2.602599
H	2.537098	0.763783	-4.070544
H	3.610923	2.168242	-4.216228
H	3.819339	1.016565	-2.88199

H	-5.972984	1.068977	0.727201
H	6.911778	1.77678	-0.167298
H	5.945973	1.468622	2.092318
H	-7.053735	3.293201	0.428959
H	5.531167	2.704513	-2.00246
H	-5.649266	5.342413	0.373059
H	-2.606992	-2.796894	-3.053115
H	-4.117853	-2.139079	-3.689595
H	-2.219631	-3.060236	-0.694724
H	3.510417	-0.905224	-0.959906
H	-3.272392	1.443846	-3.283608
H	-4.442391	0.290096	-3.951963
H	-4.314681	0.524162	-2.195499
H	3.197869	-5.183721	-0.614586
H	5.973282	-1.070167	-0.728148
H	-3.474249	-4.037598	2.603378
H	-2.143724	-4.144566	1.444938
H	-0.53535	-2.313673	4.166989
H	-1.617042	-3.711447	4.298059
H	-0.391731	-3.653709	3.012049
H	-1.14325	-1.437869	-4.388945
H	-2.586242	-0.84716	-5.241741
H	-1.417937	0.305811	-4.573699
H	-3.819601	-1.016568	2.882539
H	-3.611165	-2.168101	4.216889
H	-2.537553	-0.763474	4.071244
H	-6.911909	-1.778007	0.167731
H	-5.945942	-1.469357	-2.091747
H	7.054046	-3.295443	-0.43784
H	-5.531183	-2.705334	2.003011
H	5.64922	-5.344507	-0.385364

Electronic energy = -2853.50841214

Sum of electronic and zero-point energies = -2852.617967

Sum of electronic and thermal energy = -2852.559376

Sum of electronic and thermal enthalpy = -2852.558431

Table S7. Optimized coordinates of $^{1}[Rh_2(esp)_2(PhN_3)(PhN)]$ (**^{1}8a**)

Rh	0.492178	0.768488	-0.631206
O	-0.951744	0.62262	-2.099668
O	-1.975042	-1.060264	-1.005522
O	-0.662102	2.060812	0.478149
O	-1.684445	0.36096	1.543516
N	1.68848	2.830891	-1.472246
N	0.976586	3.817996	-1.279534
N	0.209165	4.641733	-1.14068
C	-1.855309	-0.250077	-1.976299
C	-2.895277	-0.344197	-3.090614
C	-2.151204	-0.587063	-4.408547
H	-1.43012	0.210479	-4.605386
H	-2.866663	-0.624089	-5.236793
H	-1.613219	-1.540978	-4.382747
C	-3.876517	-1.482871	-2.831352
H	-3.354924	-2.44299	-2.783457
H	-4.605511	-1.52885	-3.647494
H	-4.416876	-1.349222	-1.891496
C	-3.631669	1.018952	-3.179677
H	-2.913838	1.768134	-3.528549
H	-4.403385	0.917347	-3.951343
C	-4.244767	1.483434	-1.885824
C	-3.490786	2.261879	-1.003323
H	-2.479749	2.545816	-1.282398
C	-3.993069	2.676622	0.233259
C	-5.300346	2.316591	0.576265
H	-5.717611	2.646078	1.524582
C	-6.073267	1.555649	-0.298545
H	-7.093955	1.294922	-0.030576
C	-5.54934	1.136511	-1.519772
H	-6.160386	0.548325	-2.199945
C	-3.114322	3.465439	1.166381
H	-3.719955	4.145099	1.776763
H	-2.422004	4.077325	0.579145
C	-2.275331	2.600838	2.145077
C	-1.275858	3.511939	2.867295
H	-0.655835	2.937278	3.564008
H	-1.81565	4.272047	3.441822
H	-0.618372	4.014958	2.15319

C	-3.166932	1.89487	3.16119
H	-3.884181	1.226548	2.679029
H	-3.722831	2.640802	3.739215
H	-2.56895	1.298822	3.856397
C	-1.476812	1.594282	1.321833
C	3.072747	2.928074	-1.174075
C	3.830364	1.7796	-1.407971
H	3.339476	0.887445	-1.783209
C	5.18936	1.790179	-1.118279
H	5.773909	0.89074	-1.288555
C	5.793502	2.934711	-0.598141
H	6.855068	2.937083	-0.369434
C	5.02605	4.074942	-0.368528
H	5.486694	4.970655	0.038325
C	3.663757	4.080686	-0.653882
H	3.069631	4.972252	-0.4699
Rh	-0.618382	-1.058168	0.522439
O	0.834914	-0.901412	1.97686
O	1.855649	0.788979	0.891205
O	0.555144	-2.331851	-0.600652
O	1.588386	-0.628175	-1.655096
N	-1.458047	-2.617547	1.388726
C	1.740791	-0.017541	1.852611
C	2.768259	0.067876	2.979201
C	2.015427	0.350531	4.284319
H	1.279672	-0.431111	4.491591
H	2.722845	0.394687	5.119207
H	1.492844	1.312108	4.232704
C	3.772862	1.182507	2.703798
H	3.271101	2.151309	2.629101
H	4.496409	1.232194	3.524797
H	4.315525	1.018136	1.770379
C	3.479376	-1.30502	3.102304
H	2.743008	-2.037937	3.447326
H	4.237628	-1.205265	3.887557
C	4.111426	-1.797103	1.827579
C	3.355254	-2.553034	0.927955
H	2.326644	-2.796088	1.178801
C	3.876825	-2.992632	-0.291331
C	5.206095	-2.683924	-0.597409

H	5.638098	-3.033436	-1.532009
C	5.980528	-1.945807	0.295146
H	7.016487	-1.721503	0.054273
C	5.437414	-1.500125	1.498138
H	6.04864	-0.927241	2.19118
C	2.997767	-3.756673	-1.245366
H	3.600545	-4.446942	-1.846833
H	2.281309	-4.356752	-0.675368
C	2.199138	-2.86924	-2.235659
C	1.213974	-3.755801	-3.00647
H	0.625698	-3.161424	-3.71426
H	1.763265	-4.513242	-3.575622
H	0.525123	-4.262537	-2.325501
C	3.133344	-2.161581	-3.211787
H	3.848012	-1.51699	-2.694461
H	3.693684	-2.907687	-3.785505
H	2.568433	-1.542118	-3.91391
C	1.387209	-1.854137	-1.433147
C	-2.767173	-2.775329	1.535364
C	-3.760993	-1.787184	1.208212
H	-3.436406	-0.834662	0.813095
C	-5.098479	-2.056686	1.403744
H	-5.84617	-1.309626	1.155857
C	-5.494742	-3.296488	1.923122
H	-6.552712	-3.496592	2.070921
C	-4.557911	-4.283757	2.257663
H	-4.89261	-5.23481	2.65944
C	-3.216634	-4.031494	2.06809
H	-2.456396	-4.767842	2.311119

Electronic energy = -2744.08657825

Sum of electronic and zero-point energies = -2743.206648

Sum of electronic and thermal energy = -2743.150359

Sum of electronic and thermal enthalpy = -2743.149415

Sum of electronic and free energy = -2743.295725

Table S8. Optimized coordinates of $^{3}[Rh_2(esp)_2(PhN_3)(PhN)]$ (**^{3}8a**)

Rh	0.580807	0.857447	0.001011
O	-0.671786	1.546619	-1.468813
O	-1.781307	-0.413398	-1.476982
O	-0.672141	1.543319	1.47215
O	-1.782038	-0.416491	1.475031
N	1.738046	2.860345	0.003997
N	0.966221	3.822712	0.005433
N	0.152778	4.611788	0.006812
C	-1.569196	0.76104	-1.897481
C	-2.464189	1.282206	-3.018236
C	-1.563857	1.67663	-4.194732
H	-0.832135	2.43129	-3.89446
H	-2.174246	2.08529	-5.006841
H	-1.023781	0.805862	-4.582158
C	-3.460167	0.214661	-3.459205
H	-2.940589	-0.669286	-3.839619
H	-4.09077	0.613557	-4.260902
H	-4.104637	-0.105493	-2.637397
C	-3.194417	2.551413	-2.504102
H	-2.446429	3.338146	-2.36252
H	-3.86975	2.878475	-3.302922
C	-3.956938	2.356256	-1.221096
C	-3.315489	2.56946	0.001877
H	-2.283045	2.907079	0.002545
C	-3.957595	2.353528	1.224028
C	-5.292858	1.937942	1.210021
H	-5.818172	1.783067	2.149136
C	-5.955275	1.73979	0.000254
H	-6.998269	1.433923	-0.000368
C	-5.29222	1.940668	-1.208712
H	-5.817039	1.787909	-2.148451
C	-3.195733	2.545922	2.507848
H	-3.871479	2.871265	3.307019
H	-2.447694	3.332977	2.368322
C	-2.465752	1.275649	3.019681
C	-1.566214	1.6676	4.197616
H	-1.026194	0.796072	4.58341
H	-2.177186	2.074298	5.010271
H	-0.834468	2.423089	3.899502

C	-3.461949	0.207089	3.457699
H	-4.105813	-0.1114	2.634774
H	-4.093134	0.604226	4.259811
H	-2.942548	-0.67761	3.836607
C	-1.570007	0.75693	1.89838
C	3.138248	3.093268	0.003242
C	3.955816	1.961676	0.002782
H	3.507741	0.974991	0.003036
C	5.336582	2.123541	0.002019
H	5.969527	1.240855	0.001665
C	5.901684	3.397606	0.001732
H	6.98084	3.517855	0.00115
C	5.073524	4.518339	0.002181
H	5.503177	5.515873	0.001944
C	3.689548	4.376213	0.002919
H	3.051947	5.256553	0.003187
Rh	-0.61282	-1.238659	-0.001527
O	0.660002	-1.890207	1.476656
O	1.769104	0.070694	1.469286
O	0.660896	-1.887066	-1.480391
O	1.769277	0.074241	-1.468896
N	-1.906283	-2.843345	-0.003146
C	1.55562	-1.097604	1.901724
C	2.449285	-1.608556	3.028153
C	1.552075	-2.051581	4.188761
H	0.847497	-2.823689	3.869102
H	2.167792	-2.454307	4.999839
H	0.980707	-1.205359	4.585672
C	3.403739	-0.51415	3.495461
H	2.850105	0.347753	3.878821
H	4.035862	-0.901974	4.30142
H	4.048455	-0.163336	2.686557
C	3.230258	-2.842666	2.502921
H	2.5147	-3.657875	2.3553
H	3.918703	-3.149116	3.298793
C	3.982471	-2.606774	1.220655
C	3.350933	-2.84766	-0.002151
H	2.333041	-3.227758	-0.002872
C	3.983142	-2.604033	-1.224075
C	5.297528	-2.126612	-1.210175

H	5.816071	-1.949536	-2.149142
C	5.949084	-1.895266	-0.000373
H	6.976314	-1.539919	0.000308
C	5.296867	-2.129337	1.208548
H	5.814893	-1.954382	2.148198
C	3.231637	-2.837139	-2.507276
H	3.920522	-3.141909	-3.303412
H	2.515993	-3.652653	-2.361782
C	2.450977	-1.601935	-3.030362
C	1.55452	-2.042528	-4.192494
H	0.983229	-1.195522	-4.587844
H	2.170784	-2.443321	-5.004114
H	0.849908	-2.815489	-3.874975
C	3.405679	-0.506492	-3.494739
H	4.049764	-0.157252	-2.684651
H	4.038419	-0.892615	-4.30103
H	2.85224	0.356134	-3.876745
C	1.5565	-1.093385	-1.903486
C	-3.222594	-2.986955	-0.002926
C	-4.115945	-1.867958	-0.002554
H	-3.697422	-0.869485	-0.002327
C	-5.48024	-2.08163	-0.002477
H	-6.148641	-1.225404	-0.002197
C	-6.00465	-3.380516	-0.002739
H	-7.079819	-3.532016	-0.002676
C	-5.143252	-4.48519	-0.003085
H	-5.552343	-5.491414	-0.003291
C	-3.773965	-4.306796	-0.003185
H	-3.092731	-5.15206	-0.003486

Electronic energy = -2744.10396693

Sum of electronic and zero-point energies = -2743.225106

Sum of electronic and thermal energy = -2743.168665

Sum of electronic and thermal enthalpy = -2743.167721

Sum of electronic and free energy = -2743.316249

Table S9. Optimized coordinates of $^{1}[Rh_2(esp)_2(pMePhN_3)_2]$ (**3b**)

Rh	0.72984	-0.862581	-0.387784
O	1.991573	-0.364116	1.142656
O	1.579264	0.540982	-1.624543
O	0.625551	1.267831	1.881919
O	0.203511	2.16537	-0.890113
N	1.57139	-3.654082	-1.038421
N	2.154738	-2.56604	-1.032686
N	0.921337	-4.582009	-1.057844
C	1.139907	1.726983	-1.625339
C	1.677042	0.560189	1.945607
C	2.640089	0.854075	3.092825
C	3.360577	3.418226	-0.684493
C	2.880508	3.135932	0.596653
H	1.82424	3.279674	0.806189
C	1.777999	2.723756	-2.588295
C	3.713388	2.661474	1.613082
C	1.86865	0.712474	4.409611
H	1.010573	1.38922	4.437928
H	2.526887	0.947456	5.252749
H	1.504347	-0.312438	4.540204
C	4.724593	3.241203	-0.938148
H	5.124051	3.474245	-1.922077
C	3.12515	2.321737	2.956257
H	2.272356	2.979624	3.152503
H	3.861875	2.492358	3.749697
C	2.82992	2.041857	-3.456983
H	3.634253	1.608454	-2.858129
H	3.266232	2.774775	-4.144031
H	2.383992	1.238674	-4.050465
C	4.18259	-1.296046	-0.922201
H	3.580205	-0.409035	-1.085267
C	3.566726	-2.547631	-0.867056
C	5.697836	-3.585182	-0.474399
H	6.282364	-4.484656	-0.298596
C	2.401531	3.872944	-1.751905
H	2.90377	4.546974	-2.455353
H	1.583952	4.432556	-1.285723
C	5.556178	-1.207631	-0.748367
H	6.026971	-0.228267	-0.7849

C	3.816614	-0.116952	3.071565
H	3.472065	-1.148087	3.191115
H	4.496892	0.115583	3.898002
H	4.374022	-0.060324	2.134094
C	0.668752	3.306375	-3.471493
H	0.196592	2.522418	-4.073657
H	1.091303	4.050102	-4.155248
H	-0.103409	3.787983	-2.865846
C	4.320806	-3.697756	-0.643928
H	3.845822	-4.674439	-0.598907
C	5.07322	2.492398	1.334944
H	5.743013	2.14196	2.116291
C	6.340365	-2.345525	-0.52008
C	5.57389	2.785484	0.06812
H	6.635128	2.66541	-0.134213
C	7.824068	-2.226208	-0.326986
H	8.059731	-1.60027	0.541246
H	8.300403	-1.759674	-1.196653
H	8.28646	-3.204757	-0.17277
Rh	-0.729822	0.862728	0.388439
O	-1.991596	0.364187	-1.141931
O	-1.579147	-0.540842	1.625283
O	-0.625497	-1.267637	-1.88132
O	-0.203568	-2.165298	0.890662
N	-1.571701	3.654722	1.036453
N	-2.154848	2.566552	1.032443
N	-0.921807	4.582781	1.05446
C	-1.139929	-1.726898	1.625919
C	-1.67704	-0.560059	-1.944938
C	-2.640137	-0.853972	-3.092102
C	-3.360572	-3.418214	0.685151
C	-2.880476	-3.135847	-0.595966
H	-1.824185	-3.279472	-0.805451
C	-1.777988	-2.723649	2.588923
C	-3.71336	-2.661472	-1.612432
C	-1.868787	-0.712244	-4.40893
H	-1.010655	-1.388916	-4.437328
H	-2.527054	-0.947242	-5.252039
H	-1.504577	0.312705	-4.539496
C	-4.724622	-3.241351	0.938739

H	-5.124107	-3.474466	1.922641
C	-3.125092	-2.321669	-2.95558
H	-2.272253	-2.979503	-3.151815
H	-3.861782	-2.492314	-3.749046
C	-2.82988	-2.04175	3.457646
H	-3.634281	-1.608426	2.858825
H	-3.266113	-2.774656	4.144759
H	-2.383954	-1.238515	4.051057
C	-4.182512	1.296134	0.923151
H	-3.580093	0.409475	1.088023
C	-3.566777	2.54769	0.866176
C	-5.697833	3.58434	0.470896
H	-6.282413	4.483468	0.293497
C	-2.401521	-3.872871	1.752592
H	-2.903747	-4.54688	2.456068
H	-1.583939	-4.43249	1.286426
C	-5.55602	1.20726	0.748866
H	-6.02673	0.227916	0.786931
C	-3.816739	0.116962	-3.070706
H	-3.472286	1.148136	-3.190202
H	-4.497044	-0.115574	-3.89712
H	-4.374084	0.060217	-2.133205
C	-0.668684	-3.306216	3.472093
H	-0.19652	-2.522226	4.074212
H	-1.091184	-4.049935	4.155889
H	0.103466	-3.787821	2.866428
C	-4.320899	3.697364	0.64088
H	-3.846043	4.674054	0.594668
C	-5.073222	-2.492553	-1.334361
H	-5.743014	-2.142167	-2.115732
C	-6.340216	2.344665	0.518212
C	-5.573919	-2.785714	-0.067565
H	-6.63518	-2.665754	0.134718
C	-7.823627	2.224746	0.323249
H	-8.05764	1.6087	-0.552539
H	-8.299458	1.747004	1.187015
H	-8.287811	3.204117	0.180033

Electronic energy = -2932.05879041

Sum of electronic and zero-point energies = -2931.113478

Sum of electronic and thermal energy = -2931.051171
Sum of electronic and thermal enthalpy = -2931.050226
Sum of electronic and free energy = -2931.212481

Table S10. Optimized coordinates of $^{1}[Rh_2(esp)_2(pMePhN_3)(pMePhN)]$ (**^{1}8b**)

Rh	0.580081	0.774128	-0.629503
O	-2.035202	-0.79707	-1.176955
O	-0.483814	2.120372	0.506619
O	-0.821999	0.835962	-2.146534
O	-1.705015	0.478004	1.447027
N	2.043834	2.769573	-1.319871
N	1.465654	3.80956	-1.002593
C	-1.806352	0.047698	-2.097298
C	-2.81133	0.111145	-3.246039
N	0.816926	4.709771	-0.764238
C	-2.099027	2.732256	2.14621
C	-1.370395	1.693656	1.297461
C	-3.405058	1.544095	-3.290376
C	-3.224168	2.663228	-1.050418
C	3.405509	2.615745	-0.946701
C	4.015276	1.4205	-1.33061
C	-3.909829	-0.932917	-3.073718
C	4.113709	3.560288	-0.206219
C	5.329197	1.175415	-0.961974
C	-2.813009	3.722041	1.187378
C	-1.044737	3.504001	2.948327
C	-2.049782	-0.144314	-4.551546
C	-3.729729	3.069708	0.187597
C	-3.09313	2.068723	3.0934
C	-4.017602	2.007422	-1.995772
C	-5.889397	2.191155	-0.468969
C	-5.363501	1.778363	-1.691582
C	6.06213	2.101774	-0.208722
C	-5.078546	2.828437	0.468158
C	5.432131	3.294228	0.154943
Rh	-0.741359	-0.991353	0.39419
O	1.882114	0.589596	0.936311
O	0.344204	-2.326069	-0.746301
O	0.666262	-1.043765	1.9029
O	1.567496	-0.680627	-1.684033
N	-1.764105	-2.486158	1.196032
C	1.656074	-0.247316	1.850674
C	2.648774	-0.315428	3.010205
C	1.986247	-2.93913	-2.357287

C	1.244911	-1.890464	-1.529154
C	3.223588	-1.753729	3.085027
C	3.06136	-2.878275	0.847937
C	-3.078478	-2.499796	1.32097
C	-3.963123	-1.41559	0.968457
C	3.76313	0.70875	2.819031
C	-3.679441	-3.692084	1.856822
C	-5.318249	-1.536625	1.143849
C	2.668866	-3.9419	-1.39066
C	0.949896	-3.694047	-3.197867
C	1.883574	-0.024524	4.306114
C	3.582465	-3.309448	-0.374555
C	3.01259	-2.277459	-3.270956
C	3.852905	-2.242342	1.807711
C	5.75412	-2.500893	0.330445
C	5.212523	-2.060833	1.536212
C	-5.881006	-2.719813	1.67078
C	4.94535	-3.116888	-0.622469
C	-5.039427	-3.793344	2.024932
H	-0.315398	3.974814	2.283716
H	-1.529928	4.283863	3.54476
H	-0.509644	2.836972	3.633101
H	-1.610912	-1.14803	-4.556927
H	-2.735765	-0.070216	-5.402016
H	-1.246222	0.584286	-4.686603
H	-4.153372	1.557717	-4.09116
H	-2.603755	2.232488	-3.577085
H	-2.179538	2.85414	-1.280157
H	3.438277	0.680172	-1.874847
H	-4.467683	-0.788032	-2.145809
H	-4.610247	-0.867555	-3.913343
H	-3.488925	-1.942182	-3.056489
H	3.644122	4.49195	0.099327
H	-2.042954	4.289402	0.654862
H	-3.371657	4.428852	1.811646
H	-2.582899	1.383108	3.775868
H	-3.59626	2.836487	3.690963
H	-3.852334	1.498718	2.552802
H	5.790237	0.233182	-1.247151
H	-6.94059	2.023347	-0.24877

H	-6.003651	1.288358	-2.421051
H	-5.496934	3.154422	1.417218
H	5.97754	4.030415	0.740316
H	2.410021	-2.429294	3.368178
H	3.958618	-1.764769	3.898198
H	2.005776	-3.031348	1.053813
H	-3.535143	-0.507528	0.56781
H	3.359136	1.724371	2.790179
H	4.467812	0.642546	3.655295
H	4.308503	0.542842	1.887578
H	-3.01264	-4.507312	2.122025
H	-5.975687	-0.713737	0.875824
H	3.225523	-4.655988	-2.008628
H	1.882558	-4.499387	-0.871827
H	0.441385	-3.015316	-3.891505
H	1.445574	-4.472027	-3.788219
H	0.195951	-4.16555	-2.562032
H	1.071461	-0.741559	4.453243
H	2.564035	-0.086919	5.162072
H	1.455076	0.983683	4.287874
H	3.765247	-1.727047	-2.701584
H	3.521026	-3.044862	-3.864664
H	2.530272	-1.575995	-3.9574
H	6.814845	-2.366851	0.133901
H	5.850035	-1.583394	2.276487
H	5.375783	-3.462961	-1.559121
H	-5.480548	-4.699176	2.430437
C	-7.356518	-2.818334	1.844853
H	-7.859108	-2.693822	0.878036
H	-7.656203	-3.77452	2.277552
H	-7.717239	-2.007404	2.488638
C	7.474741	1.803075	0.202199
H	7.883128	2.596196	0.834291
H	7.52907	0.861839	0.761228
H	8.129807	1.695999	-0.670154

Electronic energy = -2822.64185233

Sum of electronic and zero-point energies = -2821.707429

Sum of electronic and thermal energy = -2821.647276

Sum of electronic and thermal enthalpy = -2821.646331

Sum of electronic and free energy = -2821.801997

Table S11. Optimized coordinates of $^3[Rh_2(esp)_2(pMePhN_3)(pMePhN)]$ (**^{3}8b**)

Rh	0.660165	0.746899	-0.404471
O	-1.921121	-0.620716	-1.322924
O	-0.394579	1.968974	0.855186
O	-0.635419	1.11822	-1.953606
O	-1.688282	0.240686	1.495285
N	2.038699	2.550821	-0.930934
N	1.394264	3.60382	-0.9248
C	-1.633888	0.349082	-2.083557
C	-2.566219	0.617711	-3.261817
N	0.692278	4.493136	-0.948625
C	-2.074305	2.379514	2.494307
C	-1.32839	1.452404	1.53931
C	-3.127375	2.057302	-3.117999
C	-3.035254	2.822029	-0.729366
C	3.429233	2.598885	-0.63865
C	4.124739	1.392255	-0.731325
C	-3.69334	-0.408969	-3.308277
C	4.086385	3.767123	-0.258625
C	5.480632	1.366712	-0.438815
C	-2.71057	3.52191	1.658323
C	-1.048134	2.988996	3.456456
C	-1.734727	0.540436	-4.547418
C	-3.591927	3.054324	0.531124
C	-3.134413	1.613656	3.278793
C	-3.794802	2.339207	-1.79844
C	-5.736461	2.355883	-0.351113
C	-5.159508	2.110765	-1.595567
C	6.168178	2.524191	-0.052229
C	-4.958926	2.818246	0.708659
C	5.447398	3.718139	0.029027
Rh	-0.726383	-1.106301	0.275164
O	1.876458	0.290426	1.170808
O	0.357713	-2.301764	-0.998428
O	0.591488	-1.442122	1.819786
O	1.648605	-0.566448	-1.628251
N	-2.171298	-2.479839	0.812285
C	1.590065	-0.667483	1.942638
C	2.520649	-0.923162	3.12485
C	2.045495	-2.700452	-2.634034

C	1.293104	-1.77888	-1.677951
C	3.115214	-2.348722	2.975192
C	3.034377	-3.11046	0.586106
C	-3.489713	-2.456766	0.906093
C	-4.263464	-1.284483	0.620331
C	3.624969	0.128264	3.176053
C	-4.182819	-3.640456	1.308896
C	-5.634746	-1.322252	0.7366
C	2.719634	-3.821542	-1.79908
C	1.024008	-3.339218	-3.581549
C	1.685863	-0.870326	4.409059
C	3.592376	-3.327681	-0.676216
C	3.080344	-1.917964	-3.43619
C	3.785474	-2.610503	1.652957
C	5.720907	-2.572769	0.198219
C	5.142863	-2.346627	1.445633
C	-6.316241	-2.490125	1.132534
C	4.952046	-3.055705	-0.858738
C	-5.559078	-3.639587	1.414001
H	-0.270954	3.530886	2.911031
H	-1.5477	3.685934	4.137523
H	-0.568531	2.210716	4.060003
H	-1.315738	-0.462838	-4.681361
H	-2.369149	0.760528	-5.412454
H	-0.910901	1.258749	-4.527402
H	-3.834054	2.209905	-3.941729
H	-2.299438	2.759148	-3.260481
H	-1.977275	3.01634	-0.880946
H	3.594161	0.488996	-1.013043
H	-4.295074	-0.394894	-2.396721
H	-4.346989	-0.193671	-4.160357
H	-3.294485	-1.420053	-3.428951
H	3.547843	4.708296	-0.182603
H	-1.899571	4.134509	1.251116
H	-3.28117	4.148771	2.353036
H	-2.677545	0.822914	3.880482
H	-3.655682	2.300762	3.95384
H	-3.871151	1.14795	2.620374
H	6.013604	0.42151	-0.504961
H	-6.801451	2.192061	-0.208038

H	-5.773624	1.753934	-2.418646
H	-5.417495	3.010804	1.67537
H	5.956564	4.63094	0.327743
H	2.30428	-3.070224	3.117439
H	3.827151	-2.487446	3.796916
H	1.981107	-3.327945	0.74031
H	-3.746931	-0.383182	0.315458
H	3.203879	1.130153	3.299228
H	4.282143	-0.075224	4.02841
H	4.226279	0.13071	2.264321
H	-3.602755	-4.531649	1.528088
H	-6.20545	-0.423512	0.515344
H	3.305023	-4.432278	-2.495935
H	1.929795	-4.458239	-1.387816
H	0.524867	-2.576286	-4.188934
H	1.531559	-4.033155	-4.259785
H	0.261424	-3.890078	-3.024957
H	0.876831	-1.604995	4.383569
H	2.323017	-1.082037	5.274208
H	1.245912	0.123331	4.547859
H	3.825373	-1.447268	-2.790504
H	3.597255	-2.596773	-4.122907
H	2.602799	-1.130951	-4.026647
H	6.780336	-2.379139	0.050908
H	5.750618	-1.974985	2.266905
H	5.412051	-3.236614	-1.82709
H	-6.070364	-4.548292	1.721714
C	-7.808658	-2.493616	1.245082
H	-8.274783	-2.255007	0.281763
H	-8.184619	-3.465629	1.573783
H	-8.150359	-1.734905	1.958835
C	7.634853	2.473475	0.262722
H	8.002652	3.443427	0.607802
H	7.845855	1.733143	1.042374
H	8.219024	2.18576	-0.619048

Electronic energy = -2822.6556666

Sum of electronic and zero-point energies = -2821.722275

Sum of electronic and thermal energy = -2821.661958

Sum of electronic and thermal enthalpy = -2821.661014

Sum of electronic and free energy = -2821.818979

Table S12. Optimized coordinates of $^1[Rh_2(esp)_2(pCF_3PhN_3)_2]$ (**3c**)

Rh	-1.041666	-0.010806	0.579589
F	-8.687488	-1.603105	-0.278505
F	-8.456936	0.293253	-1.280885
F	-9.221223	0.22122	0.744296
O	-0.208869	-1.333703	1.904707
O	1.746926	-1.318478	0.787396
O	-1.621892	-1.518803	-0.698761
O	0.355326	-1.479518	-1.77761
N	-2.983439	-0.055418	1.822981
N	-2.727042	-0.010429	3.032099
N	-2.346656	0.033587	4.09637
C	-4.332288	-0.109458	1.407999
C	-5.403419	-0.118153	2.303847
H	-5.232024	-0.080888	3.375989
C	-6.699536	-0.170385	1.810351
H	-7.536531	-0.173114	2.500833
C	-6.924046	-0.210514	0.435414
C	-5.84815	-0.202684	-0.452289
H	-6.023437	-0.229159	-1.523041
C	-4.54916	-0.151437	0.029153
H	-3.700154	-0.136124	-0.644446
C	-8.3195	-0.319452	-0.092291
C	0.995405	-1.695293	1.731973
C	1.568502	-2.664586	2.760719
C	1.457775	-2.004122	4.140206
H	2.055075	-1.086579	4.182182
H	1.832678	-2.687186	4.909625
H	0.419932	-1.750685	4.373306
C	3.026956	-2.985515	2.451474
H	3.142194	-3.437399	1.463591
H	3.414048	-3.684177	3.200828
H	3.640659	-2.080595	2.47929
C	0.697583	-3.949184	2.75338
H	1.147511	-4.646662	3.469156
H	-0.295175	-3.684704	3.131518
C	0.55939	-4.60332	1.404229
C	1.454632	-5.58451	0.966683
H	2.252107	-5.917328	1.626525
C	1.320524	-6.14466	-0.301538

H	2.014449	-6.914658	-0.62827
C	0.29838	-5.728193	-1.15123
H	0.196417	-6.173082	-2.13807
C	-0.609897	-4.7485	-0.737752
C	-0.470459	-4.210968	0.544895
H	-1.177806	-3.457673	0.879888
C	-1.704531	-4.249916	-1.643833
H	-2.574078	-3.96967	-1.040704
H	-2.021395	-5.044799	-2.328711
C	-1.314813	-3.026731	-2.51586
C	-0.248437	-3.396199	-3.5418
H	0.664582	-3.75803	-3.063153
H	0.016191	-2.53199	-4.15796
H	-0.631123	-4.183673	-4.19977
C	-2.571237	-2.511745	-3.228418
H	-2.969038	-3.290539	-3.887461
H	-2.339963	-1.63462	-3.842868
H	-3.347108	-2.23618	-2.508924
C	-0.816136	-1.920643	-1.591851
Rh	1.041547	0.03132	-0.588358
F	8.753653	1.518616	0.186232
F	8.416921	-0.257217	1.365588
F	9.192414	-0.421778	-0.64959
O	0.209111	1.354249	-1.913556
O	-1.74727	1.338295	-0.797058
O	1.621356	1.539624	0.690489
O	-0.355834	1.50001	1.769171
N	2.988283	0.070773	-1.823961
N	2.739876	0.009162	-3.034025
N	2.36601	-0.045794	-4.100132
C	4.334819	0.101632	-1.39893
C	5.412909	0.06216	-2.285949
H	5.248576	0.004425	-3.358264
C	6.705821	0.092633	-1.783212
H	7.547944	0.057474	-2.466792
C	6.92095	0.159224	-0.4073
C	5.838676	0.200567	0.470978
H	6.006434	0.248515	1.542039
C	4.542266	0.171176	-0.020061
H	3.688308	0.194548	0.646885

C	8.317226	0.244349	0.122993
C	-0.995435	1.715086	-1.741536
C	-1.568448	2.683872	-2.770808
C	-1.454938	2.024125	-4.150398
H	-2.05152	1.106179	-4.193765
H	-1.828998	2.70726	-4.92016
H	-0.416516	1.771491	-4.381793
C	-3.027726	3.002926	-2.463491
H	-3.144957	3.453918	-1.475438
H	-3.414489	3.701699	-3.212904
H	-3.640363	2.097309	-2.493091
C	-0.699119	3.969567	-2.761717
H	-1.149386	4.667078	-3.47725
H	0.294232	3.706665	-3.139378
C	-0.562528	4.62283	-1.411964
C	-1.459522	5.602169	-0.973862
H	-2.257418	5.934158	-1.63361
C	-1.32659	6.16161	0.294799
H	-2.021884	6.930184	0.621979
C	-0.303848	5.746332	1.144355
H	-0.202769	6.190757	2.131491
C	0.606166	4.768488	0.730326
C	0.467825	4.23161	-0.552708
H	1.176497	3.479741	-0.888121
C	1.701687	4.271213	1.636075
H	2.571442	3.992328	1.032615
H	2.01765	5.066381	2.321041
C	1.313994	3.047244	2.507943
C	0.248042	3.415141	3.534888
H	-0.665696	3.776314	3.057137
H	-0.015248	2.550338	4.150803
H	0.630469	4.202642	4.192972
C	2.571517	2.533392	3.219329
H	2.968559	3.31219	3.878828
H	2.341887	1.655395	3.833133
H	3.347471	2.259679	2.499203
C	0.815548	1.941199	1.583775

Electronic energy = -3526.95950594

Sum of electronic and zero-point energies = -3526.059446

Sum of electronic and thermal energy = -3525.993476

Sum of electronic and thermal enthalpy = -3525.992532
Sum of electronic and free energy = -3526.167846

Table S13. Optimized coordinates of $^{1}[Rh_2(esp)_2(pCF_3PhN_3)(pCF_3PhN)]$ (**^{1}8c**)

Rh	0.945916	0.176045	-0.733881
F	8.310095	0.555837	-0.285089
F	7.94522	2.68191	-0.387624
F	8.508494	1.594419	-2.170607
O	0.495837	-1.605442	-1.674145
O	-1.055852	-2.189589	-0.14549
O	2.266172	-0.725661	0.552816
O	0.668816	-1.330222	2.021525
N	2.367071	0.344407	-2.057934
C	3.632177	0.651652	-1.757367
C	4.617404	0.382578	-2.756961
H	4.280863	-0.064131	-3.687245
C	5.94878	0.678929	-2.544155
H	6.693074	0.472894	-3.305315
C	6.328039	1.250995	-1.32642
C	5.393023	1.541221	-0.324443
H	5.72004	2.001112	0.60275
C	4.06174	1.247896	-0.527818
H	3.320884	1.475048	0.227586
C	7.781314	1.526801	-1.048839
C	-0.381305	-2.388867	-1.193849
C	-0.626795	-3.675172	-1.978557
C	-1.102582	-3.282084	-3.382477
H	-2.046383	-2.727969	-3.332605
H	-1.270089	-4.182918	-3.982174
H	-0.361978	-2.657771	-3.889283
C	-1.686336	-4.532053	-1.294101
H	-1.393358	-4.807379	-0.278202
H	-1.841351	-5.449957	-1.871096
H	-2.640003	-3.999392	-1.238884
C	0.719037	-4.437458	-2.102788
H	0.51247	-5.366835	-2.645796
H	1.391261	-3.835903	-2.722695
C	1.387907	-4.741541	-0.788323
C	1.143881	-5.934063	-0.099953
H	0.487202	-6.681999	-0.537638
C	1.746327	-6.172071	1.13311
H	1.559486	-7.10722	1.654467
C	2.589315	-5.219403	1.700153

H	3.057443	-5.411349	2.662541
C	2.848624	-4.017927	1.033006
C	2.253862	-3.8065	-0.213988
H	2.460453	-2.882864	-0.747013
C	3.718046	-2.949105	1.640561
H	4.244967	-2.411602	0.845666
H	4.475258	-3.401242	2.291194
C	2.950807	-1.905831	2.495509
C	2.341549	-2.547185	3.737457
H	1.623501	-3.328871	3.478994
H	1.82302	-1.801499	4.34653
H	3.136724	-2.993067	4.344293
C	3.92622	-0.795563	2.90518
H	4.724755	-1.216467	3.524925
H	3.415948	-0.022674	3.490552
H	4.379521	-0.325381	2.028263
C	1.864454	-1.276115	1.628669
Rh	-0.771086	-0.437811	0.868785
F	-7.062158	-0.199728	-1.935644
F	-7.859896	-1.938675	-0.938723
F	-8.41825	0.044648	-0.27198
O	-0.365344	1.340223	1.818327
O	1.186882	1.926244	0.298447
O	-2.109369	0.469414	-0.398716
O	-0.507681	1.068505	-1.863417
N	-2.734401	-0.581131	2.507585
N	-2.586454	0.27214	3.389231
N	-2.320511	1.001173	4.21316
C	-3.956172	-0.58857	1.794088
C	-4.921204	0.412722	1.9121
H	-4.787218	1.238094	2.605719
C	-6.056059	0.360126	1.112524
H	-6.804474	1.141693	1.19009
C	-6.227369	-0.687481	0.210767
C	-5.265346	-1.694693	0.111345
H	-5.400744	-2.510257	-0.592144
C	-4.129008	-1.648379	0.901518
H	-3.352216	-2.400067	0.811936
C	-7.39317	-0.69584	-0.724273
C	0.498595	2.130741	1.348289

C	0.738565	3.426634	2.115287
C	1.253406	3.040483	3.508238
H	2.203916	2.500159	3.437336
H	1.421499	3.944229	4.103097
H	0.532508	2.406565	4.031805
C	1.761841	4.307361	1.406653
H	1.441114	4.570834	0.396035
H	1.903592	5.231478	1.976831
H	2.729423	3.802828	1.332455
C	-0.621002	4.158095	2.273644
H	-0.424035	5.080999	2.830837
H	-1.270732	3.531062	2.892623
C	-1.312518	4.473535	0.973821
C	-1.109803	5.689098	0.31292
H	-0.473647	6.446348	0.764679
C	-1.725369	5.936073	-0.911761
H	-1.570434	6.88823	-1.412354
C	-2.538323	4.969286	-1.498525
H	-3.013767	5.166725	-2.456223
C	-2.756964	3.745057	-0.858816
C	-2.152362	3.525783	0.38227
H	-2.327832	2.584259	0.893694
C	-3.588869	2.661683	-1.491673
H	-4.113157	2.098826	-0.71313
H	-4.347915	3.102962	-2.147626
C	-2.782241	1.65149	-2.349718
C	-2.159671	2.329524	-3.565118
H	-1.462102	3.119498	-3.276479
H	-1.614564	1.606436	-4.177952
H	-2.95004	2.77327	-4.179929
C	-3.728108	0.530643	-2.800194
H	-4.532572	0.950363	-3.413117
H	-3.193257	-0.21101	-3.403658
H	-4.174528	0.023921	-1.941525
C	-1.712174	1.01581	-1.466244

Electronic energy = -3417.53458882

Sum of electronic and zero-point energies = -3416.645457

Sum of electronic and thermal energy = -3416.581765

Sum of electronic and thermal enthalpy = -3416.580821

Sum of electronic and free energy = -3416.747706

Table S14. Optimized coordinates of $^{3}[Rh_2(esp)_2(pCF_3PhN_3)(pCF_3PhN)]$ (**^{3}8c**)

Rh	0.968978	0.06915	-0.774456
F	8.013005	-3.209501	-0.646215
F	8.465428	-1.302272	0.255044
F	8.790711	-1.603629	-1.864193
O	-0.353659	-0.956665	-1.964477
O	-2.02709	-0.632847	-0.493158
O	1.388918	-1.622529	0.337974
O	-0.312142	-1.261179	1.767331
N	2.659305	-0.310751	-1.863441
C	3.908203	-0.664515	-1.603377
C	4.82215	-0.844258	-2.686081
H	4.469533	-0.68015	-3.69898
C	6.126392	-1.218409	-2.436301
H	6.818519	-1.352101	-3.26094
C	6.559103	-1.420635	-1.120578
C	5.678185	-1.248706	-0.043549
H	6.028274	-1.405147	0.972289
C	4.370995	-0.875136	-0.266451
H	3.673437	-0.732216	0.547996
C	7.958412	-1.878631	-0.848432
C	-1.558843	-1.075323	-1.579309
C	-2.509742	-1.813035	-2.517643
C	-2.477255	-1.105983	-3.877384
H	-2.835692	-0.074507	-3.788755
H	-3.130302	-1.631163	-4.582209
H	-1.464577	-1.08592	-4.288386
C	-3.931075	-1.802828	-1.96332
H	-3.990111	-2.282241	-0.983849
H	-4.594595	-2.335984	-2.652428
H	-4.29928	-0.779702	-1.856996
C	-1.986008	-3.262698	-2.697056
H	-2.710001	-3.788957	-3.329533
H	-1.04096	-3.216078	-3.247713
C	-1.775387	-4.011602	-1.408591
C	-2.791811	-4.772386	-0.822559
H	-3.7518	-4.864689	-1.324457
C	-2.574395	-5.422152	0.390267
H	-3.366359	-6.021551	0.831579
C	-1.34571	-5.313826	1.037548

H	-1.181045	-5.828492	1.981
C	-0.313777	-4.55755	0.47273
C	-0.543807	-3.928718	-0.753613
H	0.255874	-3.349144	-1.206569
C	1.013472	-4.384431	1.16146
H	1.79883	-4.264806	0.408277
H	1.256002	-5.275563	1.751563
C	1.086332	-3.170117	2.124936
C	0.177446	-3.367956	3.334183
H	-0.870217	-3.470016	3.04223
H	0.253287	-2.521088	4.02196
H	0.478671	-4.273712	3.870993
C	2.538382	-2.997724	2.585851
H	2.856071	-3.886067	3.141555
H	2.638651	-2.131252	3.248946
H	3.209774	-2.864181	1.733639
C	0.684369	-1.918618	1.351065
Rh	-0.837584	0.438031	0.777303
F	-8.081603	0.987745	-1.008031
F	-7.277064	-0.932979	-1.577001
F	-8.524474	-0.769135	0.178073
O	0.452678	1.47331	1.989047
O	2.130319	1.167358	0.517034
O	-1.290472	2.128465	-0.306847
O	0.413773	1.782192	-1.738598
N	-2.678781	0.620772	2.269541
N	-2.431655	0.013902	3.322064
N	-2.083079	-0.477883	4.277746
C	-3.95532	0.430952	1.680019
C	-4.816095	-0.605237	2.040503
H	-4.554238	-1.297823	2.835054
C	-6.008837	-0.765093	1.347734
H	-6.677212	-1.578459	1.610108
C	-6.337202	0.106002	0.311332
C	-5.478126	1.151274	-0.029583
H	-5.736579	1.828199	-0.837475
C	-4.284588	1.317377	0.654415
H	-3.582739	2.098925	0.384653
C	-7.55664	-0.146934	-0.515277
C	1.649919	1.615235	1.600142

C	2.588991	2.383384	2.52599
C	2.642139	1.629309	3.860509
H	3.051166	0.622056	3.724077
H	3.290396	2.164764	4.561932
H	1.646743	1.540471	4.303911
C	3.988793	2.481473	1.928377
H	3.98319	2.991331	0.962285
H	4.637257	3.040222	2.611541
H	4.423679	1.489244	1.78042
C	1.986551	3.791885	2.772311
H	2.681939	4.326986	3.428949
H	1.046849	3.667053	3.319752
C	1.7362	4.588433	1.519399
C	2.7032	5.449063	0.990544
H	3.646798	5.583637	1.513643
C	2.458372	6.14094	-0.193186
H	3.211761	6.816132	-0.590275
C	1.252395	5.974181	-0.869756
H	1.067311	6.517281	-1.793292
C	0.269352	5.11884	-0.362285
C	0.523523	4.450802	0.838656
H	-0.239536	3.795341	1.248109
C	-1.025826	4.881469	-1.09257
H	-1.824916	4.698626	-0.367148
H	-1.302991	5.770142	-1.670986
C	-0.994068	3.68787	-2.08312
C	-0.035459	3.954959	-3.23863
H	0.989721	4.098889	-2.88963
H	-0.036379	3.121542	-3.946492
H	-0.350293	4.858186	-3.771943
C	-2.410825	3.458393	-2.624766
H	-2.744757	4.346414	-3.171435
H	-2.432431	2.607852	-3.314736
H	-3.118784	3.263792	-1.814564
C	-0.586046	2.434256	-1.315007

Electronic energy = -3417.55408263

Sum of electronic and zero-point energies = -3416.665848

Sum of electronic and thermal energy = -3416.60206

Sum of electronic and thermal enthalpy = -3416.601116

Sum of electronic and free energy = -3416.769185

F. X-ray Diffraction Data

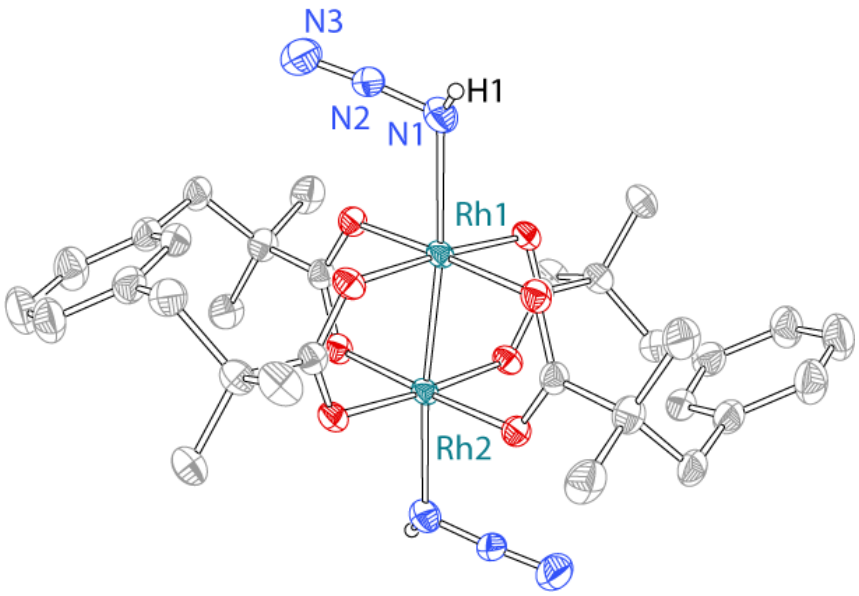

Figure S49. Displacement ellipsoid plot of **2** plotted at 50% probability. H-atoms and dichloromethane are removed for clarity. The crystalline sample used in this diffraction experiment was obtained from a concentrated CH_2Cl_2 solution at −20 °C.

Table S15. X-ray experimental details of **2** (CCDC 2404479)

Crystal data	
Chemical formula	$C_{32}H_{42}N_6O_8Rh_2 \cdot CH_2Cl_2$
M_r	929.46
Crystal system, space group	Monoclinic, $I2/a$
Temperature (K)	100
a, b, c (Å)	22.6442(3), 11.3144(2), 14.9695(2)
β (°)	92.123(1)
V (Å^3)	3832.6(1)
Z	4
Radiation type	Cu $K\alpha$
μ (mm^{-1})	8.72
Crystal size (mm)	0.17 × 0.15 × 0.1
Data collection	
Diffractometer	XtaLAB Synergy, Dualflex, HyPix
Absorption correction	Multi-scan *CrysAlis PRO* 1.171.43.142a (Rigaku Oxford Diffraction, 2024)
T_{min}, T_{max}	0.641, 1.000
No. of measured, independent and observed [$I > 2\sigma(I)$] reflections	20517, 4091, 3917
R_{int}	0.034
$(\sin \theta/\lambda)_{max}$ (Å^{-1})	0.638
Refinement	
$R[F^2 > 2\sigma(F^2)]$, $wR(F^2)$, S	0.029, 0.081, 1.11
No. of reflections	4091
No. of parameters	239
H-atom treatment	H atoms treated by a mixture of independent and constrained refinement
$\Delta\rho_{max}$, $\Delta\rho_{min}$ (e Å^{-3})	0.91, –1.11

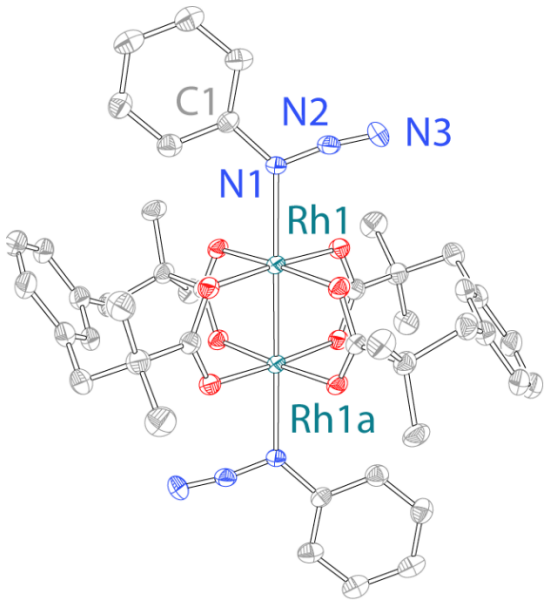

Figure S50. Displacement ellipsoid plot of **3a** plotted at 50% probability. H-atoms and dichloromethane are removed for clarity. The crystalline sample used in this diffraction experiment was obtained from a concentrated CH_2Cl_2 solution layered with pentane at −20 °C.

Table S16. X-ray experimental details of **3a** (CCDC 2514304)

Crystal data	
Chemical formula	$C_{44}H_{50}N_6O_8Rh_2$
M_r	996.72
Crystal system, space group	Tetragonal, $P4_2/n$
Temperature (K)	100
a, c (Å)	19.6356(1), 11.1311(1)
V (Å^3)	4291.67(6)
Z	4
Radiation type	Cu $K\alpha$
μ (mm^{-1})	6.72
Crystal size (mm)	0.37 × 0.29 × 0.24
Data collection	
Diffractometer	XtaLAB Synergy, Dualflex, HyPix
Absorption correction	Multi-scan *CrysAlis PRO* 1.171.43.142a (Rigaku Oxford Diffraction, 2024)
T_{min}, T_{max}	0.801, 1.000
No. of measured, independent and observed [$I > 2\sigma(I)$] reflections	23444, 4615, 4188
R_{int}	0.042
$(\sin\theta/\lambda)_{max}$ (Å^{-1})	0.639
Refinement	
$R[F^2 > 2\sigma(F^2)]$, $wR(F^2)$, S	0.035, 0.101, 1.10
No. of reflections	4615
No. of parameters	275
H-atom treatment	H-atom parameters constrained
$\Delta\rho_{max}$, $\Delta\rho_{min}$ (e Å^{-3})	1.10, −1.17

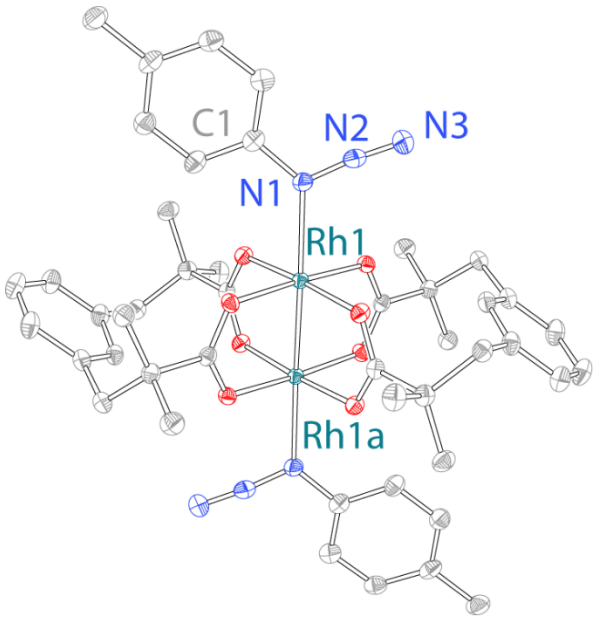

Figure S51. Displacement ellipsoid plot of **3b** plotted at 50% probability. H-atoms and dichloromethane are removed for clarity. The crystalline sample used in this diffraction experiment was obtained from a concentrated CH_2Cl_2 solution layered with pentane at −20 °C.

Table S17. X-ray experimental details of **3b** (CCDC 2516143)

Crystal data	
Chemical formula	$C_{46}H_{54}N_6O_8Rh_2 \cdot 2(CHCl_3)$
M_r	1263.50
Crystal system, space group	Triclinic, *P*–1
Temperature (K)	100
a, *b*, *c* (Å)	9.7362(1), 11.0255(2), 13.0008(2)
α, β, γ (°)	100.047(1), 93.400(1), 104.109(1)
V (Å^3)	1325.13(4)
Z	1
Radiation type	Cu *K*α
μ (mm^{-1})	8.29
Crystal size (mm)	0.39 × 0.34 × 0.26
Data collection	
Diffractometer	XtaLAB Synergy, Dualflex, HyPix
Absorption correction	Multi-scan *CrysAlis PRO* 1.171.43.142a (Rigaku Oxford Diffraction, 2024.
T_{min}, T_{max}	0.843, 1.000
No. of measured, independent and observed [$I > 2\sigma(I)$] reflections	28128, 5651, 5453
R_{int}	0.043
$(\sin \theta/\lambda)_{max}$ (Å^{-1})	0.639
Refinement	
$R[F^2 > 2\sigma(F^2)]$, $wR(F^2)$, S	0.032, 0.088, 1.12
No. of reflections	5651
No. of parameters	321
H-atom treatment	H-atom parameters constrained
$\Delta\varrho_{max}$, $\Delta\varrho_{min}$ (e Å^{-3})	0.61, –1.04

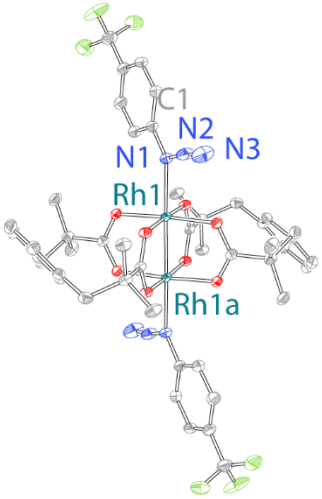

Figure S52. Displacement ellipsoid plot of **3c** plotted at 50% probability. H-atoms and dichloromethane are removed for clarity. The crystalline sample used in this diffraction experiment was obtained from a concentrated CH_2Cl_2 solution layered with pentane at −20 °C.

Table S18. X-ray experimental details of **3c** (CCDC 2514293)

Crystal data	
Chemical formula	$2(C_{23}H_{24}F_3N_3O_4Rh)$
M_r	1132.72
Crystal system, space group	Triclinic, *P*–1
Temperature (K)	100
a, *b*, *c* (Å)	11.4456(2), 14.6808(2), 16.3018(2)
α, β, γ (°)	90.120(1), 95.341(1), 109.552(1)
V (Å^3)	2568.43(7)
Z	2
Radiation type	Cu *K*α
μ (mm^{-1})	5.86
Crystal size (mm)	0.31 × 0.23 × 0.18
Data collection	
Diffractometer	XtaLAB Synergy, Dualflex, HyPix
Absorption correction	
T_{min}, T_{max}	0.646, 1.000
No. of measured, independent and observed [$I > 2\sigma(I)$] reflections	38177, 10960, 10012
R_{int}	0.031
$(\sin\theta/\lambda)_{max}$ (Å^{-1})	0.639
Refinement	
$R[F^2 > 2\sigma(F^2)]$, $wR(F^2)$, S	0.037, 0.107, 1.07
No. of reflections	10960
No. of parameters	649
No. of restraints	54
H-atom treatment	H-atom parameters constrained
$\Delta\rho_{max}$, $\Delta\rho_{min}$ (e Å^{-3})	1.87, –1.16

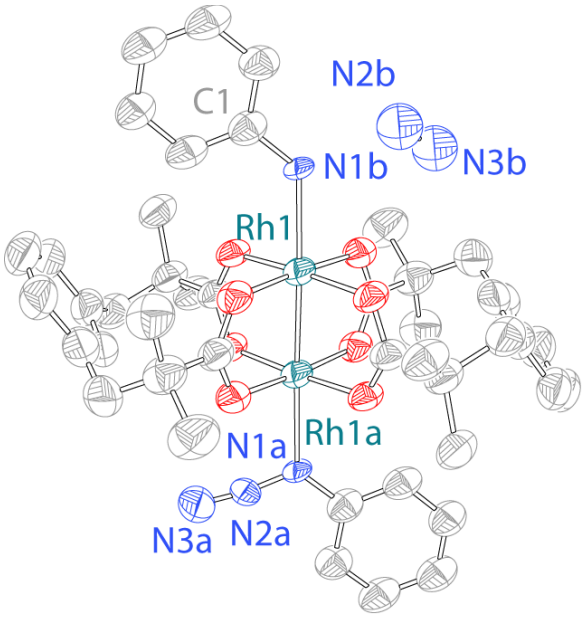

Figure S53. Displacement ellipsoid plot of $Rh_2(esp)_2(C_6H_5N)(C_6H_5N_3)$ (**8a**) plotted at 50% probability. H-atoms and solvent molecules are removed for clarity. The crystal used in this picture was obtained by in situ photolysis of **3a** which resulted in the expulsion of N_2 with 30 % photoconversison.

Table S19. X-ray experimental details of **8a** (CCDC 2523419)

Crystal data	
Chemical formula	$C_{44}N_{4.383}O_8Rh_2 \cdot 0.149(N_2)$
M_r	982.39
Crystal system, space group	Tetragonal, $P4_2/n$
Temperature (K)	100
a, c (Å)	19.8111(4), 11.0700(3)
V (Å^3)	4344.7(2)
Z	4
Radiation type	Cu $K\alpha$
μ (mm^{-1})	6.62
Crystal size (mm)	0.2 × 0.17 × 0.15
Data collection	
Diffractometer	XtaLAB Synergy, Dualflex, HyPix
Absorption correction	Multi-scan *CrysAlis PRO* 1.171.43.142a (Rigaku Oxford Diffraction, 2024)
T_{min}, T_{max}	0.579, 1.000
No. of measured, independent and observed [$I > 2\sigma(I)$] reflections	22190, 4640, 3607
R_{int}	0.060
$(\sin \theta/\lambda)_{max}$ (Å^{-1})	0.640
Refinement	
$R[F^2 > 2\sigma(F^2)]$, $wR(F^2)$, S	0.078, 0.238, 1.06
No. of reflections	4640
No. of parameters	282
No. of restraints	5
$\Delta\rho_{max}$, $\Delta\rho_{min}$ (e Å^{-3})	2.31, −0.83

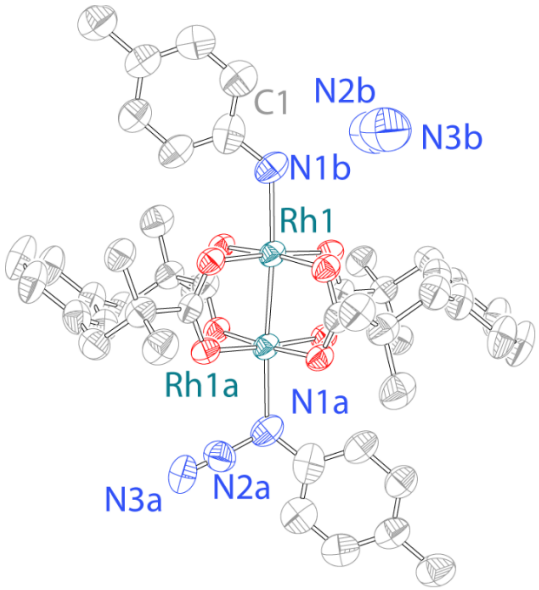

Figure S54. Displacement ellipsoid plot of $Rh_2(esp)_2(C_6H_5N)(C_6H_5N_3)$ (**8b**) plotted at 50% probability. H-atoms and solvent molecules are removed for clarity. The crystal used in this picture was obtained by in situ photolysis of **3b** which resulted in the expulsion of N_2 with 35 % photoconversison.

Table S20. X-ray experimental details of **8b** (CCDC 2524966)

Crystal data	
Chemical formula	$C_{46}H_{54}N_{4.6}O_8Rh_2 \cdot 0.41(N_2) \cdot 2(CHCl_3)$
M_r	1255.38
Crystal system, space group	Triclinic, *P*–1
Temperature (K)	100
a, *b*, *c* (Å)	9.8820(4), 10.9681(6), 13.0253(5)
α, β, γ (°)	99.241(4), 93.779(3), 104.961(4)
V (Å^3)	1337.7(1)
Z	1
Radiation type	Cu *K*α
μ (mm^{-1})	8.21
Crystal size (mm)	0.39 × 0.34 × 0.26
Data collection	
Diffractometer	XtaLAB Synergy, Dualflex, HyPix
Absorption correction	Multi-scan *CrysAlis PRO* 1.171.43.142a (Rigaku Oxford Diffraction, 2024)
T_{min}, T_{max}	0.735, 1.000
No. of measured, independent and observed [$I > 2\sigma(I)$] reflections	25638, 5646, 4673
R_{int}	0.085
$(\sin \theta/\lambda)_{max}$ (Å^{-1})	0.640
Refinement	
$R[F^2 > 2\sigma(F^2)]$, $wR(F^2)$, S	0.076, 0.216, 1.04
No. of reflections	5646
No. of parameters	343
No. of restraints	5
H-atom treatment	H-atom parameters constrained
$\Delta\rho_{max}$, $\Delta\rho_{min}$ (e Å^{-3})	2.73, −1.41

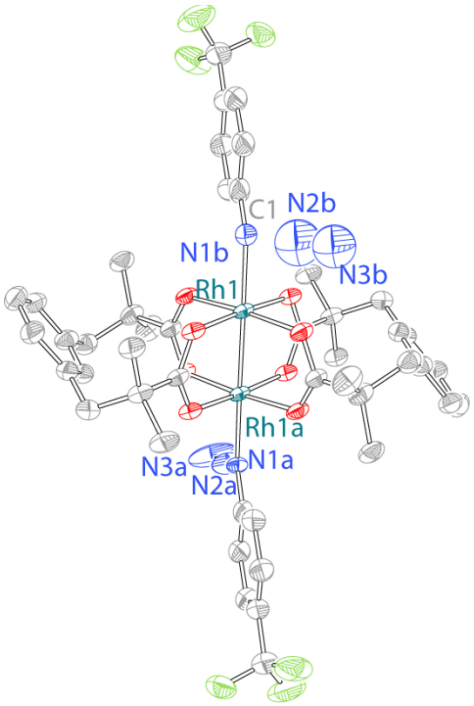

Figure S55. Displacement ellipsoid plot of $Rh_2(esp)_2(C_6H_5N)(C_6H_5N_3)$ (**8c**) plotted at 50% probability. H-atoms and solvent molecules are removed for clarity. The crystal used in this picture was obtained by in situ photolysis of **3c** which resulted in the expulsion of N_2 with 50 % (avg.) photoconversison.

Table S21. X-ray experimental details of **9c** (CCDC 2523425)

Crystal data	
Chemical formula	$2(C_{23}H_{24}F_3N_{2.107}O_4Rh)\cdot 0.934(N_2)\cdot 1[CH3Cl_2]$
M_r	1218.66
Crystal system, space group	Triclinic, *P*–1
Temperature (K)	100
a, *b*, *c* (Å)	11.5718(3), 14.6728(3), 16.2451(3)
α, β, γ (°)	89.822(2), 83.587(2), 70.620(2)
V (Å^3)	2584.0(1)
Z	2
Radiation type	Cu *K*α
μ (mm^{-1})	6.80
Crystal size (mm)	0.3 × 0.3 × 0.3
Data collection	
Diffractometer	XtaLAB Synergy, Dualflex, HyPix
Absorption correction	Multi-scan *CrysAlis PRO* 1.171.44.128a (Rigaku Oxford Diffraction, 2025)
T_{min}, T_{max}	0.596, 1.000
No. of measured, independent and observed [$I > 2\sigma(I)$] reflections	40204, 10984, 9171
R_{int}	0.037
$(\sin\theta/\lambda)_{max}$ (Å^{-1})	0.639
Refinement	
$R[F^2 > 2\sigma(F^2)]$, $wR(F^2)$, S	0.048, 0.142, 1.10
No. of reflections	10984
No. of parameters	675
No. of restraints	579
H-atom treatment	H-atom parameters constrained
$\Delta\rho_{max}$, $\Delta\rho_{min}$ (e Å^{-3})	1.85, −1.63

G. NMR Data

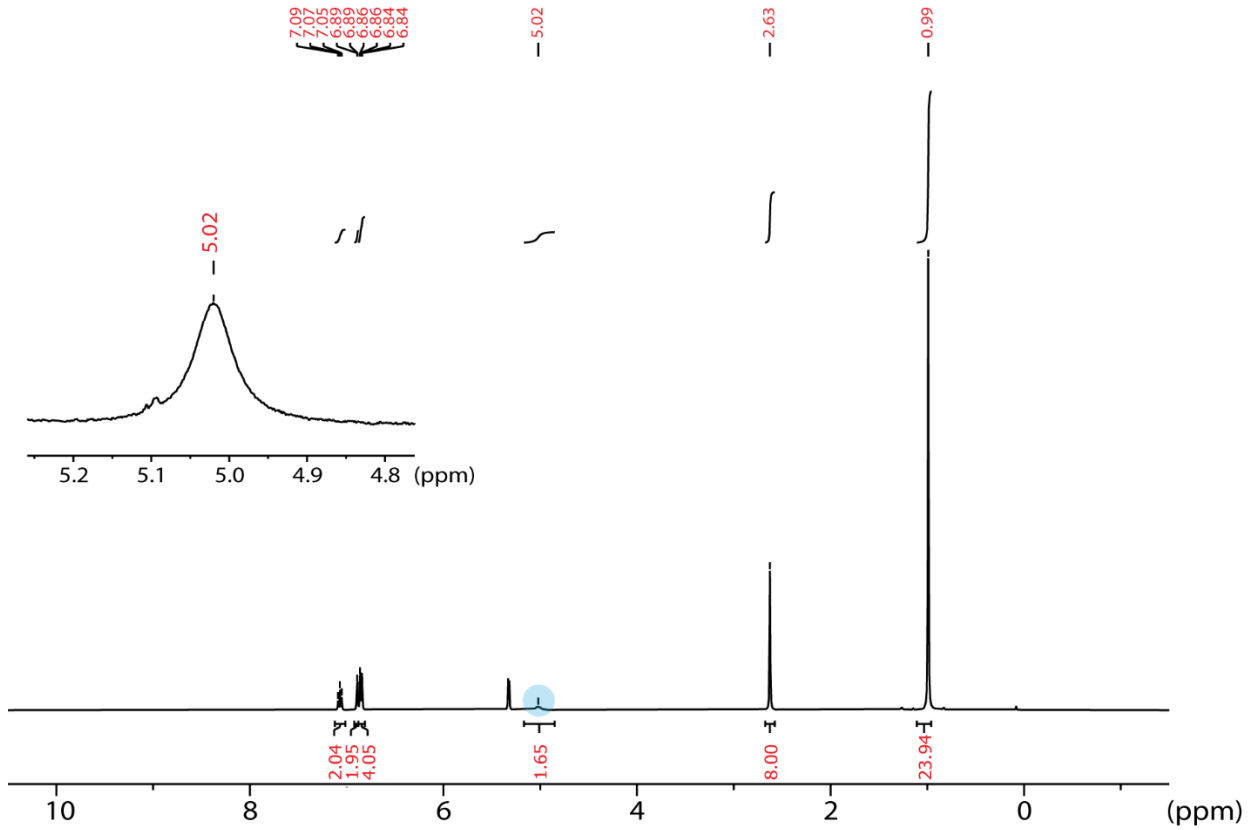

Figure S56. ^{1}H NMR spectrum of **2** recorded in CD_2Cl_2 with an instrument operating at 500 MHz at 23 °C. Inset: Expansion of the spectral window between 5.9 to 4.9 to highlight the resonance attributed to the N–H of coordinated HN_3. The position of this resonance is temperature and concentration dependent (see Figure S5 for the concentration dependence and S3a for temperature dependence of the N–H peak).

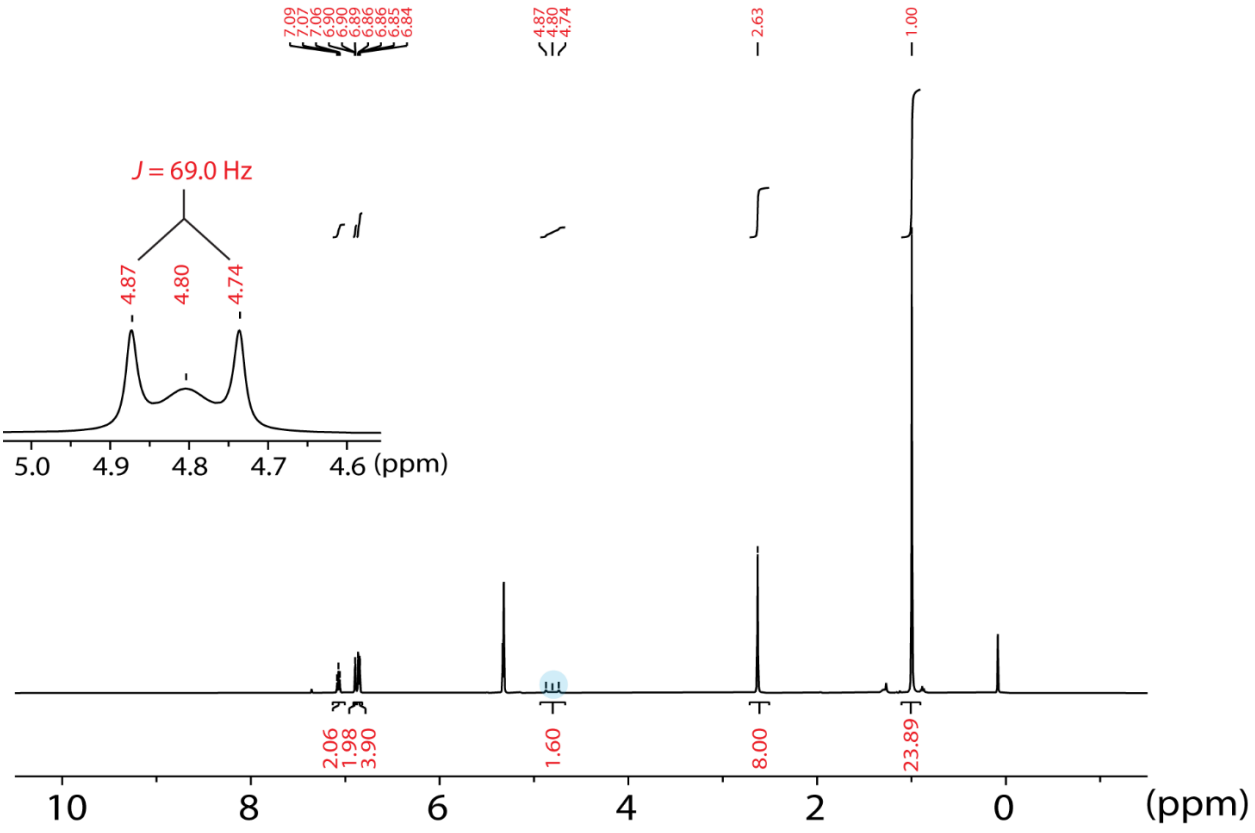

Figure S57. ^{1}H NMR spectrum of [^{15}N]-**2** recorded in CD_2Cl_2 with an instrument operating at 500 MHz at 23 °C. Inset: Expansion of the spectral window between 5.0 to 4.6 to highlight the resonance attributed to the N–H of coordinated [^{15}N]-HN_3. The position of this resonance is temperature and concentration dependent (see Figure S5 for the concentration dependence and S3a for temperature dependence of the N–H peak).

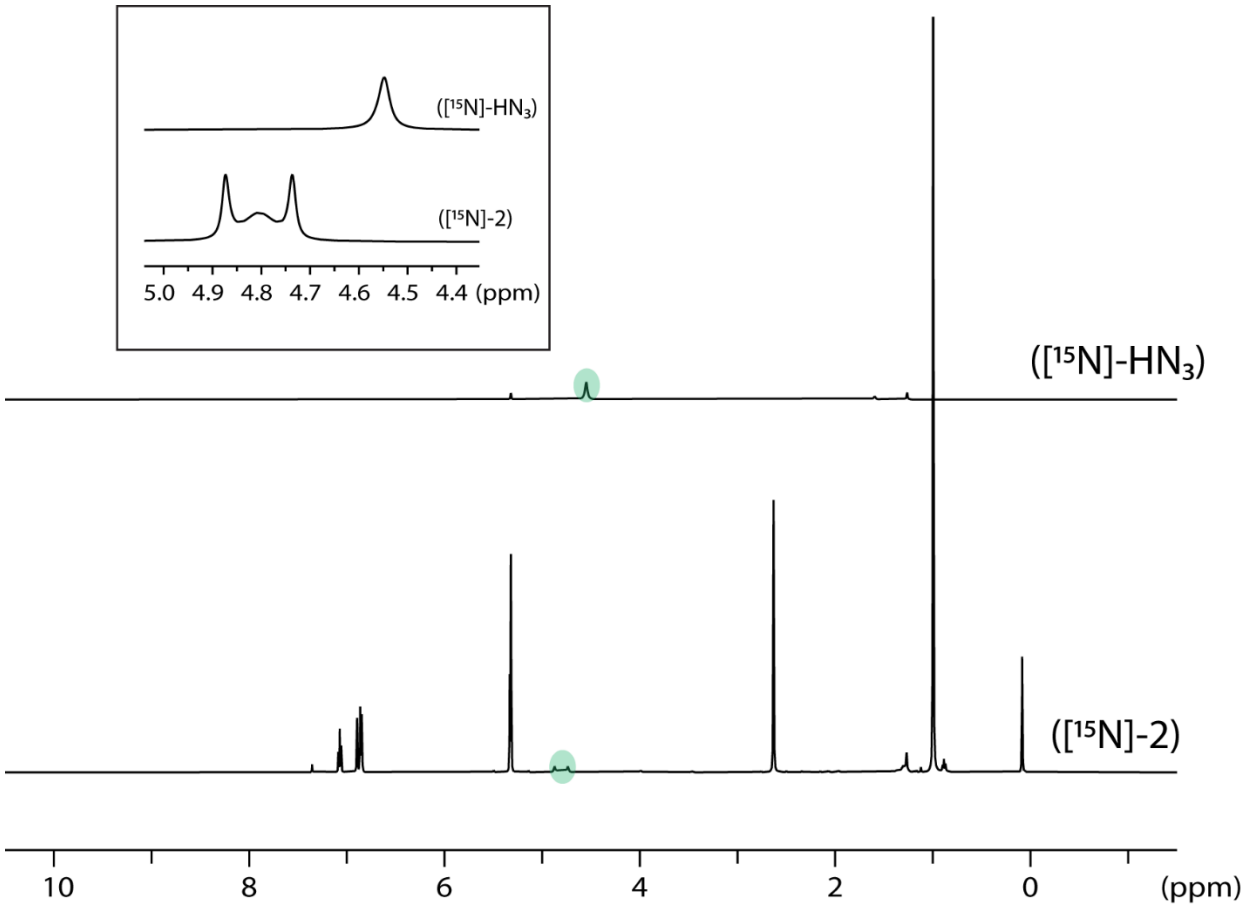

Figure S58. ^{1}H NMR spectra of [^{15}N]-HN_3 (top) and [^{15}N]-**2** (bottom); the N–H resonances are highlighted in green. Inset: Expanded spectral window that highlights the peak splitting for [^{15}N]-**2** due to the ^{1}H-^{15}N coupling (J = 69.0 Hz). Spectra were measured at 500 MHz in CD_2Cl_2 at 23 °C. In contrast to [^{15}N]-HN_3, the doublet splitting in case of the ^{1}H NMR for compound [^{15}N]-**2**, indicates the difference in chemical environment of the (α)-N–H upon coordination of the HN_3 to the Rh_2(II,II) core.

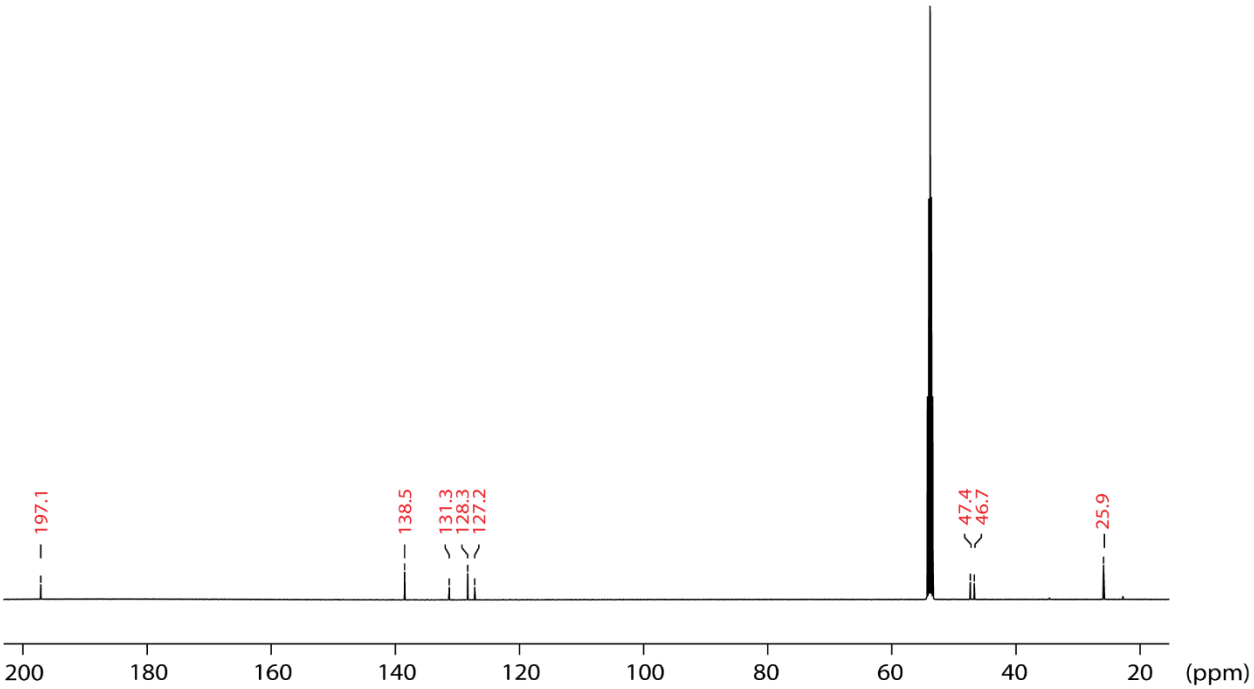

Figure S59. ^{13}C NMR spectrum of **2** recorded in CD_2Cl_2 with an instrument operating at 125.6 MHz at 23 °C.

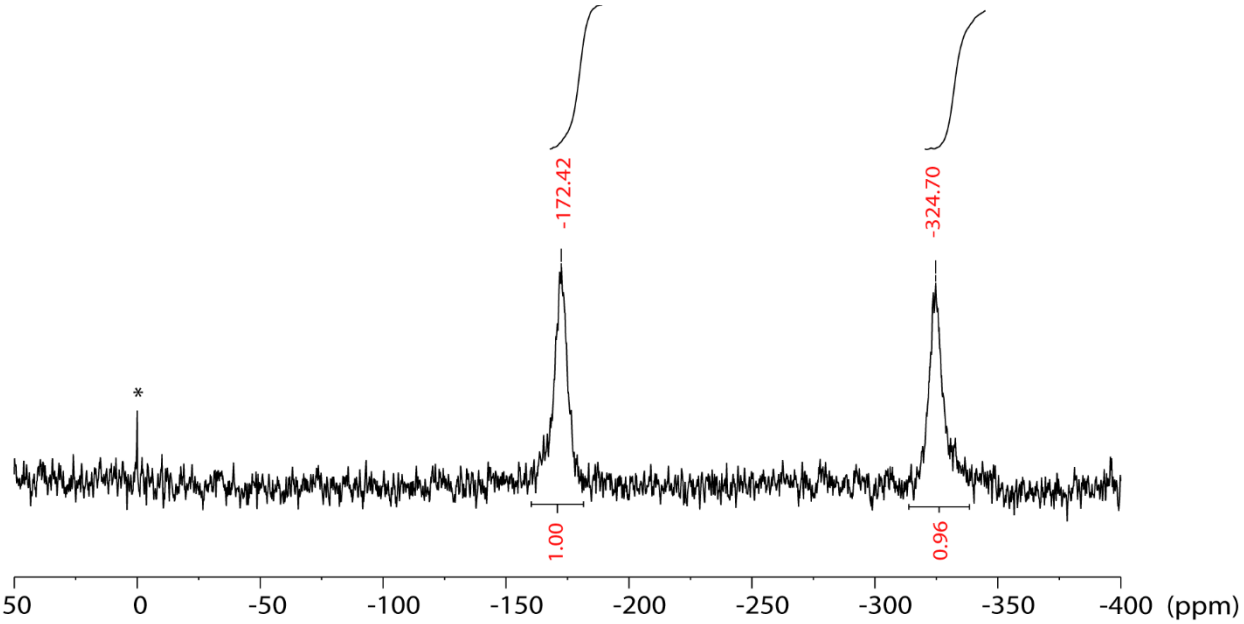

Figure S60. ^{15}N NMR spectrum of [^{15}N]-HN_3 recorded in CD_2Cl_2 with an instrument operating at 50.7 MHz at 23 °C. The (*) indicates the peak of CH_3NO_2 at 380.5 ppm, which has been used as a reference.

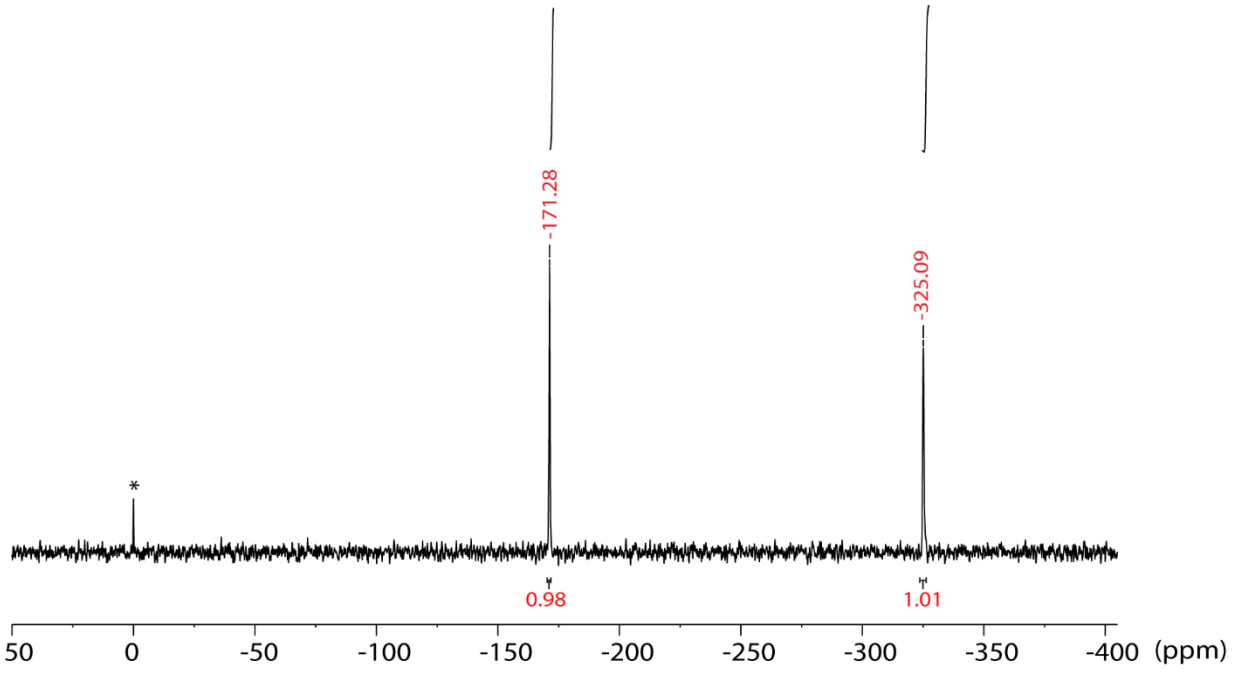

Figure S561. $^{15}N\{^{1}H\}$ NMR spectrum of compound [^{15}N]-**2** recorded in CD_2Cl_2 with an instrument operating at 50.7 MHz at 23 °C. The (*) indicates the peak of CH_3NO_2 at 380.5 ppm, which has been used as a reference.

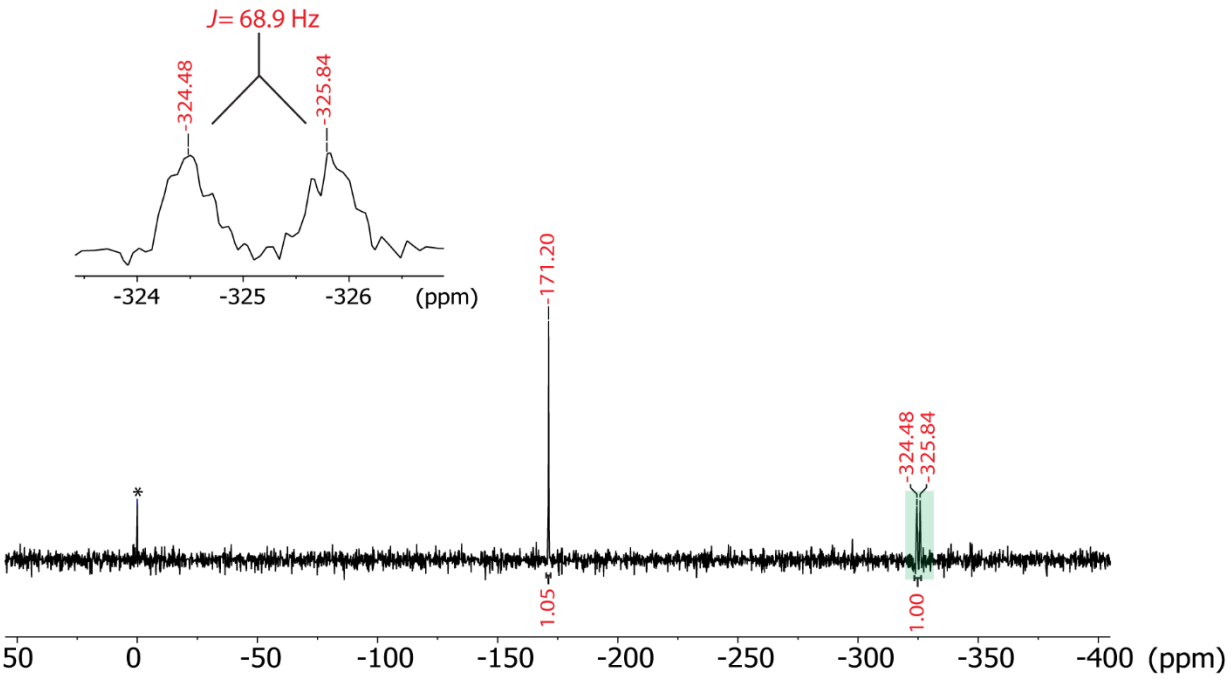

Figure S62. ^{15}N NMR spectrum of c [^{15}N]-**2** recorded in CD_2Cl_2 with an instrument operating at 50.7 MHz at 23 °C. The (*) indicates the peak of CH_3NO_2 at 380.5 ppm, which has been used as a reference. Expansion of the shaded (green) area shows the doublet splitting for ^{15}N-^{1}H coupling (J = 69.7).

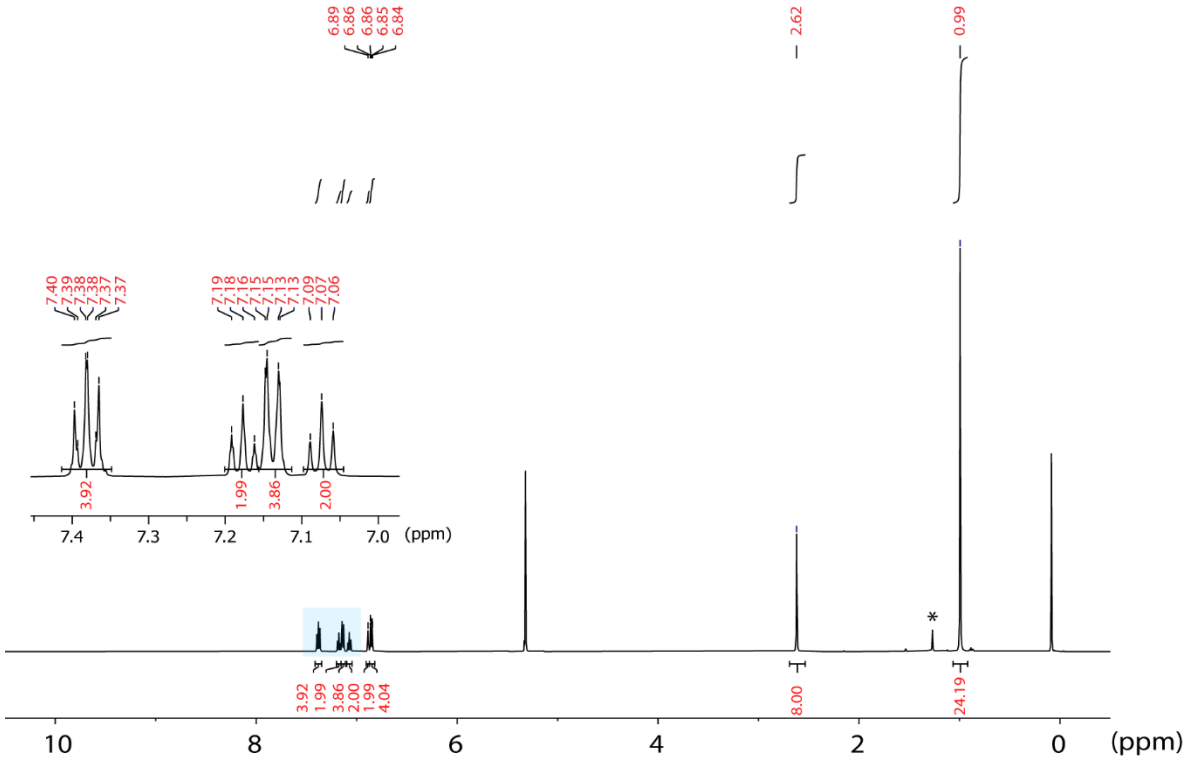

Figure S63. ^{1}H NMR spectrum of **3a** recorded in CD_2Cl_2 with an instrument operating at 500 MHz at 23 °C. Inset: Expansion of the spectral window between 7.5 to 7.0 to highlight the resonance attributed to the phenyl ring of the of coordinated $C_6H_5N_3$. The residual pentane after drying is indicated by the * sign.

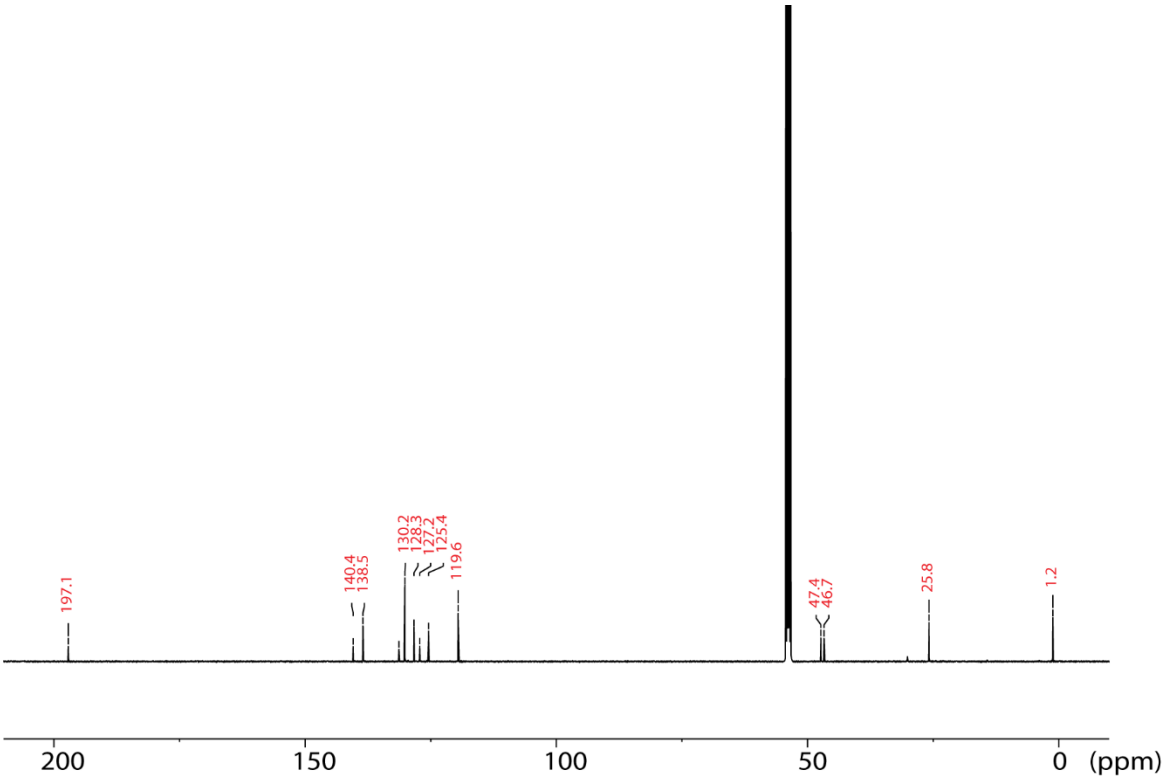

Figure S64. ^{13}C NMR spectrum of **3a** recorded in CD_2Cl_2 with an instrument operating at 125.6 MHz at 23 °C.

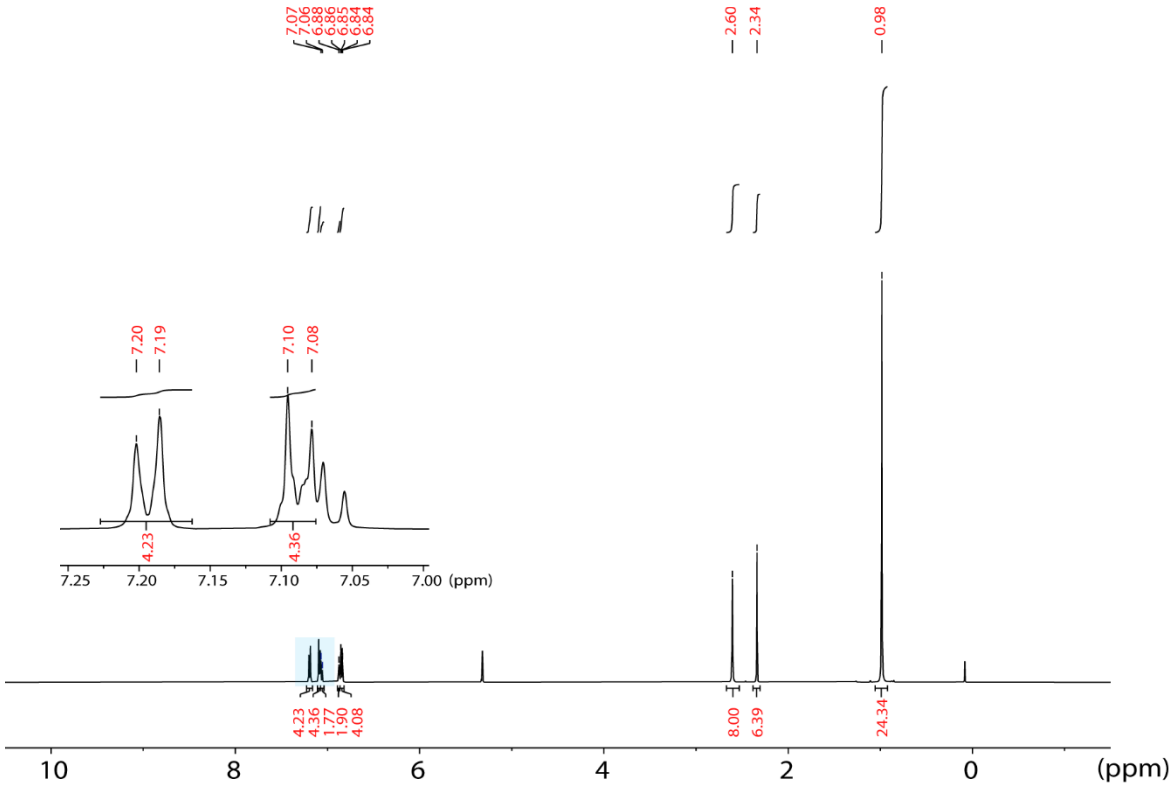

Figure S65. ^{1}H NMR spectrum of **3b** recorded in CD_2Cl_2 with an instrument operating at 500 MHz at 23 °C. Inset: Expansion of the spectral window between 7.05 to 7.25 to highlight the resonance attributed to the aryl ring of the of coordinated 4-CH_3-$C_6H_4N_3$.

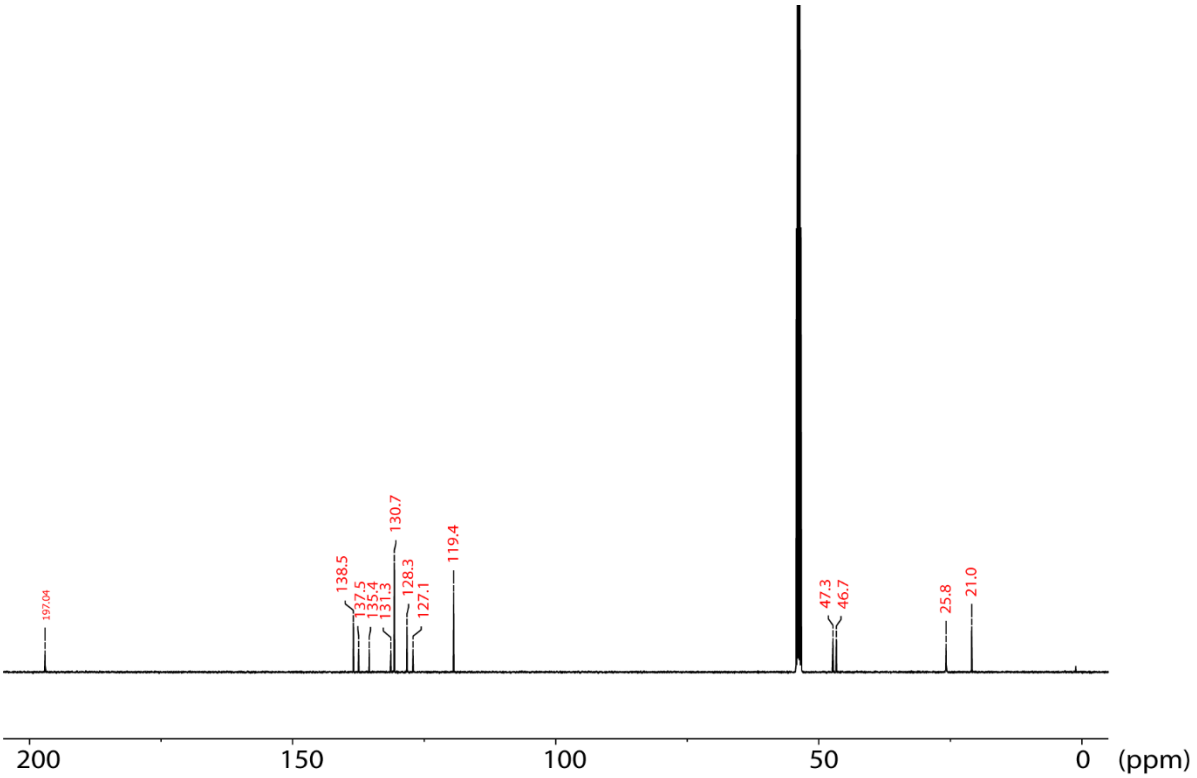

Figure S66. ^{13}C NMR spectrum of **3b** recorded in CD_2Cl_2 with an instrument operating at 125.6 MHz at 23 °C.

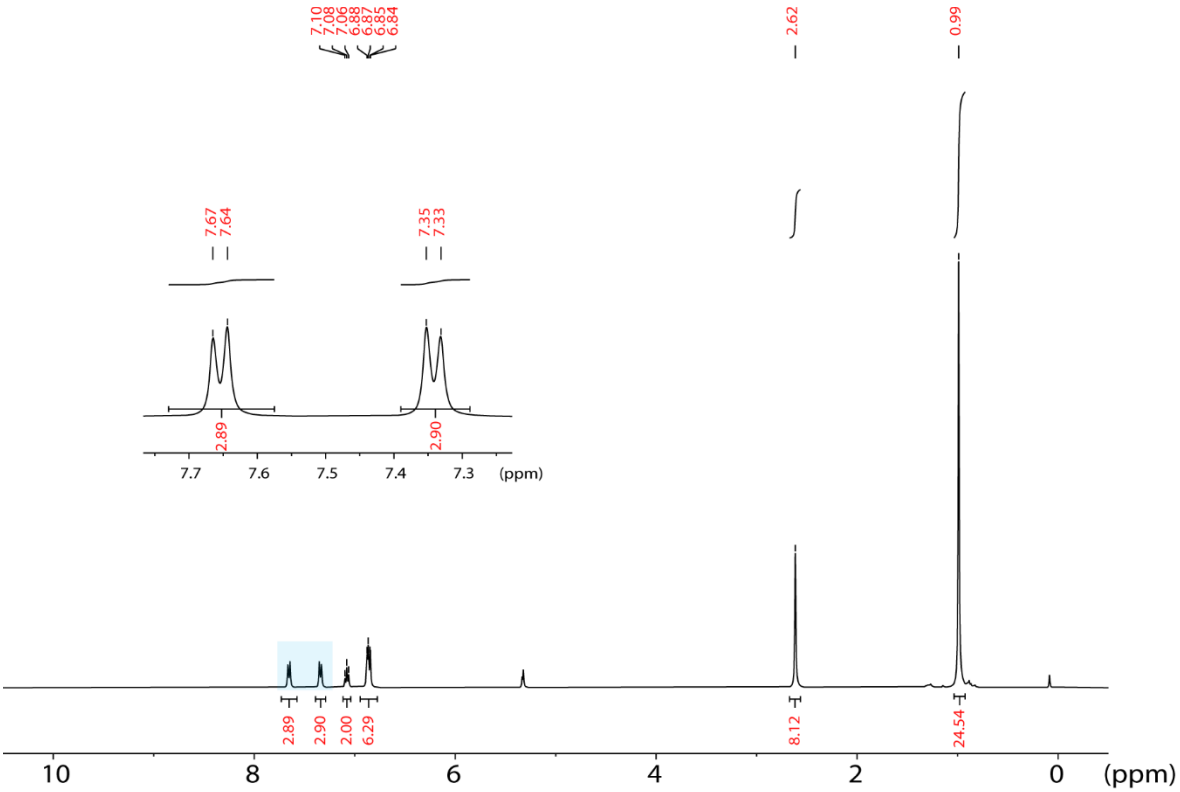

Figure S67. ^{1}H NMR spectrum of **3c** recorded in CD_2Cl_2 with an instrument operating at 500 MHz at 23 °C. Inset: Expansion of the spectral window between 7.05 to 7.25 to highlight the resonance attributed to the aryl ring of the of coordinated 4-CF_3-$C_6H_4N_3$.

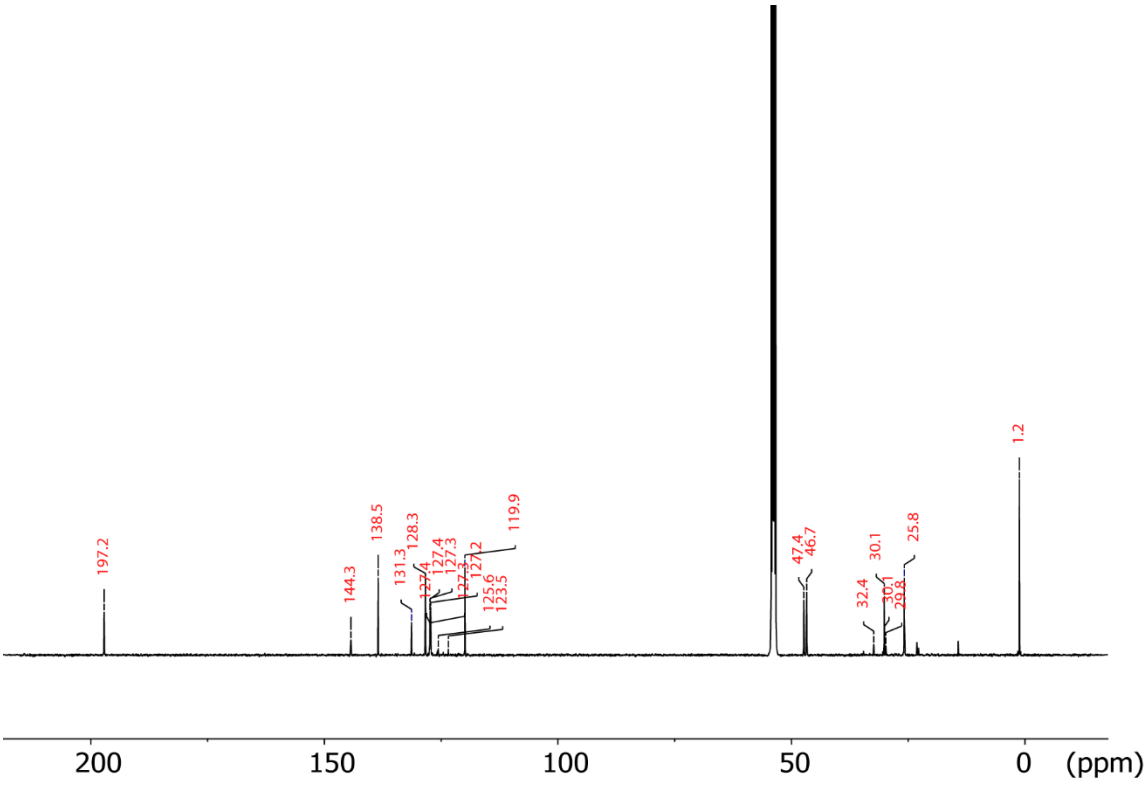

Figure S68. ^{13}C NMR spectrum of **3c** recorded in CD_2Cl_2 with an instrument operating at 125.6 MHz at 23 °C.

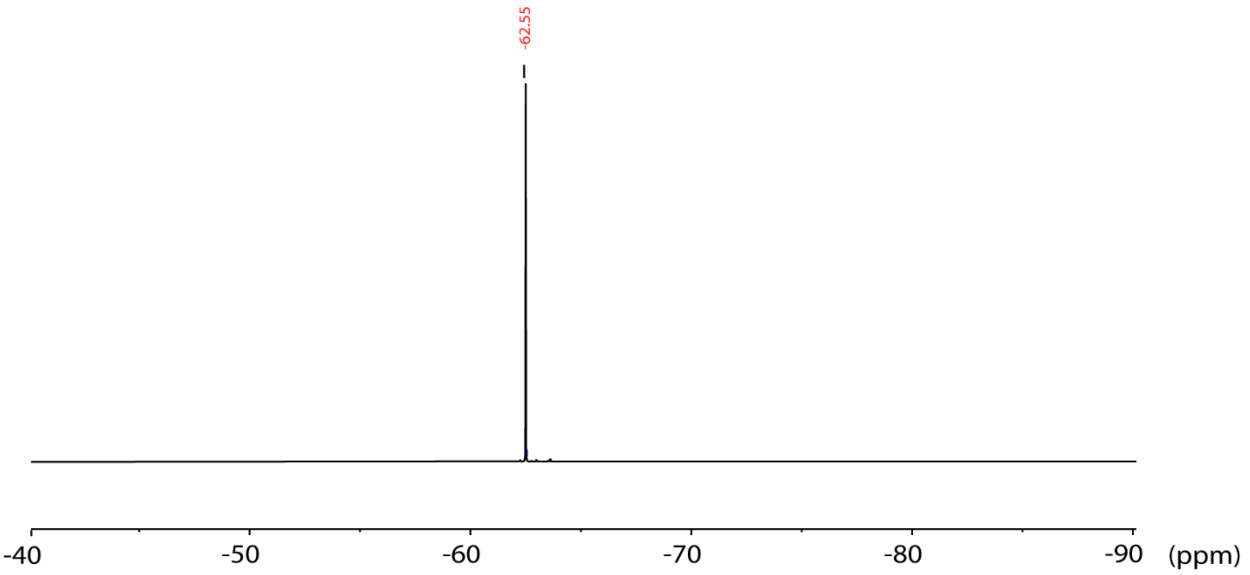

Figure S69. ^{19}F NMR spectrum of **3c** recorded in CD_2Cl_2 with an instrument operating at 376 MHz at 23 °C.

References

1. A. B. Pangborn, M. A. Giardello, R. H. Grubbs, R. K. Rosen and F. J. Timmers, *Organometallics*, 1996, **15**, 1518–1520.
2. A. Das, Y.-S. Chen, J. H. Reibenspies and D. C. Powers, *J. Am. Chem. Soc.*, 2019, **141**, 16232–16236.
3. G. R. Fulmer, A. J. M. Miller, N. H. Sherden, H. E. Gottlieb, A. Nudelman, B. M. Stoltz, J. E. Bercaw and K. I. Goldberg, *Organometallics*, 2010, **29**, 2176–2179.
4. O. V. Dolomanov, L. J. Bourhis, R. J. Gildea, J. A. K. Howard and H. Puschmann, *J. Appl. Crystallogr.*, 2009, **42**, 339–341.
5. G. M. Sheldrick, *Acta Crystallogr., Sect. A*, 2008, **64**, 112–122.
6. K. Bläsing, J. Bresien, R. Labbow, D. Michalik, A. Schulz, M. Thomas and A. Villinger, *Angew. Chem., Int. Ed.*, 2019, **58**, 6540–6544.
7. K. Rosenstengel, A. Schulz and A. Villinger, *Inorg. Chem.*, 2013, **52**, 6110–6126.
8. X. Zeng, H. Beckers, H. Willner and J. S. Francisco, *Angew. Chem., Int. Ed.*, 2012, **51**, 3334–3339.
9. R. S. Drago, *Physical Methods for Chemists*, University of Florida, Gainesville, FL, 1992.
10. Y. Huang, S.-Y. Zhu, G. He, G. Chen and H. Wang, *J. Org. Chem.*, 2024, **89**, 6263–6273.
11. *Gaussian 16*, Revision C.01, Gaussian, Inc., Wallingford, CT, 2016.
12. A. D. Becke, *J. Chem. Phys.*, 1993, **98**, 5648–5652.
13. S. Grimme, *J. Comput. Chem.*, 2006, **27**, 1787–1799.
14. S. Grimme, S. Ehrlich and L. Goerigk, *J. Comput. Chem.*, 2011, **32**, 1456–1465.
15. M. Couty and M. B. Hall, *J. Comput. Chem.*, 1996, **17**, 1359–1370.
16. R. Ditchfield, W. J. Hehre and J. A. Pople, *J. Chem. Phys.*, 1971, **54**, 724–728.
17. W. J. Hehre, R. Ditchfield and J. A. Pople, *J. Chem. Phys.*, 1972, **56**, 2257–2261.
18. P. C. Hariharan and J. A. Pople, *Theor. Chim. Acta*, 1973, **28**, 213–222.
19. A. V. Marenich, C. J. Cramer and D. G. Truhlar, *J. Phys. Chem. B*, 2009, **113**, 6378–6396.
20. M. A. L. Marques and E. K. U. Gross, *Annu. Rev. Phys. Chem.*, 2004, **55**, 427–455.
21. W. H. Press, S. A. Teukolsky, W. T. Vetterling and B. P. Flannery, *Numerical Recipes in FORTRAN: The Art of Scientific Computing*, Cambridge University Press, Cambridge, 1992.
22. *GaussView*, Semichem, Inc., Shawnee Mission, KS, 2016.
23. F. Weigend and R. Ahlrichs, *Phys. Chem. Chem. Phys.*, 2005, **7**, 3297–3305.
24. D. Andrae, U. Häußermann, M. Dolg, H. Stoll and H. Preuß, *Theor. Chim. Acta*, 1990, **77**, 123–141.
25. F. Neese, *WIREs Comput. Mol. Sci.*, 2012, **2**, 73–78.
26. C. Riplinger and F. Neese, *J. Chem. Phys.*, 2013, **138**, 034106.
27. C. Riplinger, B. Sandhoefer, A. Hansen and F. Neese, *J. Chem. Phys.*, 2013, **139**, 134101.
28. C. Riplinger, P. Pinski, U. Becker, E. F. Valeev and F. Neese, *J. Chem. Phys.*, 2016, **144**, 024109.

29. A. Hellweg, C. Hättig, S. Höfener and W. Klopper, *Theor. Chem. Acc.*, 2007, **117**, 587–597.